CHEMICAL CONSTITUENTS AND BIOLOGICAL ACTIVITIES FROM *Garcinia xanthochymus* Hook. f.

SIRACHUCH MAUNGPRASERT

MASTER OF SCIENCE
IN
APPLIED CHEMISTRY

SCHOOL OF SCIENCE
MAE FAH LUANG UNIVERSITY
2025

CHEMICAL CONSTITUENTS AND BIOLOGICAL ACTIVITIES FROM *Garcinia xanthochymus* Hook. f.

SIRACHUCH MAUNGPRASERT

THIS THESIS IS A PARTIAL FULFILLMENT OF
THE REQUIREMENTS FOR THE DEGREE OF
MASTER OF SCIENCE
IN
APPLIED CHEMISTRY

SCHOOL OF SCIENCE
MAE FAH LUANG UNIVERSITY
2025

THESIS APPROVAL

MAE FAH LUANG UNIVERSITY

FOR

MASTER OF SCIENCE IN APPLIED CHEMISTRY

Thesis Title: Chemical Constituents and Biological Activities from *Garcinia xanthochymus* Hook. f.

Author: Sirachuch Maungprasert

Examination Committee:

Associate Professor Panupong Puttarak, Ph. D.	Chairperson
Professor Surat Laphookhieo, Ph. D.	Member
Professor Wim Vanden Berghe, Ph. D.	Member
Assistant Professor Suwanna Deachathai, Ph. D.	Member
Assistant Professor Tharakorn Maneerat, Ph. D.	Member

Advisors:

.....Advisor

(Professor Surat Laphookhieo, Ph. D.)

.....Co-Advisor

(Professor Wim Vanden Berghe, Ph. D.)

S. Deachathai

.....Co-Advisor

(Assistant Professor Suwanna Deachathai, Ph. D.)

Dean:

.....

(Professor Surat Laphookhieo, Ph. D.)

ACKNOWLEDGEMENTS

I would like to express my deepest gratitude to my advisor, Prof. Dr. Surat Laphookhieo, and co-advisor, Asst. Prof. Dr. Suwanna Deachathai and Prof. Dr. Wim Vanden Berghe, for their invaluable guidance, encouragement, and unwavering support throughout the course of this thesis. Their expertise, insightful feedback, and patience were essential to the completion of this work.

My heartfelt thanks go to my colleagues and friends in the Medicinal and Natural Products Laboratory for their assistance, motivation, and friendship. Their collaboration and encouragement created a supportive and enjoyable working environment.

I am deeply thankful for the support and care I received during my time overseas at College of Pharmacy, Sungkyunkwan University, South Korea. I would like to express my sincere appreciation to Prof. Dr. Chung Sub Kim and friends in the Natural Product Chemical Biology Lab, who kindly hosted and supported me abroad. His guidance, hospitality, and encouragement made my stay both productive and memorable.

I am especially thankful to my family for their unconditional love, understanding, and encouragement. Their support has been my greatest source of strength throughout this journey.

Finally, I would like to thank Mae Fah Luang University for the overseas research training scholarship, the postgraduate scholarship and research grant for master's thesis , and the provision of laboratory facilities.

Sirachuch Maungprasert

Thesis Title	Chemical Constituents and Biological Activities from *Garcinia xanthochymus* Hook. f.
Author	Sirachuch Maungprasert
Degree	Master of Science (Applied Chemistry)
Advisor	Professor Surat Laphookhieo, Ph. D.
Co-Advisor	Professor Wim Vanden Berghe, Ph. D. Assistant Professor Suwanna Deachathai, Ph. D.

ABSTRACT

Phytochemical investigation of bark and twig of *Garcinia xanthochymus* Hook. f. led to the isolation of 22 known compounds, including 13 xanthones (**GXBA-sm1** (formoxanthone C), **GXBA-sm2** (euxanthone), **GXBA-sm3** (pyranojacreubin), **GXBA-sm4** (7-geranyloxy-1,3-dihydroxyxanthone), **GXBA-sm7** (6-hydroxy-2,3-dimethoxy xanthone), **GXBA-sm8** (xanthone V1), **GXBA-sm10** (morusignin I), **GXBA-sm11** (dulxanthone B), **GXBA-sm12** (1,5-dihydroxy-3-methoxyxanthone), **GXTM-sm19** (2,5-dihydroxy-1-methoxyxanthone), **GXTM-sm20** (2,6-dihydroxy-1,5-dimethoxyxanthone), **GXTM-sm21** (1,2,5-trihydroxyxanthone), and **GXTM-sm22** (1,2,5-trihydroxy-6-methoxyxanthone)), six of flavonoid scaffolds (**GXBA-sm6** (kaempferol), **GXBA-sm9** ((*2R,3S*)-morelloflavone), **GXTM-sm13** (GB-2a), **GXTM-sm14** (GB-1), **GXTM-sm15** (*(2S,2'S,3R)*-GB-1a), and **GXTM-sm16** (volkensiflavone)), two of benzene derivatives (**GXTM-sm17** (4-hydroxybenzoic acid) and **GXTM-sm18** (4-hydroxy-3-methoxybenzoic acid)), and one anthraquinone (**GXBA-sm5** (damnacanthal)). In addition, metabolite profiling by UHPLC-QTOF-MS was also investigated, resulting in the identification of 14 xanthones, 6 flavonoids, and 2 benzene derivatives.

The extracts and some isolated compounds were also evaluated for their antioxidant and in vitro anticancer activities against four human cancer cell lines: MDA-MB-231 (breast), Huh-7 (liver), A549 (lung), and SW480 (colon). Antioxidant assays revealed that the methanol bark extract (GXBM) showed the highest DPPH scavenging activity (IC_{50} = 23.4 ± 1.0 µg/mL), while the dichloromethane bark extract

(GXBD) showed the strongest activity in ABTS (IC_{50} = 133.8 ± 1.7 µg/mL) and FRAP (IC_{50} = 104.1 ± 3.2 µg/mL) assays. The isolated compound, *(2R,3S)*-morelloflavone (**GXBA-sm9**) exhibited potent antioxidant activity across all assays: DPPH (34.5 ± 0.7 µM), ABTS (298.7 ± 11.0 µM), and FRAP (92.2 ± 0.2 µM), surpassing standard antioxidants ascorbic acid and BHT (IC_{50} = 44.1 ± 6.6 µM and 414.3 ± 12.6 µM in DPPH assay, 129.6 ± 0.8 µM and 174.7 ± 3.4 µM in ABTS assay, and 245.4 ± 8.6 µM and 1162.1 ± 16.8 µM in FRAP assay). Cytotoxicity, apoptosis, and colony formation were assessed via MTT, Annexin V-FITC/PI staining, and colony formation assays. Among all extracts, the hexane extract (GXBH) demonstrated the strongest cytotoxicity with IC_{50} values of 66.9 ± 5.1 µg/mL (MDA-MB-231), 64.7 ± 14.9 µg/mL (Huh-7), 80.0 ± 11.9 µg/mL (A549), and 65.4 ± 7.8 µg/mL (SW480). 7-Geranyloxy-1,3-dihydroxyxanthone (**GXBA-sm4**) also showed strong activity against MDA-MB-231 (IC_{50} = 24.5 ± 2.31 µM). GXBH significantly induced apoptosis and inhibited colony formation in all four cell lines. These findings demonstrate the potential of *G. xanthochymus* as a natural source of antioxidants and anticancer agents, supporting its development as an alternative therapeutic candidate.

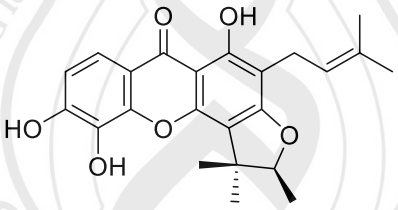

GXBA-sm1

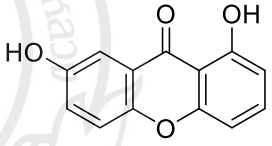

GXBA-sm2

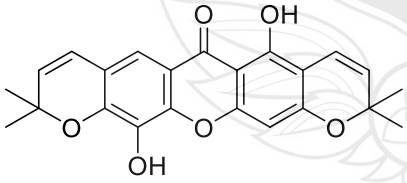

GXBA-sm3

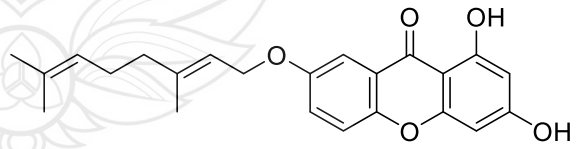

GXBA-sm4

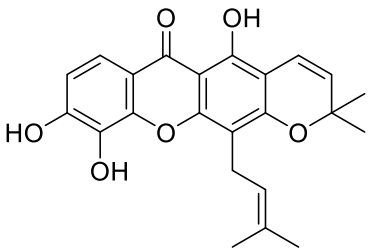

GXBA-sm8

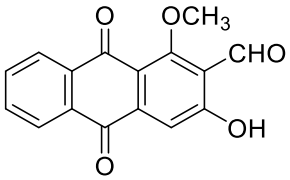

GXBA-sm5

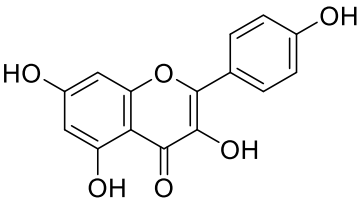

GXBA-sm6

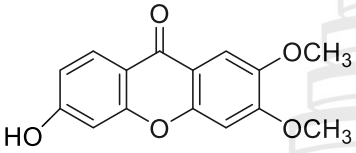

GXBA-sm7

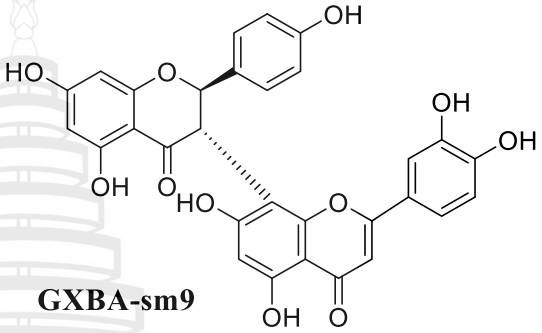

GXBA-sm9

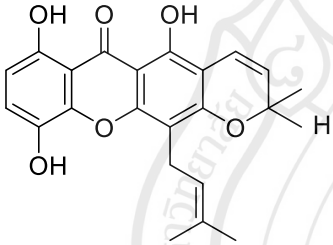

GXBA-sm10

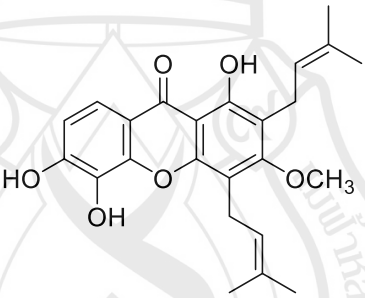

GXBA-sm11

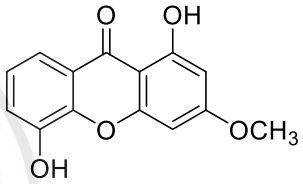

GXBA-sm12

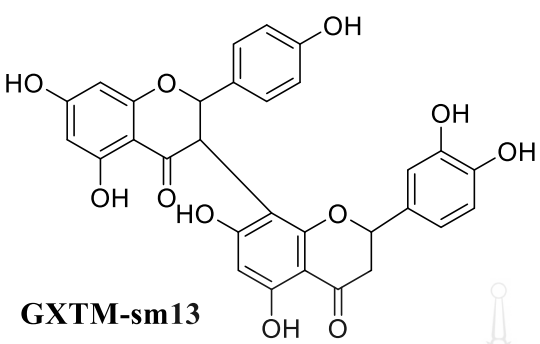

GXTM-sm13

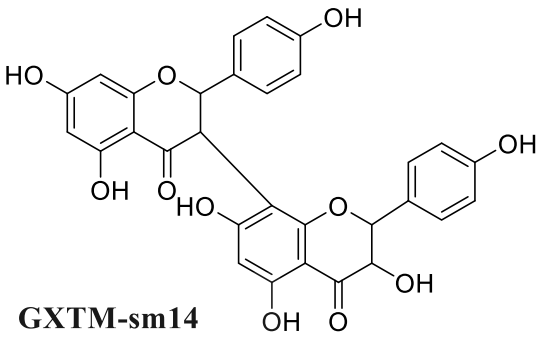

GXTM-sm14

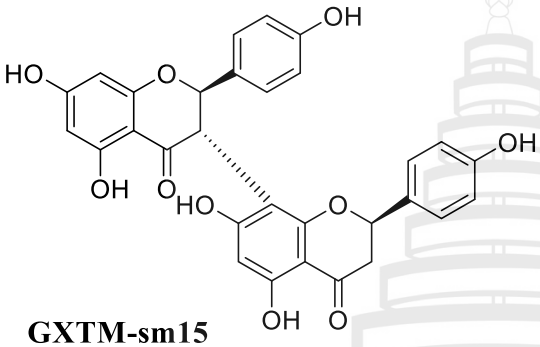

GXTM-sm15

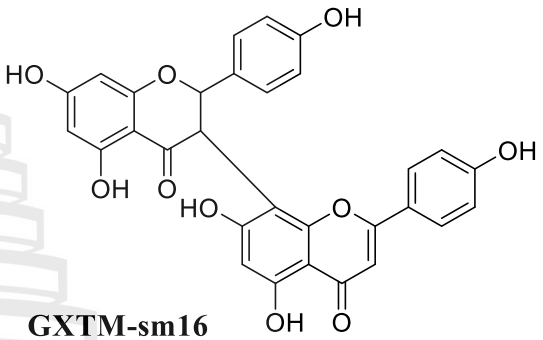

GXTM-sm16

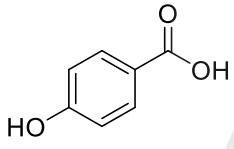

GXTM-sm17

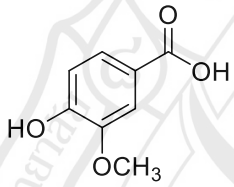

GXTM-sm18

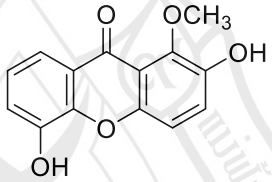

GXTM-sm19

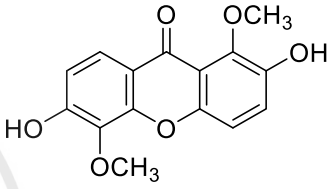

GXTM-sm20

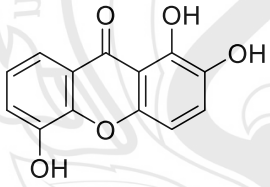

GXTM-sm21

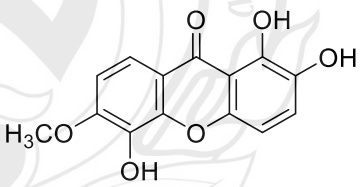

GXTM-sm22

Keywords: *Garcinia xanthochymus*, Antioxidation Activity, Anticancer Activity

TABLE OF CONTENTS

TABLE OF CONTENTS

LIST OF TABLES

LIST OF TABLES

LIST OF FIGURES

LIST OF FIGURES

ABBREVIATIONS AND SYMBOLS

ABTS	2,2'-azino-bis(3-ethylbenzothiazoline-6-sulfonic acid)
%	Percentage
% v/v	Percentage of Volume by Volume
<	Less Than
>	More Than
±	Plus Or Minus
°C	Degrees Celsius
µL	Microliter
13C NMR	Carbon-13 Nuclear Magnetic Resonance
1H NMR	Proton Nuclear Magnetic Resonance
Å	Angstrom
A549	Non-Small Cell Lung Carcinoma Cell Line
ACN	Acetonitrile
AH	Antioxidant Compound
AkT	Ak Strain Transforming
ATCC	American Type Culture Collection
BHT	Butylated Hydroxytoluene
br s	Broad Singlet
C18	Octadecyl Alkyl Substituent
CA	California
CC	Column Chromatography
CD	Circular Dichroism
CH_2Cl_2	Dichloromethane
cm	Centimeter
CO_2	Carbon Dioxide

ABBREVIATIONS AND SYMBOL

A549	Non-Small Cell Lung Carcinoma Cell Line
d	Doublet
dd	Doublet of Doublet
DMEM	Dulbecco's Modified Eagle Medium
DMSO	Dimethyl Sulfoxid
DPPH	2,2-diphenyl-1-picrylhydrazyl
dt	Doublet of Triplet
ESI	Electrospray Ionization
FBS	Fetal Bovine Serum
FRAP	Ferric Reducing Antioxidant Power
g	Gram
h.	Hour
H_2O	Water
H_2O_2	Hydrogen Peroxide
HepG2	Human Hepatocellular Carcinoma Cells
HL-60	Human Leukemia Cell Line
HO-1	Heme Oxygenase 1
HPLC	High-Performance Liquid Chromatography
Huh-7	Hepatocellular Carcinoma Cell Line
Hz	Hertz
IC_{50}	50% Inhibition Concentration
IL-1β	Interleukin-1 Beta
IL-6	Interleukin 6
J	Coupling Constant
JCRB	Japanese Collection of Research Bioresources

ABBREVIATIONS AND SYMBOL

kg	Kilogram
L	Liter
LC	Liquid Chromatography
LC-MS	Liquid Chromatography-Mass Spectrometry
m	Multiplet
m/z	Mass Per Charge
MCF-7	Human Breast Cancer Cell Line
MDA-MB-231	Human Triple-Negative Breast Adenocarcinoma Cell Line
Me_2CO	Acetone
MeOH	Methanol
mg	Milligram
MHz	Megahertz
min	Minute
mL	Milliliter
mm	Millimeter
mM	Millimolar
MS	Mass Spectrometry
MTT	3-[4,5-dimethylthiazol-2-yl]-2,5 diphenyl tetrazolium bromide
MW	Molecular Weight
NF-kB	Nuclear Factor Kappa-Light-Chain-Enhancer of Activated B Cells
nm	Nanometer

ABBREVIATIONS AND SYMBOL

NRF2	Nuclear Factor Erythroid 2-Related Factor 2
OD	Optical Density
P	P-Value
PC12	Catecholamine Cells
PC12D	Cellosaurus Cell Line
PI3K	Phosphoinositide-3-Kinase
ppm	Parts Per Million
QCC	Quick Column Chromatography
QE	Quercetin Equivalent
s	Singlet
SCG7901	Human Gastric Adenocarcinoma Cell Line
SD	Standard Deviation
SMMC-7721	Human Hepatocarcinoma Cell Line
SW480	Colon Cancer Cell Line
t	Triplet
td	Triplet Of Doublet
THP-1	Monocytic Leukemia Cell Line
TLC	Thin Layer Chromatography
TNF-α	Tumor Necrosis Factor
TPTZ	2,4,6-tri(2-pyridyl)-s-triazine
UHPLC-QTOF	Ultra-High Performance Liquid Chromatography-Quadrupole Time-of-Flight Mass Spectrometry
USA	The United States of America
UV	Ultraviolet
V	Volt

ABBREVIATIONS AND SYMBOL

VA	Virginia
δ	Chemical Shift
µg	Microgram
µM	Micromolar

CHAPTER 1

INTRODUCTION

1.1 Introduction

The genus *Garcinia* belongs to the Clusiaceae family, which includes 200 species found in the tropics as trees or shrubs and rarely as subshrubs (Chen et al., 2010). *Garcinia xanthochymus* Hook. f. is a medicinal plant known as "Ma-Da-Luang" or "Mang-Khud-Pa" in Thailand. The main phytochemicals found in *Garcinia* are xanthones, benzophenones, flavonoids, depsidones, and isocoumarins (Che Hassan et al., 2018). The genus *Garcinia* comprises a group of medicinal plants with potential therapeutic agents such as inflammation, oxidative stress, microbial infection, cancer, and obesity (Hemshekhar et al., 2011). A number of studies have reported the most chemical constituents of *G. xanthochymus* are xanthones and flavonoids and some of them showed interesting biological activities such as anti-inflammatory, antioxidant, antibacterial, antiviral, antidiabetic, antitumor, and cytotoxic properties (He et al., 2021). Several xanthones exhibited many bioactivities including antimalarial, antimicrobial, antiplasmodial, cytotoxic, trypanocidal, and antioxidant (Baggett et al., 2005; Chen et al., 2008). The essential one of flavonoid is bioflavonoids (flavonoid-flavonoid dimers) which present antibacterial, antifungal, antiallergic, antiviral, antihepatotoxic, anticancer, and immune suppressive activities (Kim et al., 2008).

One of the causes of death that also increases mortality and incidence in many countries is cancer (García et al., 2024; Tourinho-Barbosa et al., 2016). Cancer remains one of the leading causes of disease and death in the world, and its impact has worsened in recent times. In 2022, around 20 million new cases of cancer were diagnosed worldwide, and 9.7 million people died from the disease (Bizuayehu et al., 2024). It is predicted that by 2050, there will be an additional 35 million cases of cancer, a 77% increase from 2022 (World Health Organization [WHO], 2024). This growing burden highlights the urgent need for effective action against cancer. Cancer has become a serious public health problem in Thailand. In 2022, more than 180,000 new cases of

cancer were reported nationwide, and it is estimated that the incidence will increase by 50% by 2045 (All.Can international, 2025). In particular, the age-standardized incidence rate (ASIR) for breast cancer in Chiang Mai is expected to rise to 36.7 cases per 100,000 woman-years by 2024 (Sripan et al., 2017). There are still problems, such as late diagnosis and unequal access to care, especially in rural areas, even after universal health coverage was introduced in 2002. Cancer control strategies are essential for tackling the problems of prevention, early detection, and efficient treatment in order to reduce the rising incidence of cancer both internationally and in Thailand (National Cancer Institute, 2024). The treatment of cancer has been transformed by the advent of immunotherapy, targeted medicines, and customized medicine. These methods target cancer cells while minimizing harm to healthy tissue, which reduces side effects and improves therapy results. In recent years, natural extracts from marine organisms, fungi, and plants have drawn interest as potential sources of anti-cancer medications (Begg et al., 2011). These bioactive substances, which include terpenoids, polyphenols, alkaloids, and flavonoids, have distinct anti-cancer properties because of their various modes of action (Khan et al., 2020). Natural extracts provide a kinder and more effective alternative to traditional treatments like radiation and chemotherapy, which frequently have serious side effects. Furthermore, these extracts are often rich in antioxidants, which help mitigate oxidative stress, a key factor in cancer development (Asma et al., 2022). The capacity of natural extracts to specifically target cancer cells while reducing harm to healthy tissue is one of their primary benefits. Furthermore, natural extracts are essential to combo treatments. They can improve side effects, decrease medication resistance, and boost efficacy when used with traditional therapies (Safe, 2024).

Antioxidants have become a focus of scientific interest due to their numerous benefits, including anti-aging and anti-inflammatory properties. Antioxidants are substances that may protect cells from free radicals, which have been connected to heart disease, cancer, and other diseases. Free radicals are created when the body breaks down food, is exposed to radiation, or is exposed to tobacco smoke. Potent antioxidants can help reduce the risk of several diseases, including heart disease and certain types of cancer. Antioxidants prevent or lessen oxidative damage by scavenging free radicals from bodily cells (Francenia Santos-Sánchez et al., 2019; Seifried et al., 2003;

Zehiroglu & Ozturk Sarikaya, 2019). Antioxidants are a biological activity that inhibits the oxidative mechanisms of free radicals and therefore inhibits the oxidative mechanisms that will lead to degenerative diseases. Free radicals such as hydroxyl radical ($OH^{\bullet}$), nitric oxide ($NO^{\bullet}$), or peroxyl radical ($ROO^{\bullet}$) were scavenged by antioxidative compounds, which inhibit the oxidative mechanism (Chen et al., 2023; Gulcin, 2020). Phytochemicals such as phenolic compounds or terpenoids have been investigated that provide the diversity of the medicinal plant, which proposes that highly effective antioxidation activity provides the antiproliferation that is the primary prevention or treatment of cancer (Tran et al., 2020).

In this study, the evaluation of the biological activities of *G. xanthochymus* Hook. f. was focused on the evaluation of antioxidation and anticancer activities of the crude extracts and the isolated pure compounds.

1.2 Research Objectives

G. xanthochymus has long been used in traditional medicine across South and Southeast Asia. Various parts of the plant, particularly the fruit and bark, have been traditionally used to treat diarrhea, dysentery, skin inflammation, infected wounds, and parasitic infections (expelling worms) (Ji et al., 2012). In addition, extracts from this species have been reported to possess antioxidant and cytotoxic activities, suggesting its potential as a source of bioactive natural products. Based on this traditional usage and previous pharmacological indications, the following research objectives are proposed:

Objectives

1. To investigate the chemical constituents of *G. xanthochymus*. This includes the extraction, isolation, purification, and structural elucidation of secondary metabolites present in various parts of the plant bark and twigs.

2. To evaluate the antioxidation and anticancer activities of the crude extracts and isolated chemical constituents from *G. xanthochymus*. Antioxidant activity may be assessed through assays such as DPPH, ABTS, or FRAP, while anticancer

(cytotoxic) activity can be evaluated using relevant cancer cell lines to determine the potential therapeutic value of the isolated compounds.

CHAPTER 2

LITERATURE REVIEWS

2.1 General Characteristics of *Garcinia xanthochymus* Hook. f.

G. xanthochymus is a medium-sized perennial species that grows up to 10–20 meters in height. It possesses green, glossy, shiny, and leathery leaves ranging from 20 to 34 cm in length and 6 to 12 cm in width, with a notably thick texture. The plant bears simple, smooth fruits that vary in color from orange to yellow or golden. Its stem is characterized by gray, hard, and thick bark, which secretes an opaque white resin. The floral structures appear in clusters or as inflorescences and are white in color, comprising both unisexual and bisexual flowers. This combination of features reflects a species well-adapted to its environment, with significant ecological and possibly pharmacological value (Figure 2.1) (Che Hassan et al., 2018).

Source A: Stem (Valke, D. (2015, January 5). *Garcinia xanthochymus Hook.f. ex T.Anderson.* Flickr. https://www.flickr.com/photos/dinesh_valke/16201182272)

B: Barks, D: Leaves (Doi Suthep Nature Center. (n.d.). *Plant.* https://doisuthep.science.cmu.ac.th/database/plant/69)

C: Flowers (Nikharge, S. (2010, July 30). *Garcinia xanthochymus flowers on the ground 2010_0717_Rani_Bagh_ e*. Flickr. https://www.flickr.com/photos/shubhada _nikharge/4842322293)

E: Fruits (NParks Flora & Fauna Web. (2022, March 31). *Garcinia xanthochymus Hook. f. ex T. Anders.* https://www.nparks.gov.sg/florafaunaweb/flora/2/9/2931)

Figure 2.1 *Garcinia xanthochymus* Hook. f.

2.2 Chemical Constituents from *Garcinia xanthochymus* Hook. f.

According to Google Scholar and Science Direct Databases, chemical constituents have been isolated from *G. xanthochymus* summarized in Table 2.1.

Table 2.1 Compounds Isolated from *Garcinia xanthochymus*

Part	Compound (Type, Structure)	References
Bark	Garcinenone A **(a, 1)**	(Zhong et al.,
	Garcinenone B **(a, 2)**	2009)
	Garcinenone C **(a, 3)**	
	Garcinenone D **(a, 4)**	
	Garcinenone E **(a, 5)**	
	Jacareubin **(a, 6)**	
	12b-Hydroxy-des-*D*-garcigerrin A (**a, 7)**	
	1,4,6-Trihydroxy- 5-methoxy-7-(3-methyl-2 buteny1) xanthone **(a, 8)**	
	1,3,5,6-Tetrahydroxy-4,7,8-tri(3-methyl-2-butenyl) xanthone **(a, 9)**	
	Garciniaxanthone E **(a, 10)**	
	Subeliptenone B **(a, 11)**	
	Symphoxanthone **(a, 12)**	
	Garciniaxanthone I **(a, 13)**	(Jin et al., 2019)
	Jacarelhyperols B **(a, 14)**	
	Garcinenones Y **(a, 15)**	
	3,4-Dihydro-3,6,7,11-tetrahydroxy-8,9-di-(3-methyl-2-butenyl)-2,2-dimenthyl-pyrano-[2,3-c] xanthone **(a, 16)**	
	7-Geranyl-1,3,5,6-tetrahydroxy-8-(3-menthyl-2-butenyl) xanthone **(a, 17)**	
	Garcinexanthone A **(a, 18)**	(Chen et al., 2008)
	Garcinexanthone B **(a, 19)**	
	Garcinexanthone C **(a, 20)**	
	Garcinexanthone D **(a, 21)**	
	Garcinexanthone E **(a, 22)**	

Table 2.1 (continued)

Part	Compound (Type, Structure)	References
Bark	1,5,6- Trihydroxy-7-(3-methyl-2-butenyl)-8-(3-hydroxy-3-methylbutyl) furano(2′,3′:3,4) xanthone **(a, 23)**	(Chen et al., 2010)
	1,5,6-Trihydroxy-7-(3-methyl-2-butenyl)- 8-(3-hydroxy-3-methylbutyl)–6′, 6′-dimethylpyrano (2′,3′:3,4) xanthone **(a, 24)**	
	1,5,6-Trihydroxy-7-(3- methyl-2-butenyl)-8-(3-hydroxy-3-methylbutyl)–5′-(1-hydroxy-1-methylethyl)-4′, 5′ dihydrofurano (2′,3′:3,4) xanthone **(a, 25)**	
	1, 2, 5, 4′-Tetrahydroxy-4-(1,1- dimethylallyl)-5′-(2-hydroxypropan-2-yl)-4′, 5′-dihydrofurano-(2′, 3′:6, 7) xanthone **(a, 26)**	
	1, 3, 5, 6-Tetrahydroxy-7-geranylxanthone **(a, 27)**	
	1, 4-dihydroxy-6′, 6′- dimethylpyrano (2′, 3′: 5, 6) xanthone **(a, 28)**	
	Garcinexanthone F **(a, 29)**	(Chen et al., 2011)
	Bigarcinenone B **(a, 30)**	
	Garciniadepsidone A **(c, 113)**	(Li et al., 2017)
	1,2,5-Trihydroxylxanthone **(a, 31)**	
	2,5-Dihydroxy-1-methoxy xanthone **(a, 32)**	
	1,6-Dihydroxy-4,5-dimethoxy xanthone **(a, 33)**	
	1,4,6-Trihydroxy-5-methoxy-7- (3-methylbut-2-enyl) xanthone **(a, 34)**	
	1,3,5-Trihydroxy-4-(3- methylbut-2-enyl)-9H-xanthen-9-one **(a, 35)**	
	6-Deoxyjacareubin **(a, 36)**	
	Asatroviridin **(a, 37)**	

Table 2.1 (continued)

Part	Compound (Type, Structure)	References
Bark	1,2,5,6-Tretrahydroxy-4-(1,1-dimethyl-2-propenyl)-7-(3- methyl-2-butenyl) xanthone **(a, 38)**	
	1,4,5,6-Tetrahydroxy-7,8-di (3-methylbut-2-enyl) xanthone **(a, 39)**	
	1,5,6-Trihydroxy-7,8-di(3-methyl-2-butenyl)-60 ,60 -dimethylpyrano (2′, 3′ :3,4) xanthone **(a, 40)**	
	Xanthochymusxanthones A **(a, 41)**	(Nguyen et al., 2017)
	Xanthochymusxanthones B **(a, 42)**	
	Subelliptenone C **(a, 43)**	
	Subelliptenone D **(a, 44)**	
	Subelliptenone F **(a, 45)**	
	Subelliptenone H **(a, 46)**	
	Subelliptenone G **(a, 47)**	
	Globuxanthone (**a, 48)**	
	1,2,7-Trihydroxyxanthone **(a, 49)**	
	1,7-Dihydroxyxanthone **(a, 50)**	
Fruit	Garcixanthochymone A **(e, 51)**	(Chen et al., 2017)
	Garcixanthochymone B **(e, 52)**	
	Garcixanthochymone C **(e, 53)**	
	Garcixanthochymone D **(e, 54)**	
	Garcixanthochymone E **(e, 55)**	
	1,4,5-Trihydroxyxanthone **(a, 47)**	
	1,3,7-Trihydroxyxanthone **(a, 56)**	
	1,3,5-Trihydroxyxanthone **(a, 57)**	
	1,5,6-Trihydroxy-3-methoxyxanthone **(a, 58)**	
	1,3,6-Trihydroxy-7-methoxyxanthone **(a, 59)**	
	2,5-Dihydroxy-1-methoxylxanthone **(a, 60)**	
	1,3,5,6-Tetrahydroxy-2-isoprenylxanthone **(a, 61)**	
	Naringenin **(b, 103)**	

Table 2.1 (continued)

Part	Compound (Type, Structure)	References
Fruit	6-Prenyl-4′ ,5,7-trihydroxyflavone **(b, 104)**	
	GB-2a **(b, 105)**	
	Fukugetin **(b, 106)**	
	Volkensiflavone **(b, 107)**	
	1,5-Dihydroxyxanthone **(a, 62)**	(Joseph et al., 2016)
	1,7-Dihydroxyxanthone **(a, 63)**	
	Maclurin **(e, 120)**	
	1,3,5,6-Tetrahydroxy-4,7,8- tri(3-methyl-2-butenyl) xanthone **(a, 64)**	
	1,4,5,6- Tetrahydroxy-7,8-di(3-methylbut-2-enyl) xanthone **(a, 65)**	
	1,2,6-Trihydroxy-5-methoxy-7-(3- methylbut-2-enyl) xanthone **(a, 66)**	
	Garciniaxanthone E **(a, 10)**	
	12b-Hydroxy-des-*D*-garcigerrin A **(a, 7)**	
	Alloathyriol **(a, 67)**	
	Xanthochymol **(e, 121)**	
	Isoxanthochymol **(e, 122)**	
	Guttiferone A **(e, 123)**	
	Guttiferone E **(e, 124)**	
	Guttiferone H **(e, 125)**	
	Gambogenone **(e, 126)**	
	Aristophenone A **(e, 127)**	
	Cycloxanthochymol **(e, 128)**	
	Epicatechin **(b, 108)**	(Prakash et al., 2022)
	Catechin **(b, 109)**	
	Gallic acid **(d, 114)**	
	Syringic acid **(d, 115)**	
	Coumaric acid **(d, 116)**	

Table 2.1 (continued)

Part	Compound (Type, Structure)	References
Fruit	Cinnamic acid **(d, 117)**	
	Sinapic acid **(d, 118)**	
	Xanthochymusones A **(e, 71)**	(Xu et al., 2022)
	Xanthochymusones B **(e, 72)**	
	Xanthochymusones C **(e, 73)**	
	Xanthochymusones D **(e, 74)**	
	Xanthochymusones E **(e, 75)**	
	Xanthochymusones F **(e, 76)**	
	Xanthochymusones G **(e, 77)**	
	Xanthochymusones H **(e, 78)**	
	Xanthochymusones I **(e, 79)**	(Xu et al., 2023)
	Xanthochymusones J **(e, 80)**	
	Xanthochymusones K **(e, 81)**	
	Xanthochymusones L **(e, 82)**	
	Xanthochymusones M **(e, 83)**	
	Garciniagifolone A **(e, 129)**	
	Garcinialiptone A **(e, 130)**	
Leaf	Vanillic acid **(d, 119)**	(Rob et al., 2021)
	Garcienone **(e, 131)**	(Rob et al., 2019)
	Fukugetin **(b, 106)**	(Joseph et al.,
	Fukugiside **(b, 110)**	2016)
	Volkensiflavone **(b, 107)**	
	GB-1a **(b, 111)**	
	GB-2 **(b, 112)**	
	GB-2a **(b, 105)**	
	Xanthochymusside **(b, 84)**	
Root	Fukugetin **(b, 106)**	(Che Hassan et
Seed	Garxanthochin A **(e, 136)**	al., 2018)
	Garxanthochin B **(e, 137)**	

Table 2.1 (continued)

Part	Compound (Type, Structure)	References
Seed	Garxanthochin C **(e, 138)**	(Quan et al., 2023)
Stem bark	Garcinenone X **(a, 85)** Garcinenone Y **(a, 86)** 1,4,5,6-Tetrahydroxy-7-(3-methylbut-2-enyl) xanthone **(a, 87)** 1,4,6-Trihydroxy-5- methoxy-7-(3-methylbut-2-enyl) xanthone **(a, 88)** 1,4,5,6- Tetrahydroxy-7,8-di(3-methylbut-2-enyl) xanthone **(a, 65)** 1,3,5,6- Tetrahydroxy-4,7,8-tri(3-methyl-but-2-enyl) xanthone **(a, 64)**	(Payamalle et al., 2017) (Ji et al., 2012)
Twig	Xanthochymones A **(e, 132)** Xanthochymones B **(e, 133)** Xanthochymones C **(e, 134)** Garcinexanthone A **(a, 18)** Volkensiflavone **(b, 107)** Morelloflavone **(b, 106)** Angelicoin B **(f, 135)** 1,3,5,6-Tetrahydroxy-4,7,8-triprenylxanthone **(a, 93)** Garciniaxanthone E **(a, 10)** 6-Prenylapigenin **(b, 104)** 1,4,6-Trihydroxy-5-methoxy-7-prenylxanthone **(a, 88)** 1,4,5,6- Tetrahydroxy-7-prenylxanthone **(a, 87)** 1,2,5,6-Tetrahydroxy-7-geranylxanthone **(a, 97)** 1,4,5,6-Tetrahydroxy-7,8-diprenylxanthone **(a, 65)**	(Trisuwan et al., 2014) (Han et al., 2007)
Wood	1,4,5,6-Tetrahydroxy-7,8-di(3-methylbut-2-enyl) xanthone **(a, 65)**	(Chanmahasathien et al., 2003)

Table 2.1 (continued)

Part	Compound (Type, Structure)	References
Wood	1,2,6-Trihydroxy-5-methoxy-7-(3- methylbut-2-enyl) xanthone **(a, 88)**	
	12b-Hydroxy-des-*D*-garcigerrin A **(a, 7)**	
	1,3,5,6-Tetrahydroxy-4,7,8- tri(3-methyl-2-butenyl) xanthone **(a, 64)**	(Joseph et al., 2016)
	Garciniaxanthone E **(a, 10)**	
	Fukugetin **(b, 106)**	
	Fukugiside (**b, 110)**	
	Volkensiflavone **(b, 107)**	
	Xanthochymusside **(a, 103)**	
	GB-1a **(b, 111)**	
	GB-2 (**b, 112)**	

Note **a**: Xanthone **b**: Flavonoid **c**: Depsidone **d**: Phenolic acid **e**: Benzophenone

a: Xanthone

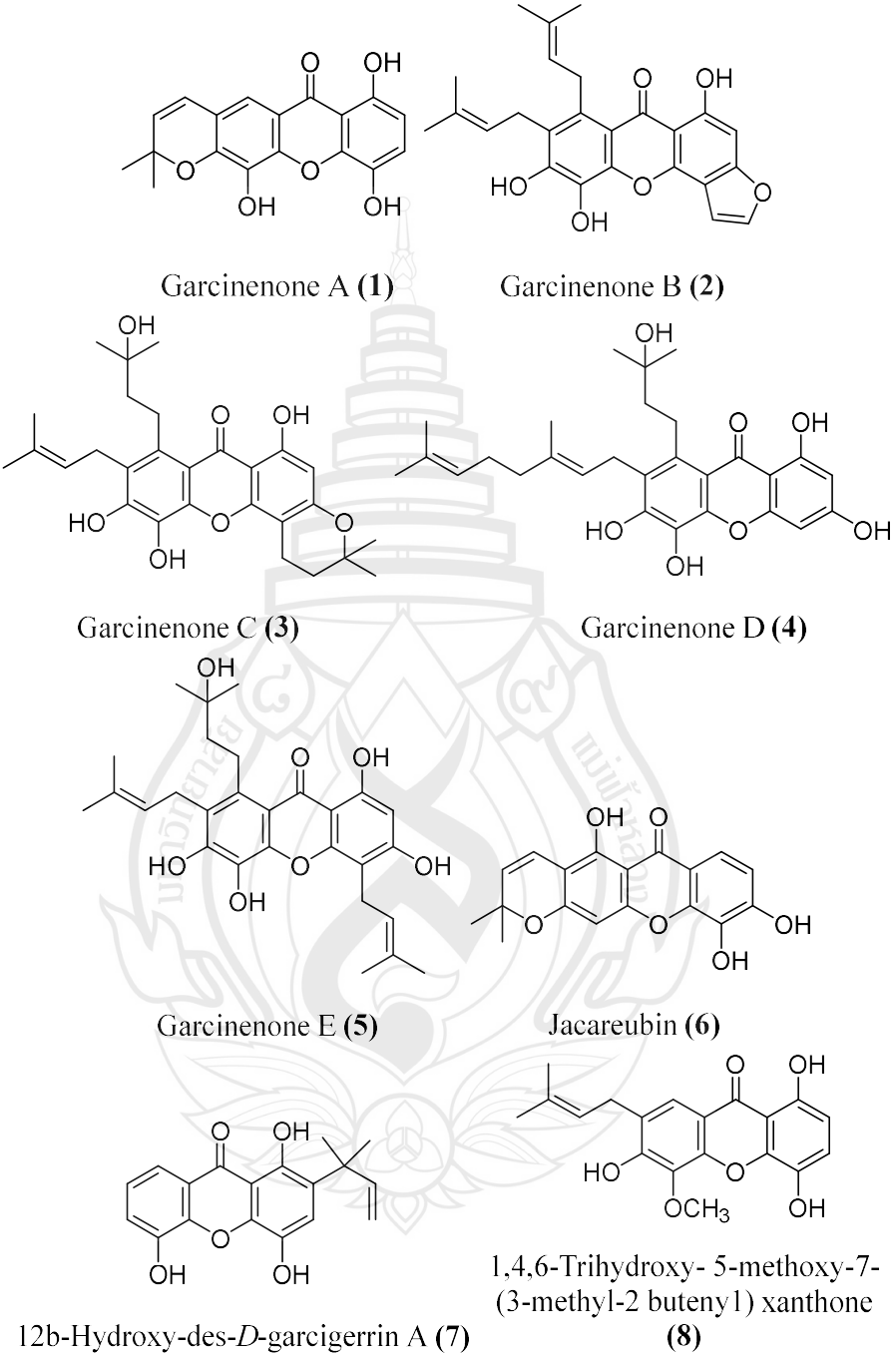

Figure 2.2 Structures of Isolated Compounds from *G. xanthochymus*.

a: Xanthone (continued)

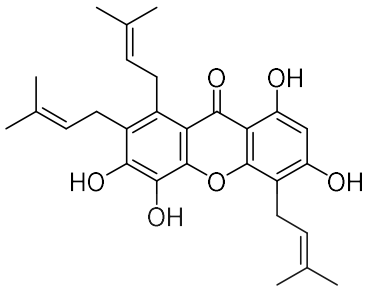

1,3,5,6-Tetrahydroxy-4,7,8-tri(3-methyl-2-butenyl) xanthone **(9)**

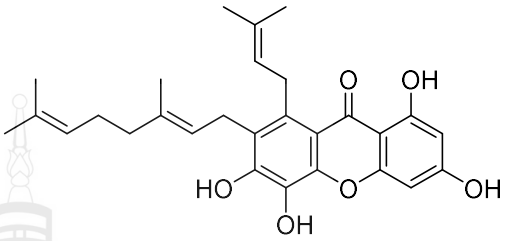

Garciniaxanthone E **(10)**

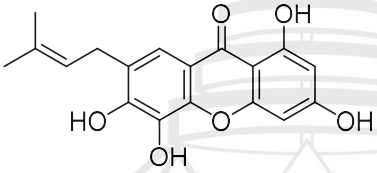

Subeliptenone B **(11)**

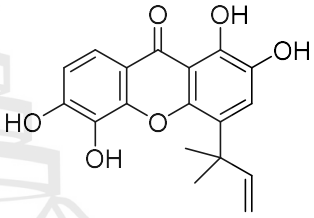

Symphoxanthone **(12)**

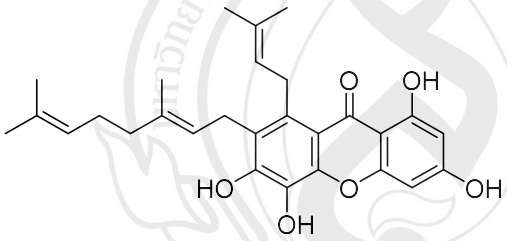

Garciniaxanthone I **(13)**

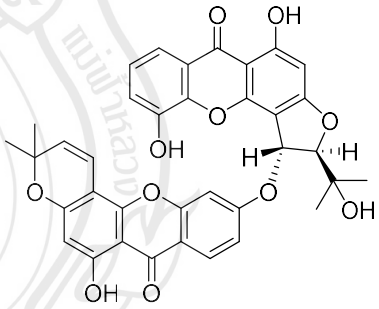

Jacarelhyperols B **(14)**

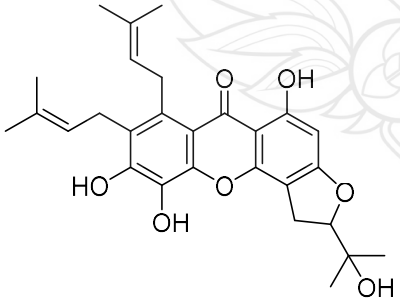

Garcinenones Y **(15)**

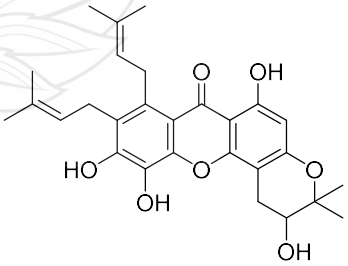

3,4-Dihydro-3,6,7,11-tetrahydroxy-8,9-di-(3-methyl-2-butenyl)-2,2-dimenthyl-pyrano-[2,3-c] xanthone **(16)**

Figure 2.2 (continued)

a: Xanthone (continued)

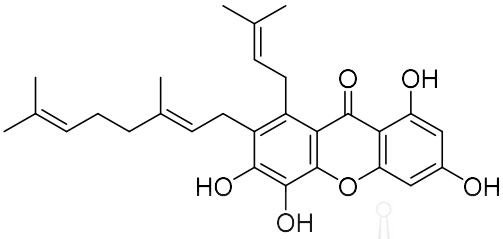

7-Geranyl-1,3,5,6-tetrahydroxy-8-(3-menthyl-2-butenyl) xanthone **(17)**

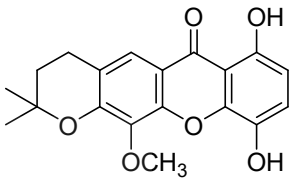

Garcinexanthone A **(18)**

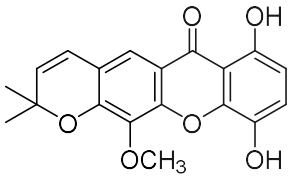

Garcinexanthone B **(19)**

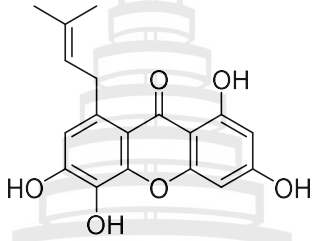

Garcinexanthone C **(20)**

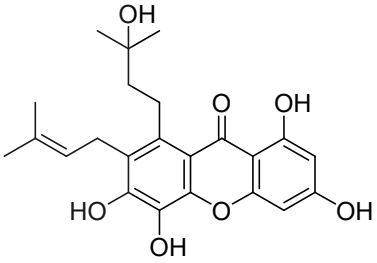

Garcinexanthone D **(21)**

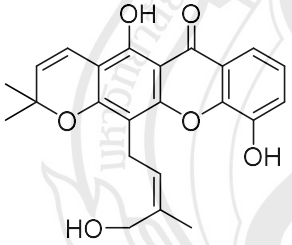

Garcinexanthone E **(22)**

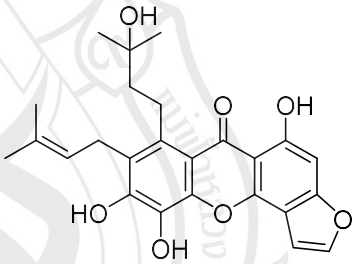

1,5,6-Trihydroxy-7-(3-methyl-2-butenyl)-8-(3-hydroxy-3-methylbutyl) furano(2',3':3,4) xanthone **(23)**

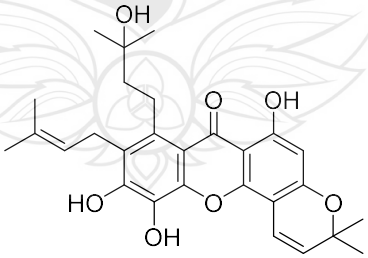

1,5,6-Trihydroxy-7-(3-methyl-2-butenyl)- 8-(3-hydroxy-3-methylbutyl)-6', 6'-dimethylpyrano (2',3':3,4) xanthone **(24)**

Figure 2.2 (continued)

a: Xanthone (continued)

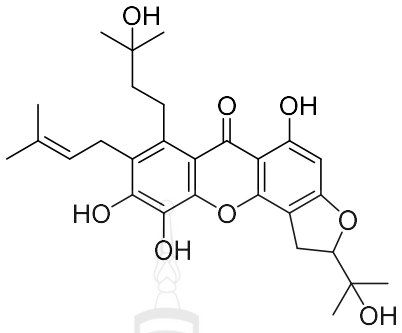

1,5,6-Trihydroxy-7-(3- methyl-2-butenyl)-8-(3-hydroxy-3-methylbutyl)-5'-(1-hydroxy-1-methylethyl)-4', 5' dihydrofurano (2',3':3,4) xanthone **(25)**

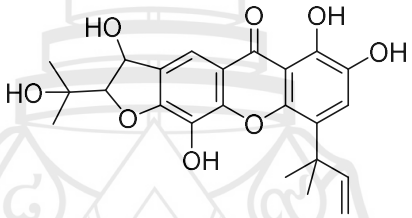

1, 2, 5, 4'-Tetrahydroxy-4-(1,1- dimethylallyl)-5'-(2-hydroxypropan-2-yl)-4', 5'-dihydrofurano-(2', 3':6, 7) xanthone **(26)**

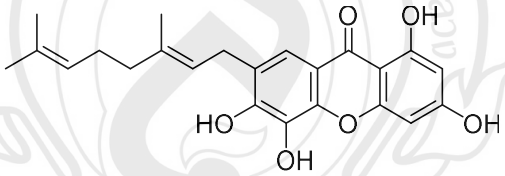

1, 3, 5, 6-Tetrahydroxy-7-geranylxanthone **(27)**

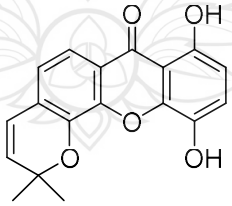

1, 4-Dihydroxy-6', 6'- dimethylpyrano (2', 3': 5, 6) xanthone **(28)**

Figure 2.2 (continued)

a: Xanthone (continued)

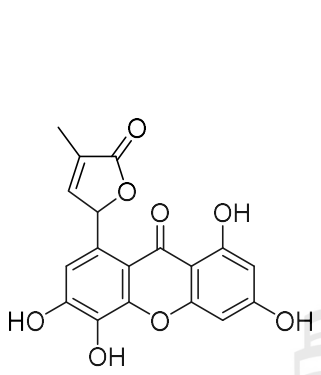

Garcinexanthone F **(29)**

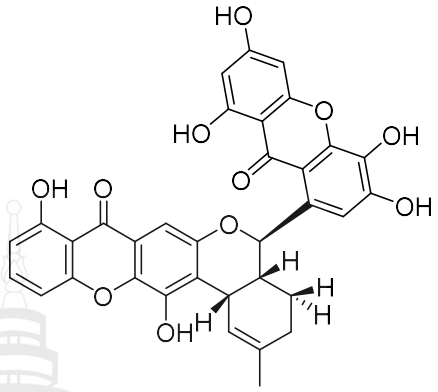

Bigarcinenone B **(30)**

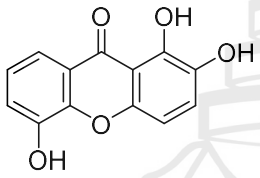

1,2,5-Trihydroxylxanthone **(31)**

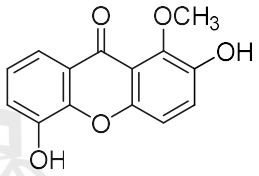

2,5-Dihydroxy-1-methoxy xanthone **(32)**

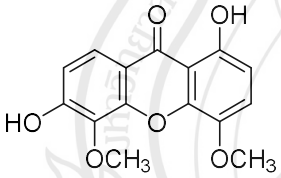

1,6-Dihydroxy-4,5-dimethoxy xanthone **(33)**

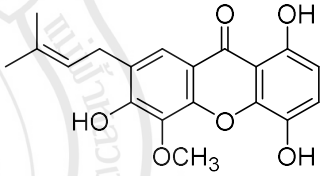

1,4,6-Trihydroxy-5-methoxy-7- (3-methylbut-2-enyl) xanthone **(34)**

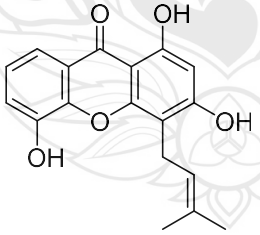

1,3,5-Trihydroxy-4-(3- methylbut-2-enyl)-9H-xanthen-9-one **(35)**

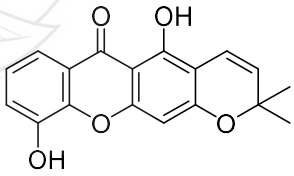

6-Deoxyjacareubin **(36)**

Figure 2.2 (continued)

a: Xanthone (continued)

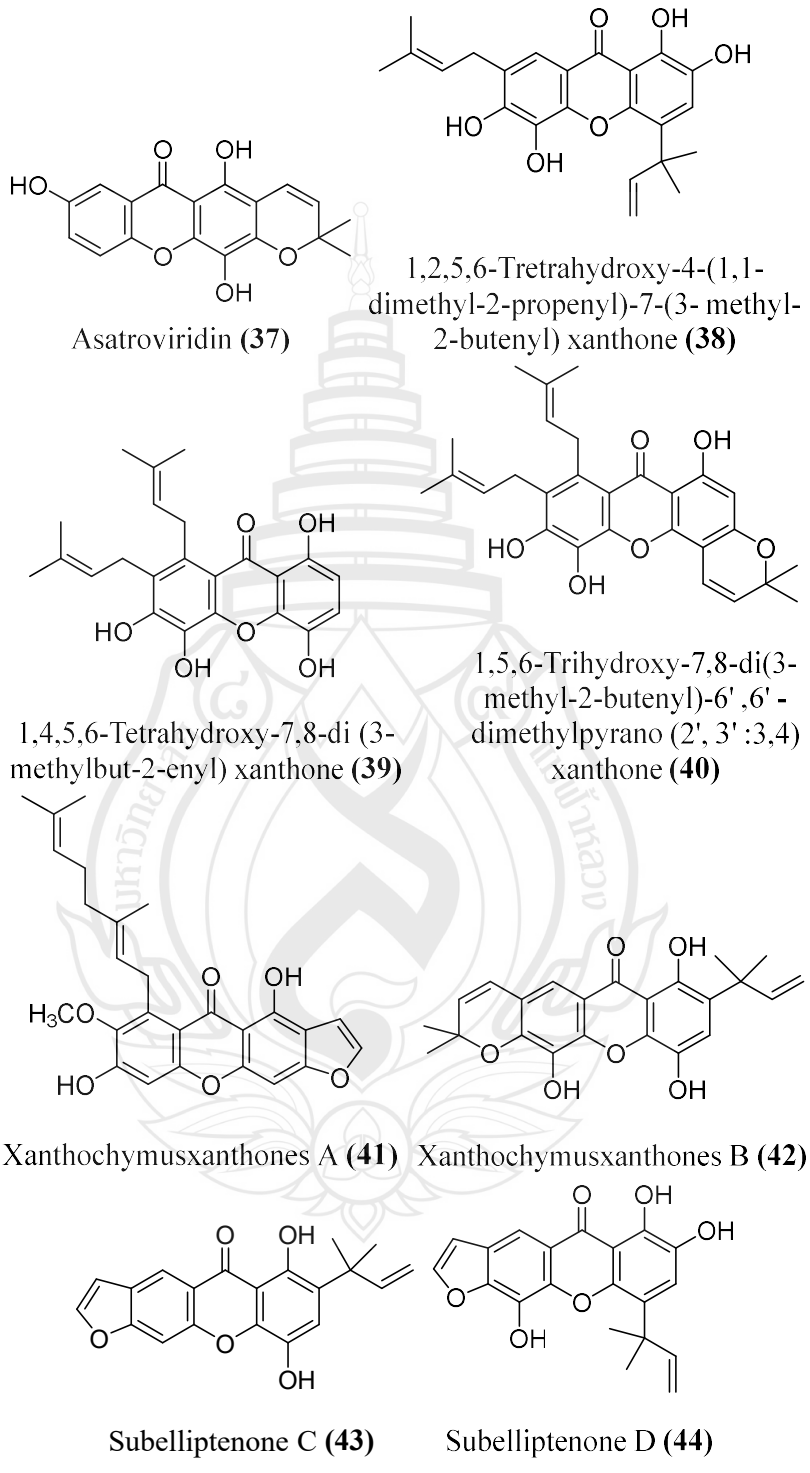

Figure 2.2 (continued)

a: Xanthone (continued)

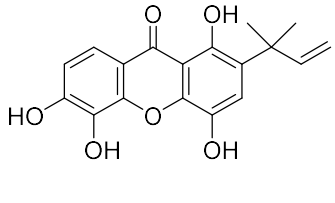

Subelliptenone F **(45)**

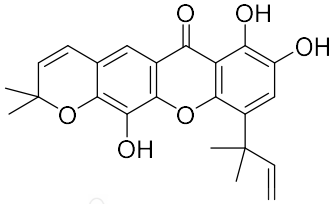

Subelliptenone H **(46)**

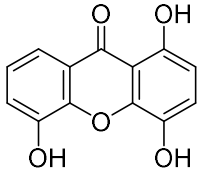

Subelliptenone G **(47)**

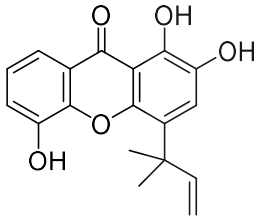

Globuxanthone **(48)**

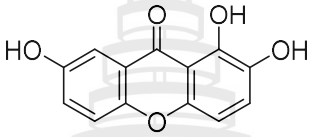

1,2,7-Trihydroxyxanthone **(49)**

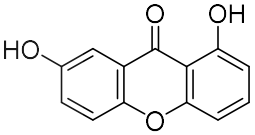

1,7-Dihydroxyxanthone **(50)**

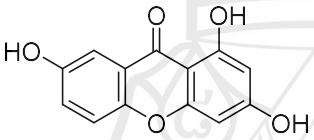

1,3,7-Trihydroxyxanthone **(56)**

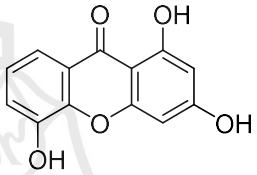

1,3,5-Trihydroxyxanthone **(57)**

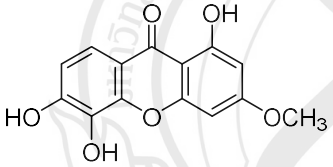

1,5,6-Trihydroxy-3-methoxyxanthone **(58)**

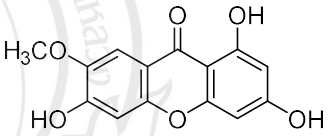

1,3,6-Trihydroxy-7-methoxyxanthone **(59)**

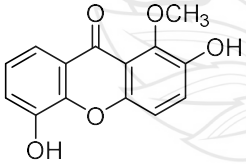

2,5-Trihydroxy-1-methoxyxanthone **(60)**

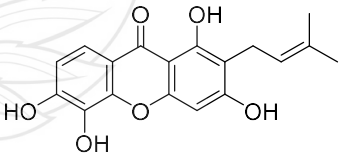

1,3,5,6-Tetrahydroxy-2-isoprenylxanthone **(61)**

Figure 2.2 (continued)

a: Xanthone (continued)

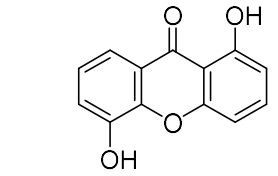

1,5-Dihydroxyxanthone **(62)**

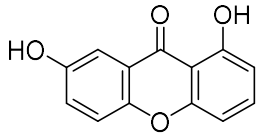

1,7-Dihydroxyxanthone **(63)**

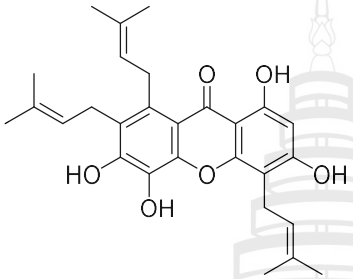

1,3,5,6-Tetrahydroxy-4,7,8- tri(3-methyl-2-butenyl) xanthone **(64)**

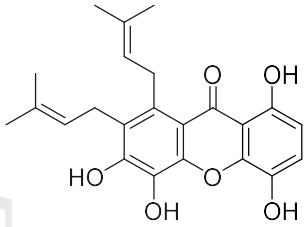

1,4,5,6- Tetrahydroxy-7,8-di(3-methylbut-2-enyl) xanthone **(65)**

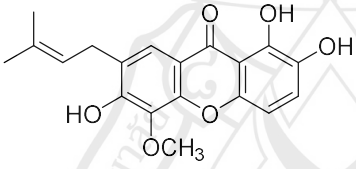

1,2,6-Trihydroxy-5-methoxy-7-(3-methylbut-2-enyl) xanthone **(66)**

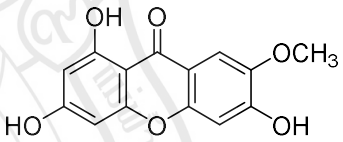

Alloathyriol **(67)**

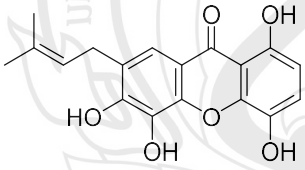

1,4,5,6-Tetrahydroxy-7-(3-methylbut-2-enyl) xanthone **(87)**

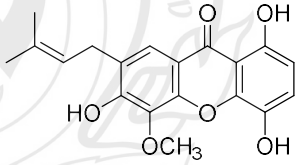

1,4,6-Trihydroxy-5- methoxy-7-(3-methylbut-2-enyl) xanthone **(88)**

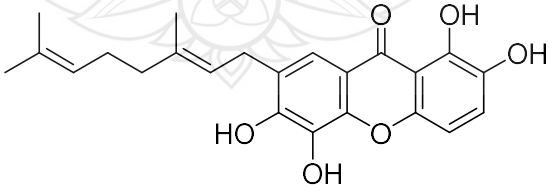

1,2,5,6-Tetrahydroxy-7-geranylxanthone **(97)**

Figure 2.2 (continued)

b: Flavonoid

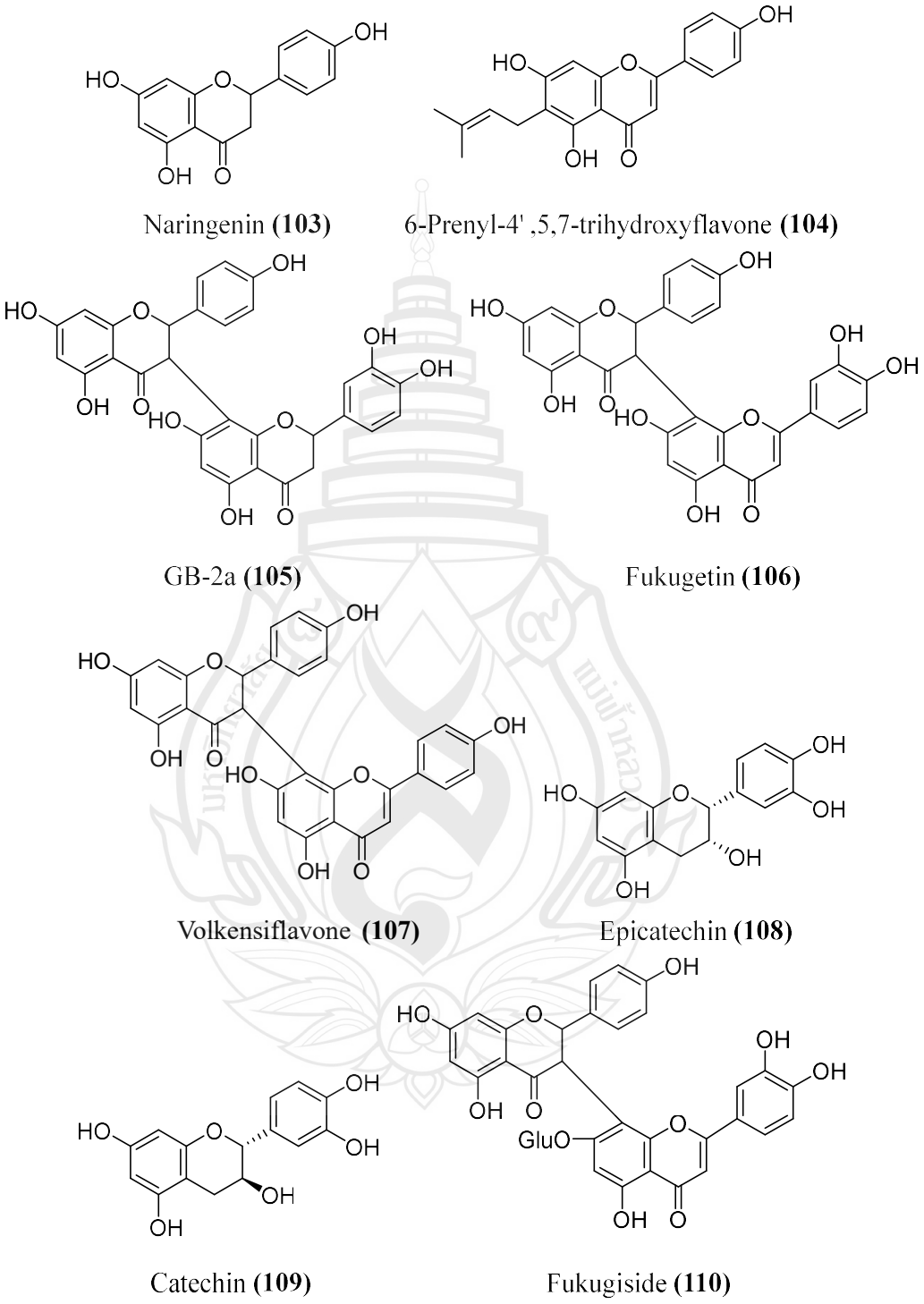

Figure 2.2 (continued)

b: Flavonoid (continued)

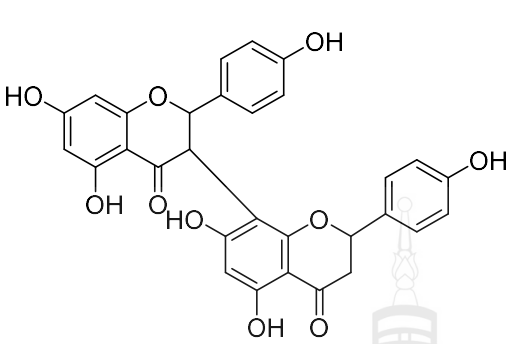

GB-1a **(111)**

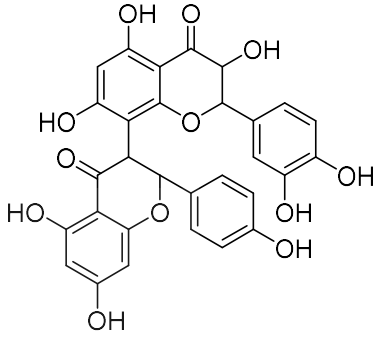

GB-2 **(112)**

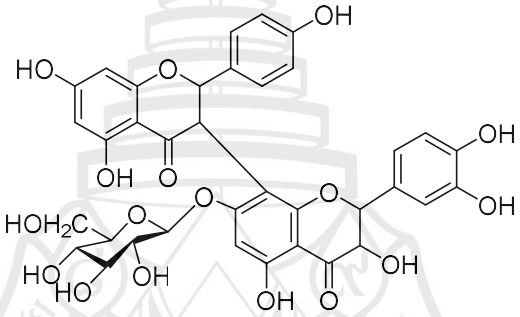

Xanthochymusside **(84)**

c: Depsidone

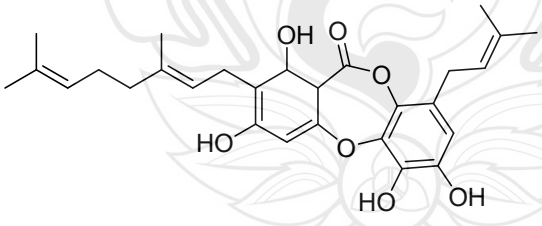

Garciniadepsidone A **(113)**

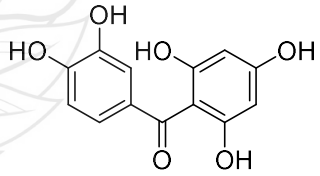

Maclurin **(120)**

Figure 2.2 (continued)

d: Phenolic acid

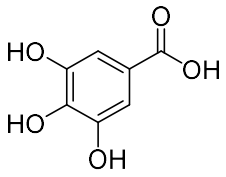

Gallic acid **(114)**

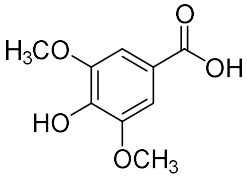

Syringic acid **(115)**

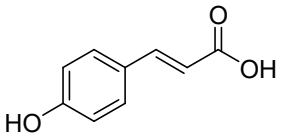

Coumaric acid **(116)**

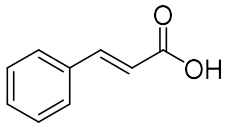

Cinnamic acid **(117)**

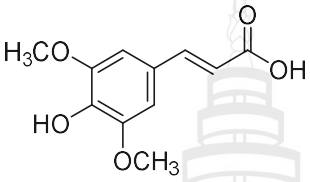

Sinapic acid **(118)**

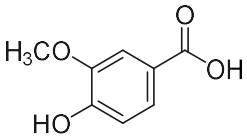

Vanillic acid **(119)**

Figure 2.2 (continued)

e: Benzophenone

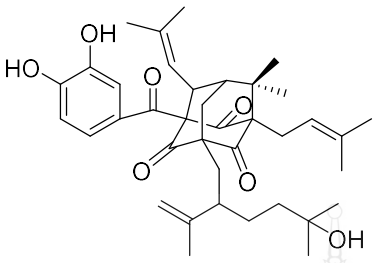

Garcixanthochymone A **(51)**

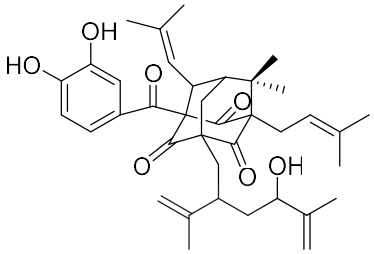

Garcixanthochymone B **(52)**

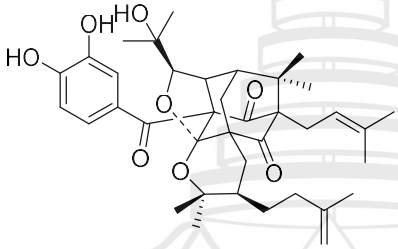

Garcixanthochymone C **(53)**

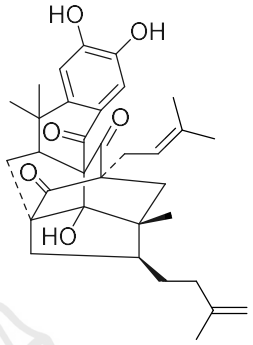

Garcixanthochymone D **(54)**

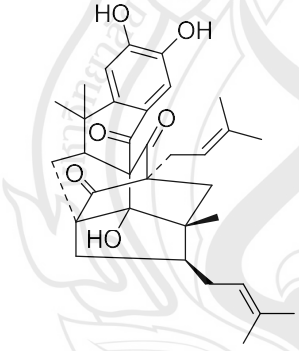

Garcixanthochymone E **(55)**

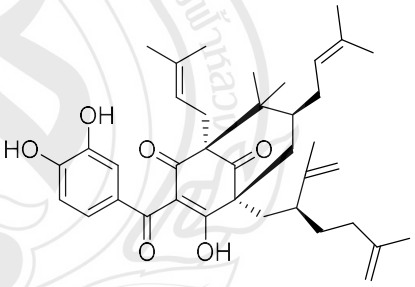

Xanthochymol **(121)**

Figure 2.2 (continued)

e: Benzophenone (continued)

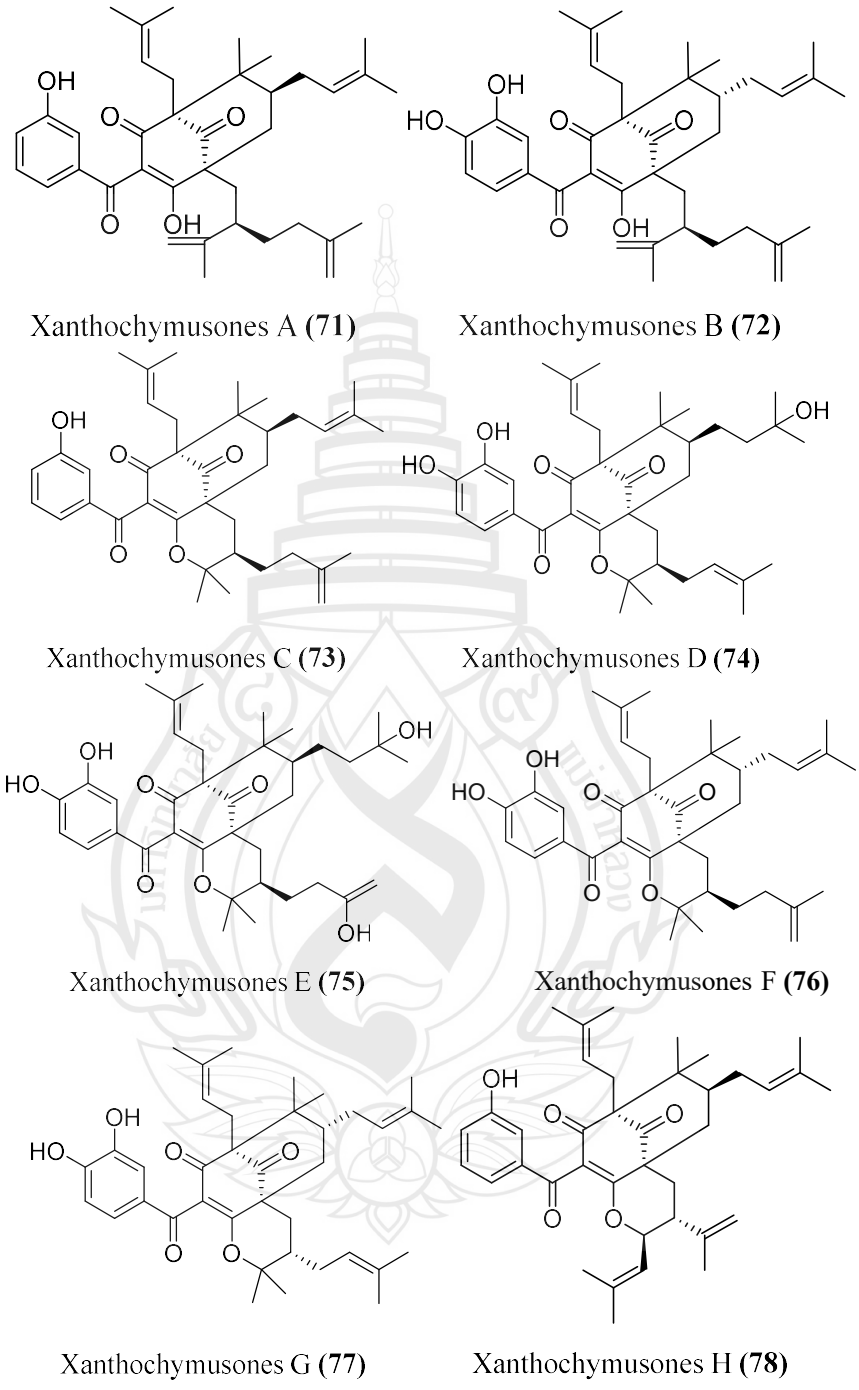

Figure 2.2 (continued)

e: Benzophenone (continued)

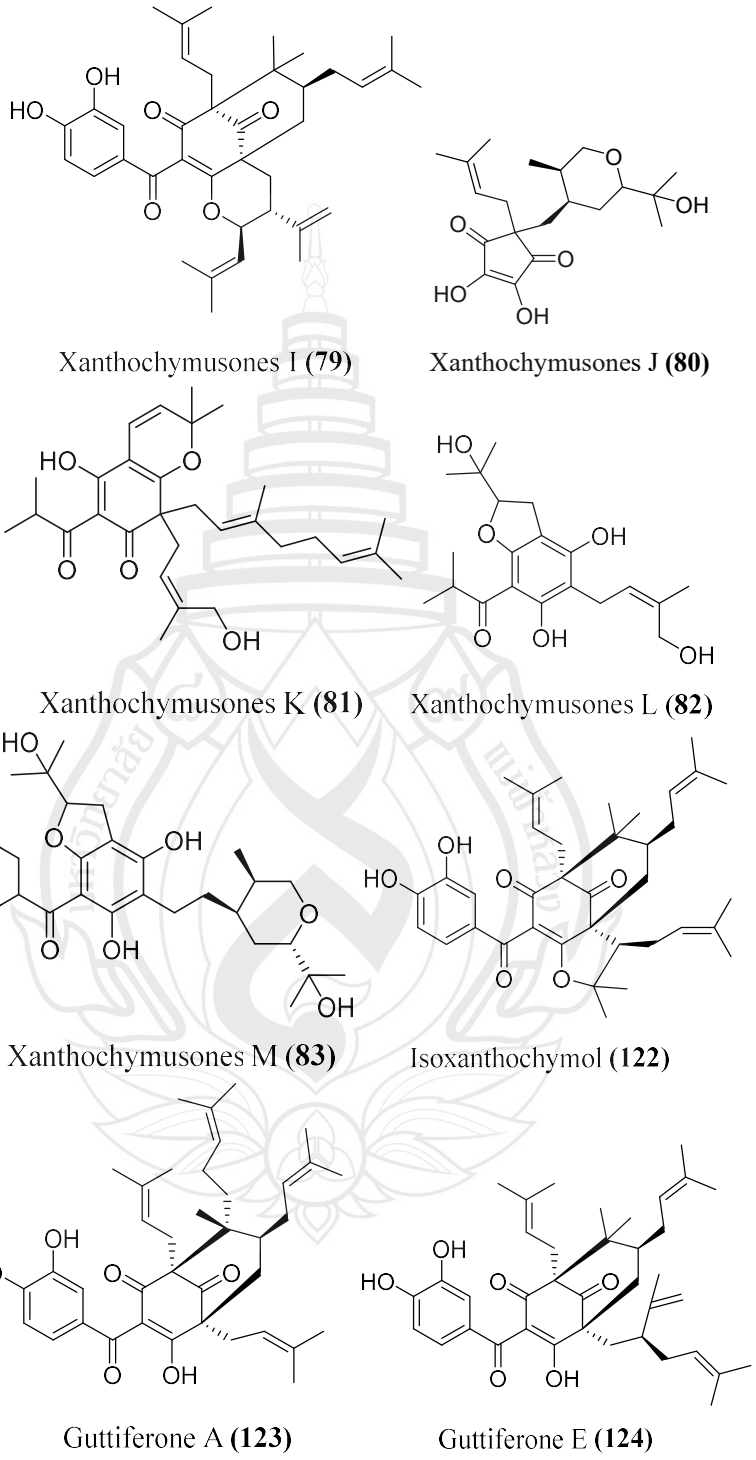

Figure 2.2 (continued)

e: Benzophenone (continued)

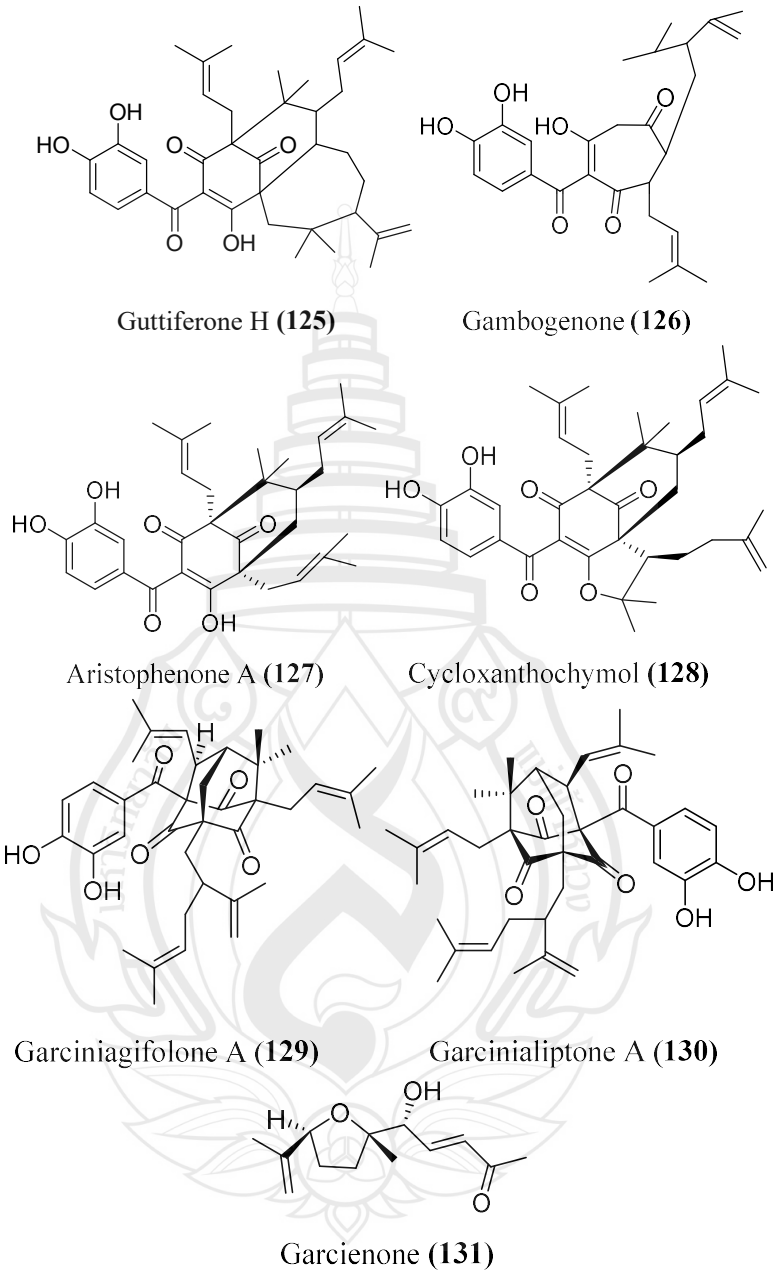

Figure 2.2 (continued)

e: Benzophenone (continued)

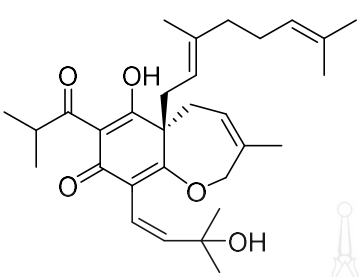

Garxanthochin A **(136)**

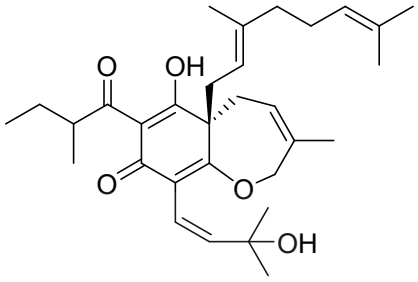

Garxanthochin B **(137)**

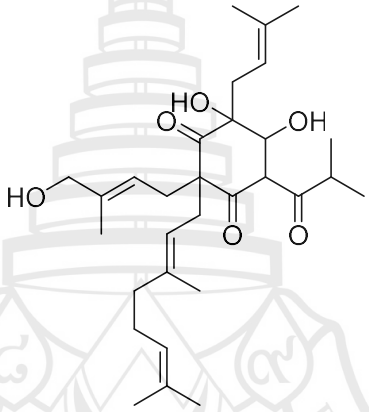

Garxanthochin C **(138)**

Figure 2.2 (continued)

2.3 Biological Activities of *Garcinia xanthochymus* Hook. f.

Numerous studies have identified xanthones as the major chemical constituents of *Garcinia xanthochymus*. According to research available on Google Scholar and Science Direct Databases, the chemical composition of *G. xanthochymus* has been extensively investigated, with particular emphasis on the isolation and characterization of bioactive compounds. Table 2.2 summarizes the key significant biological activities, including antioxidant, antimicrobial, anti-inflammatory, antidiabetic, lipase inhibitory, cytotoxic and anticancer and nerve growth factor (NGF)-potentiating properties. These findings highlight the potential of *G. xanthochymus* as a valuable source of pharmacologically active natural products.

Table 2.2 Biological Activities of *G. xanthochymus*

Biological activity	References
Antioxidant Activity	Chen et al. (2010)
	Gogoi et al. (2015)
	Xu et al. (2017)
	Jonali Brahma et al. (2025)
Antimicrobial Activity	Jackson et al. (2015)
	Jonali Brahma et al. (2025)
	Payamalle and Murthy. (2015)
	Pruksakorn et al. (2024)
	Sunkar and Nachiyar. (2012)
Anti-inflammatory Activity	Chantree et al. (2023)
	Hamidon et al. (2016)
	Winata et al. (2021)
Antidiabetic Activity	Chen et al. (2019)
	FU et al. (2014)
	Nguyen et al. (2017)
	Prakash et al. (2022)
Lipase Inhibitory Activity	Rahminiwati et al. (2025)
	Sangchan Adchara et al. (2016)

Table 2.2 (continued)

Biological activity	References
Cytotoxic and Anticancer Activities	Hamidon et al. (2016)
	Jin et al. (2019)
	Quan et al. (2023)
	Xu et al. (2020)
Nerve Growth Factor (NGF)-Potentiating Activity	Chanmahasathien et al. (2003)
	Li and Ohizumi. (2004)
	More et al. (2012)
	Joseph et al. (2016)

2.3.1 Antioxidant Activity

G. xanthochymus has garnered attention for its potent antioxidant properties, primarily attributed to its rich composition of bioactive compounds such as xanthones, flavonoids, and phenolic acids. These constituents play a crucial role in neutralizing free radicals, thereby mitigating oxidative stress and its associated cellular damage.

Several studies have evaluated the antioxidant capacity of *G. xanthochymus* using various *in vitro* models. Six new xanthones had been isolated from the bark of *G. xanthochymus* by Chen and co-workers in 2010 (Chen et al., 2010). Among these, compound **1** exhibited significant DPPH radical scavenging activity with an IC_{50} value of 19.64 μM, indicating strong antioxidant potential (Chen et al., 2010). In 2015, Gogoi and colleagues assessed the methanolic pericarp extract of *G. xanthochymus* using DPPH, ABTS, nitric oxide scavenging, and total iron-reducing power assays. The extract demonstrated high phenolic content and exhibited significant free radical scavenging activities across all assays, underscoring its robust antioxidant capacity (Gogoi et al., 2015).

Beyond chemical assays, the antioxidant efficacy of *G. xanthochymus* has been explored in cellular models. In 2017, Xu and co-workers investigated the protective effects of the ethyl acetate fraction of *G. xanthochymus* fruit on H_2O_2-induced oxidative damage in PC12 cells. The extract enhanced cell viability, increased activities of antioxidant enzymes such as superoxide dismutase and catalase and activated the

PI3K/AKT and NRF2/HO-1 signaling pathways, highlighting its potential in neuroprotection (XU et al., 2017).

The antioxidant activity of *G. xanthochymus* is closely linked to its phytochemical composition. Brahma et and colleagues (2023) conducted a comprehensive analysis of *G. xanthochymus*, revealing a high flavonoid content of 34.99 ± 0.51 mg QE/g and substantial phenolic content (Brahma et al., 2025). These compounds are known for their antioxidant properties, contributing to the plant's overall free radical scavenging activity. The strong antioxidant properties of *G. xanthochymus* suggest its potential in preventing and managing oxidative stress-related diseases, including neurodegenerative disorders, cardiovascular diseases, and certain cancers. Its rich phytochemical profile positions it as a promising candidate for the development of functional foods and nutraceuticals aimed at enhancing antioxidant defenses.

2.3.2 Antimicrobial Activity

G. xanthochymus has demonstrated significant antimicrobial properties, attributed to its diverse phytochemical constituents, including benzophenones, xanthones, and other bioactive compounds. These compounds exhibit inhibitory effects against a range of pathogenic microorganisms, encompassing both bacterial and fungal species.

The antibacterial potential of *G. xanthochymus* has been explored through various studies focusing on different plant parts and extraction methods. For instance, Pruksakorn et al. (2024) isolated benzophenones, including guttiferone E, xanthochymol, isoxanthochymol, and cycloxanthochymol, from the ethyl acetate extract of ripe fruits (Pruksakorn et al., 2024). These compounds exhibited antibacterial activity against *Streptococcus mutans*, with minimum inhibitory concentrations (MICs) ranging from 6.25 to 12.5 µg/mL. Notably, isoxanthochymol and cycloxanthochymol demonstrated lower toxicity profiles, suggesting their potential for therapeutic applications (Pruksakorn et al., 2024). In 2015, Payamalle and Murthy investigated the antibacterial effects of methanolic leaf extracts against *Staphylococcus aureus*, *Bacillus cereus*, and *Escherichia coli* (Payamalle & Murthy, 2015). The extracts showed significant inhibitory activity, with MIC values between 25 and 50 µg/mL. Atomic force microscopy revealed morphological alterations in bacterial cells, including cell size reduction and surface roughness, indicating the extract's impact on bacterial

integrity. A study by Sunkar and Nachiyar in 2012, reported the synthesis of silver nanoparticles using an endophytic Bacillus cereus strain isolated from *G. xanthochymus* (Sunkar & Nachiyar, 2012). These nanoparticles exhibited antibacterial activity against pathogens such as *E. coli*, *Pseudomonas aeruginosa*, *Staphylococcus aureus*, *Salmonella typhi*, and *Klebsiella pneumoniae*, highlighting the plant's potential in nanotechnology-based antimicrobial applications (Sunkar & Nachiyar, 2012).

The antifungal properties of *G. xanthochymus* have been primarily attributed to its benzophenone constituents. In 2015, Jackson and co-workers identified xanthochymol and garcinol as potent antifungal agents against *Candida albicans* biofilms (Jackson et al., 2015). These compounds inhibited germ tube formation and hyphal development, with MICs ranging from 1 to 3 μM. Xanthochymol induced apoptosis in fungal cells, characterized by phosphatidylserine externalization and DNA fragmentation. Moreover, xanthochymol enhanced the efficacy of fluconazole, reducing its EC_{50} from over 1,024 μg/mL to 13 μg/mL, suggesting a synergistic potential in antifungal therapy (Jackson et al., 2015). Beyond specific bacterial and fungal targets, *G. xanthochymus* exhibits a broader antimicrobial spectrum. In addition, Brahma and colleagues conducted a comprehensive analysis of *G. xanthochymus*, revealing significant antimicrobial properties alongside high flavonoid content and antioxidant activity (Brahma et al., 2025). The study supports the plant's potential in developing value-added products with health-promoting benefits (Brahma et al., 2025).

Collectively, these studies underscore the antimicrobial efficacy of *Garcinia xanthochymus*, highlighting its potential as a source of natural antimicrobial agents. The diverse mechanisms of action, ranging from direct microbial inhibition to synergistic effects with existing antibiotics, warrant further exploration for therapeutic applications.

2.3.3 Anti-inflammatory Activity

G. xanthochymus has demonstrated promising anti-inflammatory potential attributed to its diverse phytochemical constituents, including xanthones, benzophenones, and polyphenolic compounds. These compounds modulate key pro-inflammatory mediators and pathways, making the plant a valuable source of natural anti-inflammatory agents.

Hamidon et al. (2016) investigated the anti-inflammatory activity of *G. xanthochymus* root and stem bark extracts using RAW 264.7 murine macrophage cells stimulated with lipopolysaccharide (LPS) (Hamidon et al., 2016). The study employed successive maceration with *n*-hexane, dichloromethane, and methanol to obtain various extracts. Results indicated that all root extracts, along with stem bark dichloromethane and *n*-hexane extracts, significantly reduced nitric oxide (NO) production in a dose-dependent manner, suggesting potential anti-inflammatory properties of these extracts. Winata et al. (2021) evaluated the anti-inflammatory effects of *n*-hexane extracts of *G. xanthochymus* fruit, commonly known as kandis acid, in male white mice (Rattus norvegicus) (Winata et al., 2021). The study administered doses of 200, 400, and 800 mg/kg body weight to different groups of mice, with inflammation induced by carrageenan injection. The extract demonstrated significant anti-inflammatory activity, with the 400 mg/kg dose showing the most effective reduction in paw edema, comparable to the standard drug diclofenac sodium. While specific mechanistic studies on *G. xanthochymus* are limited, research on related species provides valuable insights. For instance, Chantree et al. (2023) studied garcinol, a compound extracted from *G. dulcis*, and its anti-inflammatory effects on LPS-activated THP-1 and RAW 264.7 macrophages. Garcinol inhibited the production of pro-inflammatory cytokines such as TNF-α, IL-6, and IL-1β, and downregulated the NF-kB signaling pathway, indicating its potential as an anti-inflammatory agent. These findings suggest that compounds present in *Garcinia* species, including *G. xanthochymus*, may exert anti-inflammatory effects through modulation of inflammatory mediators and signaling pathways.

Due to its dual antioxidant and anti-inflammatory actions, *G. xanthochymus* has potential applications in managing conditions such as arthritis, metabolic syndrome, and inflammatory bowel disease. However, further *in vivo* studies and clinical trials are essential to validate these effects and elucidate underlying mechanisms.

2.3.4 Antidiabetic Activity

G. xanthochymus has been extensively studied for its antidiabetic properties, attributed to its rich content of xanthones and other bioactive compounds.

In 2017, Nguyen and co-workers isolated two new xanthones, xanthochymusxanthones A and B, along with ten known xanthones from the bark of *G. xanthochymus*. These compounds exhibited significant inhibitory activity against α-

glucosidase and protein tyrosine phosphatase 1B (PTP1B), enzymes involved in glucose metabolism, with IC_{50} values of 0.3 ± 0.1 μg/mL and 2.3 ± 0.4 μg/mL, respectively (Nguyen et al., 2017).

In another study, various extracts from different parts of *G. xanthochymus* fruit were evaluated for α-glucosidase inhibitory activity. The lyophilized peel methanol extract demonstrated the highest inhibitory activity with an IC_{50} value of 21.48 ± 0.02 μg/mL, outperforming the standard acarbose (IC_{50} = 146.77 ± 1.03 μg/mL) (Prakash et al., 2022).

Further research assessed the antidiabetic potential of various fractions from the root, leaf, and fruit of *G. xanthochymus*. The ethyl acetate and n-butanol fractions showed significant α-glucosidase and α-amylase inhibitory activities, with IC_{50} values ranging from 13.01 to 18.60 μg/mL, surpassing the standard acarbose (IC_{50} > 200 μg/mL). Additionally, these fractions enhanced glucose consumption in HepG2 cells, indicating their potential in improving glucose uptake (FU et al., 2014).

Moreover, the traditional use of *G. xanthochymus* in Southeast Asia for managing diabetes has been supported by studies identifying compounds that promote glucose uptake in skeletal cells, comparable to the effects of metformin (Chen et al., 2019).

2.3.5 Lipase Inhibitory Activity

Obesity is a significant risk factor for various metabolic disorders, and pancreatic lipase plays a crucial role in the digestion and absorption of dietary fats. Inhibiting this enzyme can be an effective strategy for managing obesity. Studies have investigated the lipase inhibitory activity of *Garcinia* species, including *G. xanthochymus* (Rahminiwati et al., 2025).

In 2016, Adchara and co-workers evaluated the inhibitory effects of crude extracts from cinnamon and *Garcinia* on digestive enzymes, including lipase (Adchara et al., 2016). While cinnamon extracts significantly inhibited α-amylase and trypsin activities, *Garcinia* extracts specifically inhibited alcohol dehydrogenase activity with an IC_{50} of 43.62 μg/mL. Although this study did not directly assess lipase inhibition by *G. xanthochymus*, it highlights the potential of *Garcinia* species in modulating digestive enzymes.

Further research is needed to isolate and characterize specific compounds from *G. xanthochymus* that exhibit lipase inhibitory activity. Given the presence of bioactive compounds such as hydroxycitric acid in related Garcinia species, it is plausible that *G. xanthochymus* may also possess similar properties.

2.3.6 Cytotoxic and Anticancer Activities

G. xanthochymus has attracted considerable research interest due to its potent cytotoxic and anticancer properties. These effects are attributed to a diverse range of phytochemicals, including prenylated xanthones, benzophenones, polycyclic polyprenylated acylphloroglucinols (PPAPs), and isopentenyl phloroglucinols. These compounds act via various mechanisms, including the induction of apoptosis, inhibition of cell proliferation, and suppression of oncogenic signaling pathways, notably the signal transducer and activator of transcription 3 (STAT3) pathway.

In 2019, Jin and co-workers isolated 26 xanthones from the bark of *G. xanthochymus* and evaluated them against HepG2 (liver), A549 (lung), SGC7901 (gastric), and MCF-7 (breast) cancer cell lines (Jin et al., 2019). Among these, compound 8 showed the most potent antiproliferative activity, with IC_{50} values below 50 μM. The study concluded that xanthones bearing multiple prenyl groups exhibited superior cytotoxicity, highlighting the importance of structural features in their bioactivity (Jin et al., 2019).

Garcixanthochymones F–K, a group of newly isolated PPAPs from *G. xanthochymus* fruits, demonstrated notable antiproliferative activity against several cancer cell lines (SGC7901, A549, HepG2, and MCF-7) with IC_{50} values between 0.89 and 36.98 μM. Notably, compounds **2** and **5** induced apoptosis in MCF-7 cells by inhibiting the STAT3 signaling pathway, a key regulator of cancer cell survival (Xu et al., 2020).

From the seed extract, three new isopentenyl phloroglucinols—garxanthochins A–C were identified using LC-MS-based metabolomics. Among them, garxanthochin B showed moderate cytotoxicity against HL-60, A549, SMMC-7721, MCF-7, and SW480 cancer cell lines, with IC_{50} values ranging from 14.71 to 24.43 μM (Quan et al., 2023).

Extracts from the root and stem bark of *G. xanthochymus* exhibited dose-dependent cytotoxicity against MCF-7 breast cancer cells. Furthermore, the same

extracts displayed anti-inflammatory activity by reducing nitric oxide (NO) production in LPS-stimulated RAW 264.7 macrophages. This dual cytotoxic and anti-inflammatory activity suggests a synergistic therapeutic potential for cancer and inflammation-related diseases (Hamidon et al., 2016).

Collectively, these studies underscore the significant anticancer potential of *Garcinia xanthochymus*, attributed to its diverse phytochemical constituents. The mechanisms of action, including apoptosis induction and inhibition of key oncogenic pathways like STAT3, warrant further investigation to develop novel therapeutic agents derived from this plant.

2.3.7 Nerve Growth Factor (NGF)-Potentiating Activity

Garcinia xanthochymus has demonstrated significant potential in enhancing nerve growth factor (NGF)-mediated neurite outgrowth, a critical process in neuronal development and regeneration.

Bioactivity-guided fractionation of *G. xanthochymus* wood led to the isolation of several prenylated xanthones, notably: 1,4,5,6-tetrahydroxy-7,8-di(3-methylbut-2-enyl)xanthone, 1,2,6-trihydroxy-5-methoxy-7-(3-methylbut-2-enyl)xanthone, and 12b-hydroxy-des-*D*-garcigerrin A (Chanmahasathien et al., 2003). These compounds were structurally elucidated using spectroscopic methods and subsequently evaluated for their ability to potentiate NGF-induced neurite outgrowth in PC12D cells. At concentrations of 10 μM, all three compounds significantly enhanced NGF-mediated neurite extension, indicating their potential as neurotrophic agents (Y. Li & Ohizumi, 2004). Further studies revealed that these prenylated xanthones do not independently induce neurite outgrowth but significantly amplify the effects of suboptimal NGF concentrations. For instance, treatment with 1,3,5,6-tetrahydroxy-4,7,8-tri(3-methyl-2-butenyl)xanthone at 3 μM and garciniaxanthone E at 10 μM increased the proportion of neurite-bearing PC12D cells by 8.3% and 24.9%, respectively, in the presence of 2 ng/mL NGF. These findings suggest that the compounds enhance NGF signaling pathways, possibly by modulating receptor sensitivity or downstream signaling cascades (More et al., 2012).

The NGF-potentiating activity of *G. xanthochymus* compounds positions them as promising candidates for the development of therapeutic agents targeting neurodegenerative disorders such as Alzheimer's disease. By enhancing NGF-mediated

neuronal differentiation and survival, these compounds could contribute to neuroprotection and the restoration of neuronal networks compromised in such conditions (Joseph et al., 2016)

CHAPTER 3

RESEARCH METHODOLOGY

3.1 General Methods

All experiments were carried out using standard analytical and spectroscopic techniques. One-dimensional (1D) ^{1}H and ^{13}C NMR spectra were recorded on a Bruker Avance III 700 MHz Fourier Transform-Nuclear Magnetic Resonance Spectrometer (Sungkyunkwan University, South Korea) and a Bruker Avance NEO 500 MHz spectrometer (Mae Fah Luang University, Chiang Rai, Thailand), with samples dissolved in dimethyl sulfoxide-d_6, chloroform-d_6, acetone-d_6, and methanol-d_4 and chemical shifts expressed in ppm. Analytical thin-layer chromatography (TLC) was performed on pre-coated silica gel 60 F254 aluminum plates (20 × 20 cm, 0.2 mm thickness, Merck, Germany), and spots were visualized under UV light at 254 nm. Preparative HPLC was conducted on a Waters HPLC Alliance 1525 system equipped with a Phenomenex™ Luna C18(2) 100 Å column (250 × 100 mm, 5 µm, Sungkyunkwan University), while circular dichroism (CD) spectra were obtained using a CD spectropolarimeter (Sungkyunkwan University). UHPLC-QTOF analysis was performed on an Agilent 1290 Infinity II system coupled to a 6545B QTOF mass spectrometer with a Dual AJS ESI source in positive ion mode, using an Agilent Poroshell 120 EC-C18 column (2.1 × 150 mm, 2.7 µm particle size) (Mae Fah Luang University). Absorbance for antioxidant assays was measured with a Tecan Infinite M Nano Microplate Reader, and optical density (OD) at 570 nm for cytotoxicity assays was determined using a PerkinElmer EnVision 2105 Multi-Mode Microplate Reader (Mae Fah Luang University). Apoptotic cell detection was assessed by flow cytometry using a DxFLEX flow cytometer (Mae Fah Luang University, Chiang Rai, Thailand). Column chromatography (CC) and quick column chromatography (QCC) were carried out on silica gel 100 (0.063–0.200 mm) and silica gel 60 (0.063–0.230 mm) (Merck, Germany), respectively, with bands detected under short-wavelength UV light, and organic solvents were freshly distilled prior to use.

3.2 Plant Materials and Cell Culture

Dried barks, leaves, and twigs of *Garcinia xanthochymus* Hool.f. were collected from Chiang Rai, Thailand, in November 2017. Human cancer cell lines MDA-MB-231 (breast; HTB-26, American Type Culture Collection (ATCC), Manassas, VA, USA), Huh-7 (liver; JCRB0403, Japanese Collection of Research Bioresources (JCRB), Osaka, Japan), A549 (lung; CCL-185, ATCC), and SW480 (colon; CCL-228, ATCC) were cultured in Dulbecco's modified Eagle medium (DMEM) with 10% fetal bovine serum (FBS) and 1% penicillin-streptomycin solution. The cells were maintained at 37°C in a humidified atmosphere containing 5% CO_2. Subculturing was performed at 90% confluence using standard trypsinization methods. Cell viability and counting were assessed using trypan blue exclusion staining.

3.3 Chemical Investigation of the *Garcinai xanthochymus* Barks

3.3.1 Extraction, Isolation, and Purification

The dried barks (2.10 kg) of *G. xanthichymus* were grind into the small pieces sequentially extracted with hexanes (9 liters for 3 days), dichloromethane (9 liters for 3 days), acetone (9 liters for 7 days), and methanol (9 liters for 7 days) at room temperature, after evaporation, yielding GXBH (17.28 g), GXBD (25.48 g), GXBA (53.94 g), and GXBM (156.80 g) (Figure 3.1).

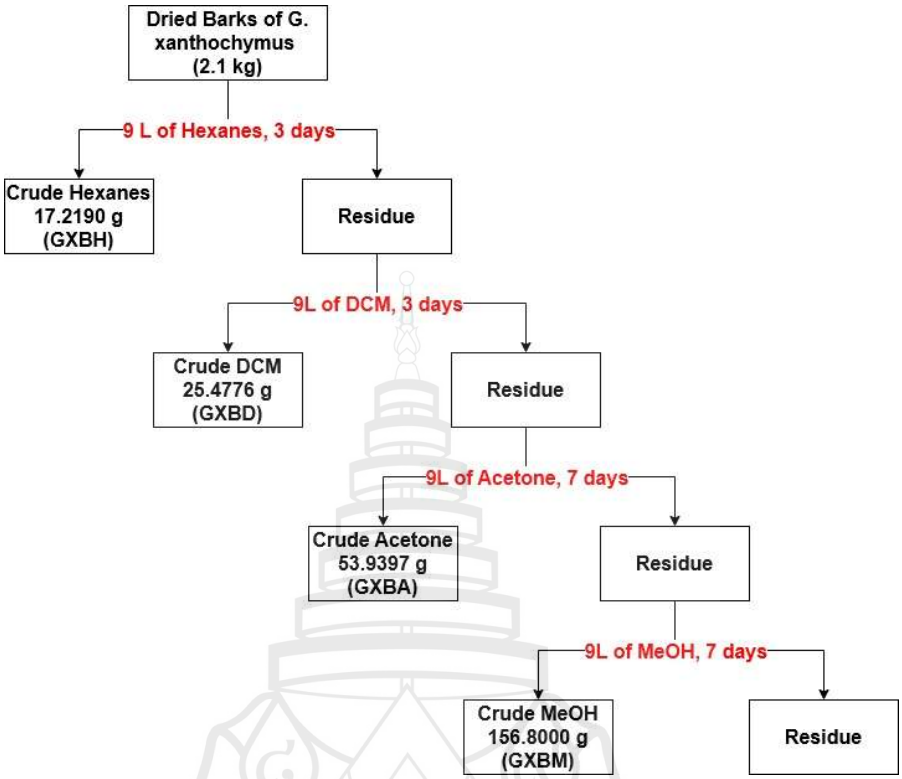

Figure 3.1 Extraction of Crude GXBH, GXBD, GXBA and GXBM Extracts from Bark of *G. xanthochymus*.

The acetone extract (47.0894 g) was subjected to QCC (silica gel 60, 30% Me_2CO/Hexanes to 100% Me_2CO) to give 21 fractions (GXBA1-GXBA21). The collective fractions were characterized by TLC and the physical character of each fraction, as shown in Table 3.1. The selected fraction was further purified as shown in Figure 3.2.

Table 3.1 Extraction of Cude GXBA and its physical characteristic

Fraction	Weight (g)	Physical characteristic
GXBA1	0.0591	Yellow viscous liquid
GXBA2	3.3372	Dark-yellow viscous liquid
GXBA3	0.3304	Dark-brown viscous liquid
GXBA4	0.5264	Dark-brown viscous liquid
GXBA5	0.5028	Dark-brown viscous liquid
GXBA6	0.6050	Dark-brown viscous liquid
GXBA7	0.5679	Dark-brown viscous liquid
GXBA8	0.6645	Dark-brown viscous liquid
GXBA9	1.4608	Dark-brown viscous liquid
GXBA10	1.2077	Dark-brown viscous liquid
GXBA11	5.0338	Dark-brown viscous liquid
GXBA12	3.8975	Grey-brown viscous liquid
GXBA13	3.9789	Dark-brown viscous liquid
GXBA14	0.7781	Black viscous liquid
GXBA15	1.8302	Black viscous liquid
GXBA16	2.3607	Black viscous liquid
GXBA17	3.1892	Dark-brown viscous liquid
GXBA18	2.2727	Black viscous liquid
GXBA19	2.2011	Black viscous liquid
GXBA20	3.4328	Black viscous liquid
GXBA21	6.2362	Black viscous liquid

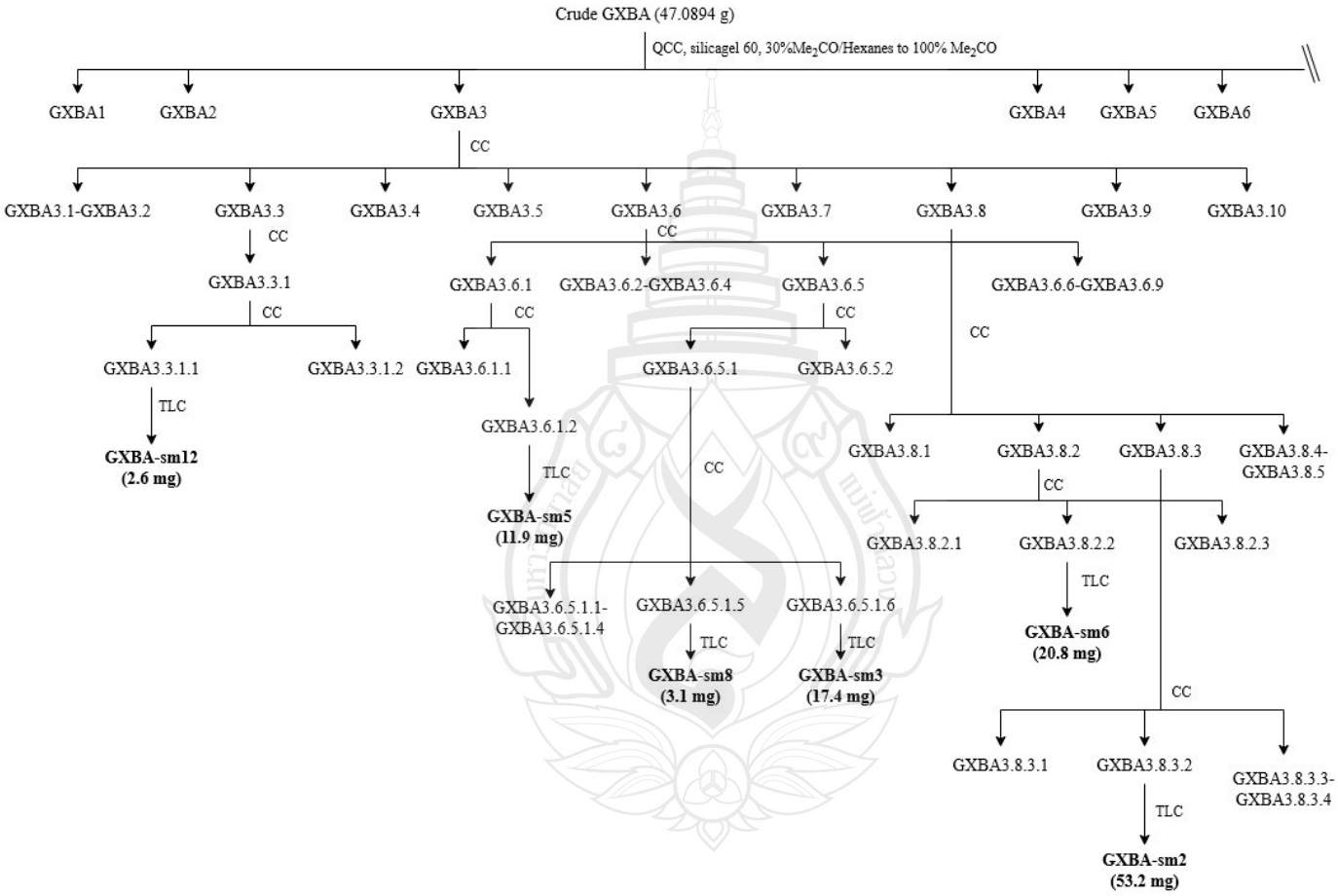

Figure 3.2 Isolation of Pure Compounds from Crude GXBA of *G. xanthochymus*

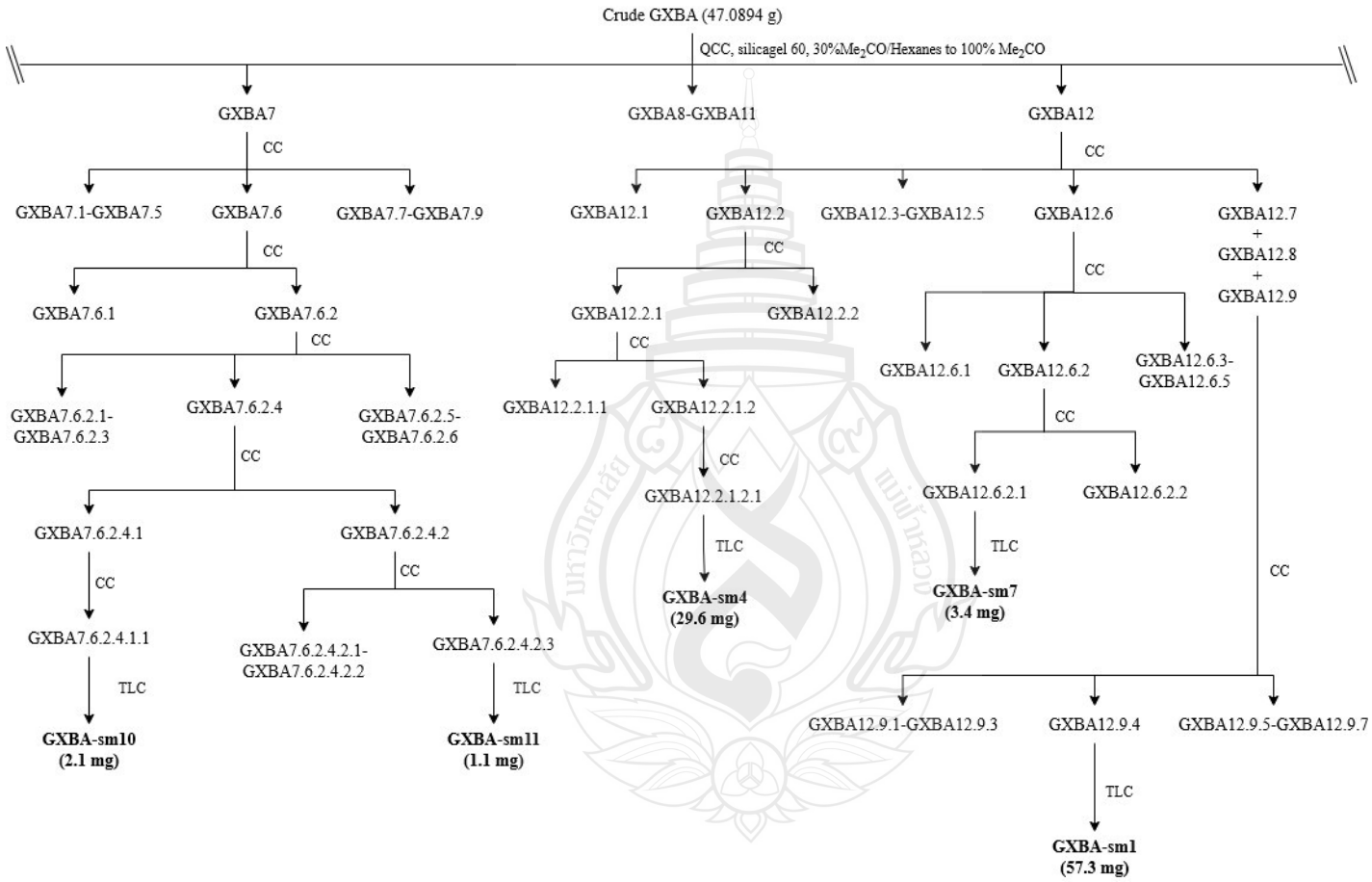

Figure 3.2 (continued)

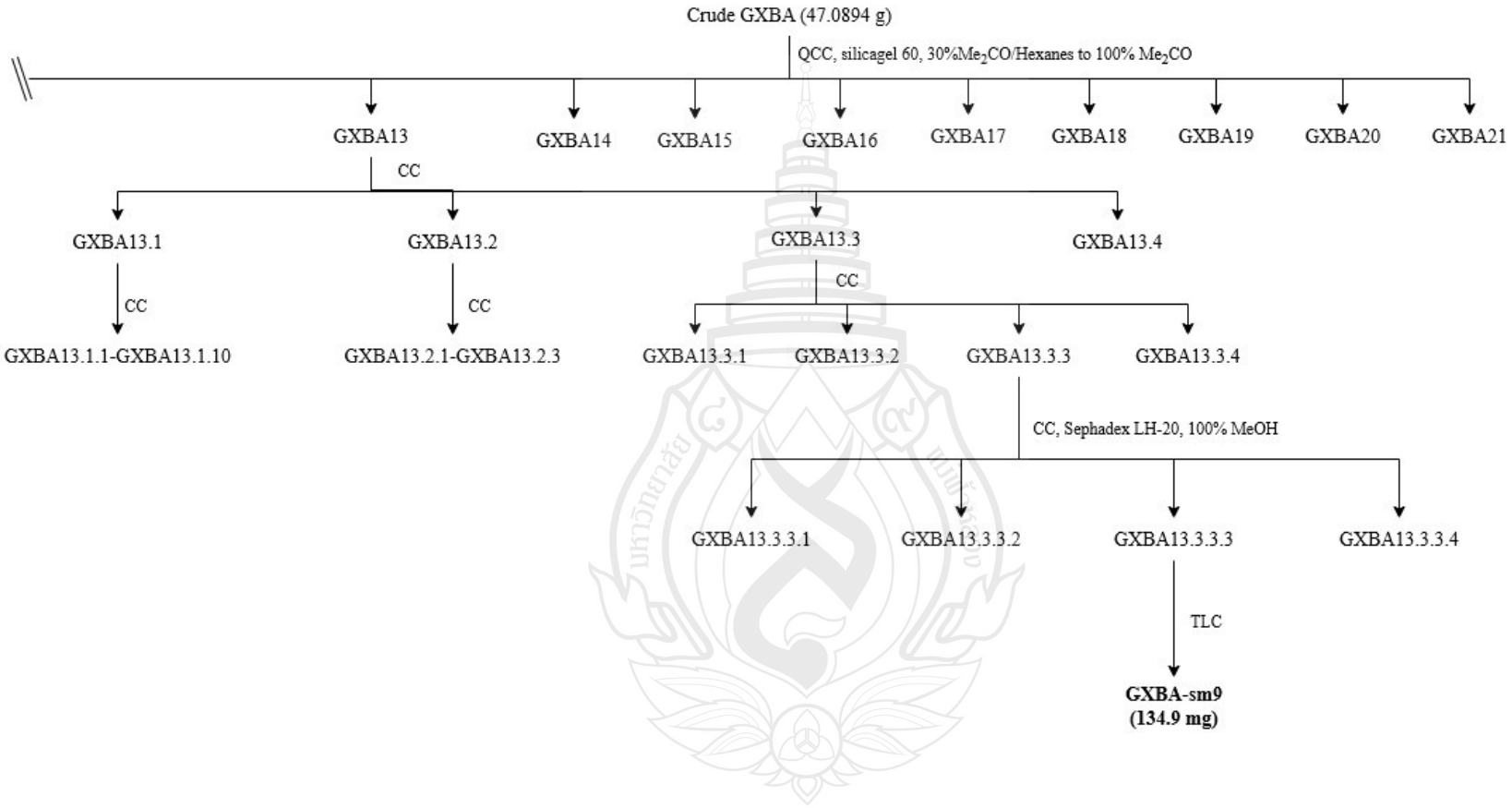

Figure 3.2 (continued)

GXBA3 (0.2779 g) was purified by CC (100%CH_2Cl_2 to 20%Me_2CO/ CH_2Cl_2) to give ten-subfractions (GXBA3.1-GXBA3.10) which GXBA3.3 (0.0546 g) was subject to CC (80%CH_2Cl_2/Hexanes, 3 times) to obtained yellow solid of **GXBA-sm12** (2.6 mg) as a yellow solid. Then subfraction GXBA3.6 (0.0871 g) was purified by CC (100%CH_2Cl_2) to give nine subfractions (GXBA3.6.1-GXBA3.6.9). GXBA3.6.1 (0.0319 g) continued to be purified by being subjected to CC with 3%Me_2CO/ CH_2Cl_2 to give a yellow solid of **GXBA-sm5** (11.9 mg). GXBA3.6.5 (0.0184 g) was subjected to CC (5%Me_2CO/ CH_2Cl_2) to obtain a yellow solid of **GXBA-sm8** (3.1mg) and an orange solid of **GXBA-sm3** (17.4 mg). Fraction GXBA3.8 (0.1470 g) was subjected to CC (100%CH_2Cl_2 to 5%Me_2CO/ CH_2Cl_2) to give five subfractions (GXBA3.8.1-GXBA3.8.5) which GXBA3.8.2 (0.0422 g) was purified by CC using 5%Me_2CO/ CH_2Cl_2 to obtain a yellow solid of **GXBA-sm6** (20.8 mg), and GXBA3.8.3 (0.0857) was subjected to CC (5%Me_2CO/ CH_2Cl_2) to give a pale yellow solid of **GXBA-sm2** (55.2 mg).

Fraction GXBA7 (0.4128 g) was subject to CC (25%Me_2CO/Hexanes) to give nine-subfraction (GXBA7.1-GXBA7.9), which GXBA7.6 (0.1002 g) was purified by CC with 20%Me_2CO/ CH_2Cl_2 to give two subfractions (GXBA7.6.2.4.1 and GXBA7.6.2.4.2) then each fraction was further purified by CC with 10%Me_2CO/ CH_2Cl_2 and 20%Me_2CO/ CH_2Cl_2, respectively, to give yellow solid of **GXBA-sm10** (2.1mg) and **GXBA-sm11** (1.1 mg).

GXBA12 (2.7951 g) was purified by CC (30%Me_2CO/ CH_2Cl_2) to give nine subfractions (GXBA12.1-GXBA12.9), then GXBA12.2 (0.8724 g) was subjected to CC with 10%Me_2CO/ CH_2Cl_2 to 20%Me_2CO/ CH_2Cl_2 to obtain a pale-yellow solid of **GXBA-sm4** (29.6 mg). Fraction GXBA12.6 (0.3227 g) was still further investigated by subjecting it to CC (10%Me_2CO/ CH_2Cl_2) to give five subfractions (GXBA12.6.1-GXBA12.6.5), of which GXBA12.6.2 (0.0189 g) was subjected to CC with 5%Me_2CO/ CH_2Cl_2 to obtain a yellow solid of **GXBA-sm7** (3.4 mg). GXBA12.7, GXBA12.8, and GXBA12.9 (0.7103 g) were combined and subjected to CC with 15%Me_2CO/ CH_2Cl_2 to 30%Me_2CO/ CH_2Cl_2 to obtain an orange-yellow solid of **GXBA-sm1** (57.3 mg).

GXBA13 (1.9512 g) was subjected to CC (30%Me_2CO/CH_2Cl_2) to give four subfractions (GXBA13.1-GXBA13.4). GXBA 13.3 (0.5124 g) was subjected to CC (30%Me_2CO/hexanes to 40%Me_2CO/hexanes) to give four subfractions (GXBA13.3.1-

GXBA13.3.4), of which fraction GXBA13.3.3 (0.1846 g) was subjected to CC with Sephadex-LH20 with 100%MeOH to give a yellow solid of **GXBA-sm9** (134.9 mg).

3.4 Chemical Investigation of the *Garcinai xanthochymus* Twigs

3.4.1 Extraction, Isolation, and Purification

Twigs (7.80 kg) of *G. xanthochymus* were dried at room temperature then chop into small pieces and sequentially extracted by macerated with hexanes (9 liters for 6 days), dichloromethane (9 liters for 6 days), acetone (9 liters for 3 days), and methanol (9 liters for 5 days) at room temperature, after evaporation, yielding GXTH (9.42 g), GXTD (6.11 g), GXTA (70.54 g), and GXTM (125.09 g) as show in Figure 3.3.

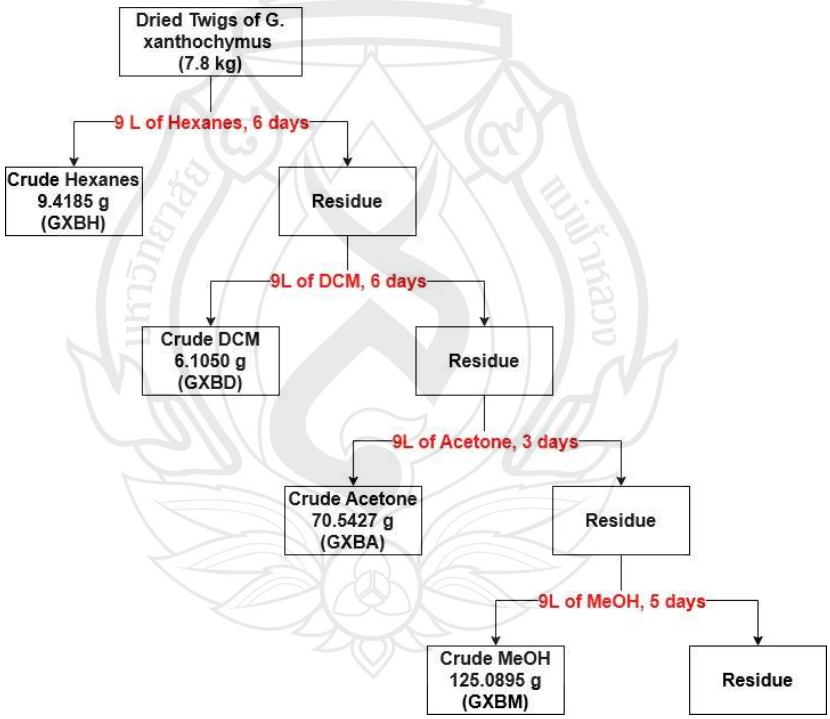

Figure 3.3 Extraction of Crude GXTH, GXTD, GXTA and GXTM Extracts from Twig of *G. xanthochymus*.

The methanol extract (50.1287 g) was purified by subjecting it to QCC (silica gel 60, 30% MeOH/Me_2CO to 100% MeOH) to give 10 fractions (GXTM1-GXTM10). The interested fraction was subject to further purification as shown in Figure 3.4.

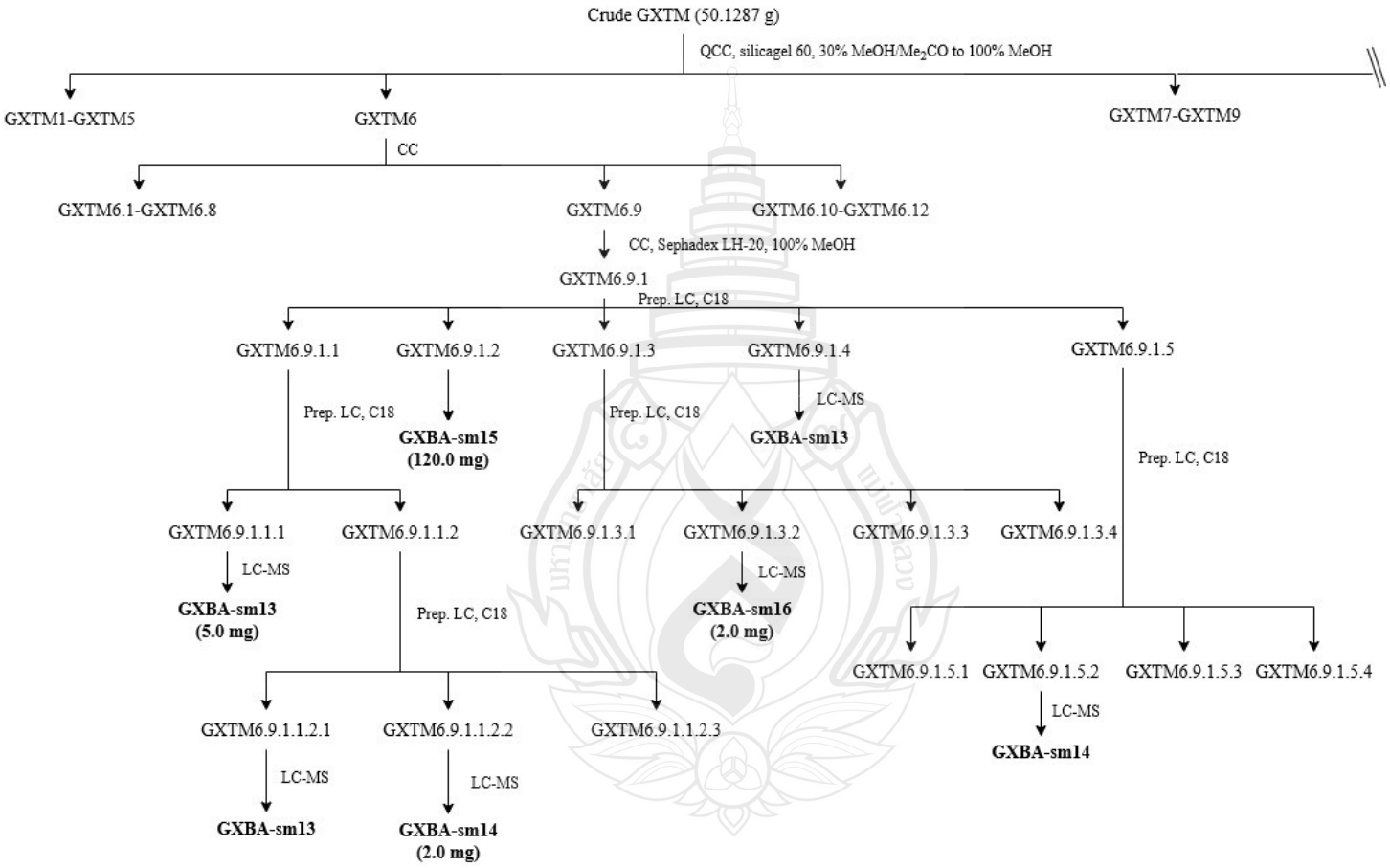

Figure 3.4 Isolation of Pure Compounds from Crude GXTM of *G. xanthochymus*

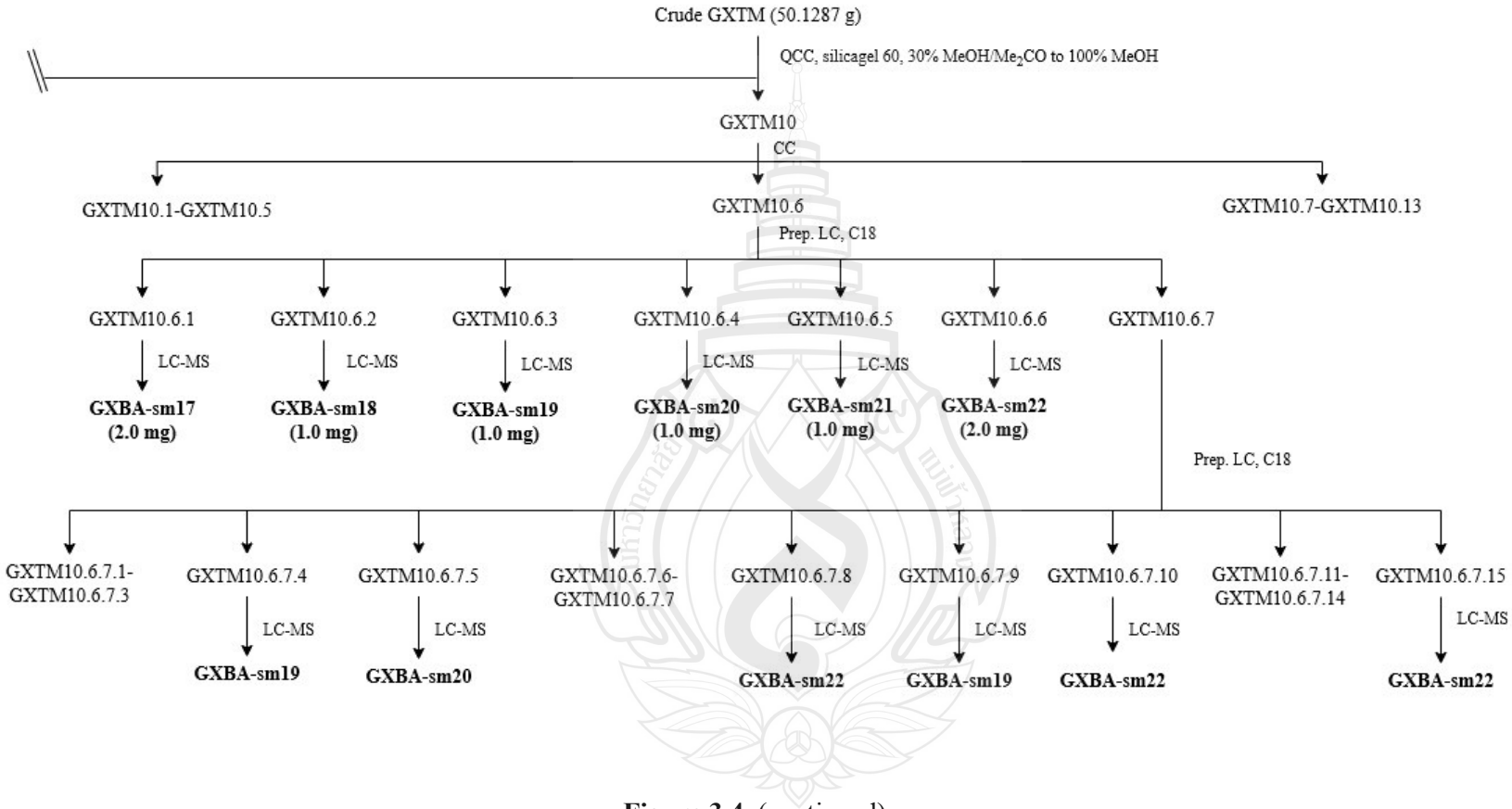

Figure 3.4 (continued)

GXTM6 was purified by CC (18%MeOH/Me_2CO to 40%MeOH/Me_2CO) to give 12 subfractions (GXTM6.1-GXTM6.12), which GXTM6.9 (0.4442 g) was subject to CC (Sephadex LH-20, 100%MeOH) to give GXTM6.9.1 (0.3321 g). Then, GXTM6.9.1 was purified by preparative LC (C18, 20%ACN/H_2O to 50%ACN/H_2O) to give five subfractions (GXTM6.9.1.1-GXTM6.9.1.5), which GXTM6.9.1.2 and GXTM6.9.1.4 obtain as a yellow solid of **GXTM-sm15** (120.0 mg) and **GXTM-sm13**. GXTM6.9.1.1 (0.0442 g) was subjected to preparative LC (C18, 27%ACN/H_2O to 50%ACN/H_2O) to give **GXTM-sm13** (5.0 mg) and subfraction GXTM6.9.1.1.2 (0.0381 g) that purified by preparative LC (C18, 25%ACN/H_2O to 50%ACN/H_2O) to give a white solid of **GXTM-sm14** (2.0 mg). GXTM6.9.1.3 (0.0401 g) was purified by preparative LC (C18, 20%ACN/H_2O to 50%ACN/H_2O) to obtain a white solid of **GXTM-sm16** (2.0 mg) and a subfraction. The fraction GXTM6.9.1.5 (0.0312) was subjected to preparative LC (C18, 20%ACN/H_2O to 100%ACN/H_2O) to obtain **GXTM-sm14** and subfractions.

GXTM10 was purified by CC (30%MeOH/Me_2CO to 100%MeOH) to give 13 subfractions (GXTM10.1-GXTM10.13), which GXTM10.6 was subjected to preparative LC (C18, 15%ACN/H_2O to 50%ACN/H_2O) to obtain a white solid of **GXTM-sm17** (2.0 mg) and **GXTM-sm18** (1.0 mg), and yellow solid of **GXTM-sm19** (1.0 mg), **GXTM-sm20** (1.0 mg), **GXTM-sm21** (1.0 mg), and **GXTM-sm22** (2.0 mg), which also give a subfraction. The subfraction GXTM10.6.7 (54 mg) was subjected to preparative LC (C18, 10%ACN/H_2O to 60%ACN/H_2O) to obtain yellow solids of **GXTM-sm19** (1.0 mg), **GXTM-sm20** (1.0 mg), **GXTM-sm22** (2.0 mg), and other subfraction. All of isolated was confirmed by using LC-MS (C18, 30%ACN/H_2O to 100%ACN/H_2O).

3.5 UHPLC-QTOF Analysis of Crude Extracts

Each extract was dissolved in chromatographic-grade methanol to achieve a final concentration of 0.2 mg/mL. The solutions were then filtered through a 0.22 µm Nylon syringe filter (13 mm diameter) and transferred into 2 mL autosampler vials. Ultra-high-performance liquid chromatography coupled with quadrupole time-of-flight mass spectrometry (UHPLC-QTOF) was performed using an Agilent 1290 Infinity II system coupled to a 6545B QTOF mass spectrometer equipped with a Dual AJS electrospray ionization (ESI) source operating in positive ion mode (Agilent Technologies, Santa Clara, CA, USA). A 1.00 µL aliquot of each sample was injected onto an Agilent Poroshell 120 EC-C18 column (2.1 × 150 mm, 2.7 µm particle size) maintained at 35.0 °C, with a flow rate of 0.2 mL/min. The binary solvent system consisted of mobile phase A (0.1% v/v formic acid in water) and mobile phase B (0.1% v/v formic acid in acetonitrile). The gradient elution profile was programmed as follows: 0–1 min, 95% A; 1–13 min, 83% A; 13–25 min, 5% A; 25–33 min, 95% A. Mass spectrometric data were acquired in AutoMS² mode with fixed collision energies of 10.0, 20.0, and 40.0 V. MS scans were collected in the m/z range of 100–1100 with a scan rate of 3.0 spectra/sec, while MS/MS scans ranged from m/z 50–1100 with the same scan rate. The nebulizer pressure was set to 35 psig, with a drying gas temperature of 300 °C and flow rate of 10 L/min. Sheath gas temperature and flow rate were maintained at 350 °C and 11 L/min, respectively. The fragmentor voltage was set to 175 V, capillary voltage at 3500 V, and nozzle voltage at 1000 V.

3.6 Evaluation of Antioxidative Activity by DPPH assay

Evaluation of antioxidative effects has been carried out by various methods. The DPPH assay is one of the methods used for antioxidant testing on free radical terminator because of the odd electron of DPPH. The DPPH free radical is a dark violet solid. Its solution shows a strong absorption band at 517 nm (in absolute ethanol). The capacity of the substances to donate electrons can be estimated from the degree of loss of color (Blois, 1958). Coexistence of an antioxidant compound (AH) and free radical (DPPH$^{\bullet}$)

leads to the disappearance of DPPH free radical and the appearance of the free radical (A•) as shown in Figure X.

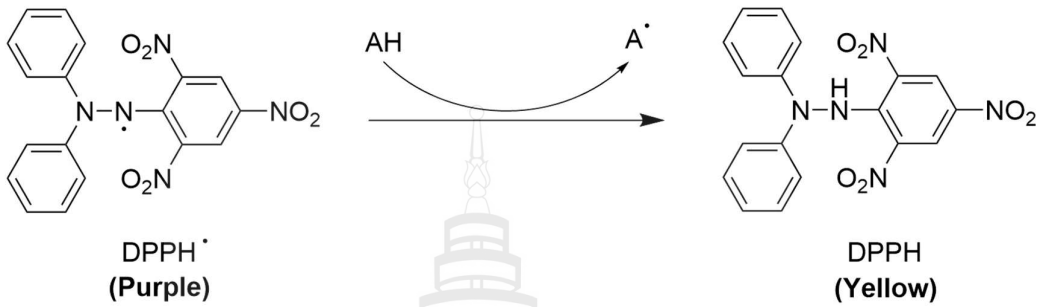

Figure 3.5 DPPH Free Radical and the Appearance of the Free Radical

3.6.1 Screening on the Free Radical Scavenging Activity of the Crude Extracts and Isolated Compounds

Crude extracts and isolated compounds will be dissolved in 10% DMSO in MeOH, and a 0.2 mM DPPH solution will be prepared in ethanol. The solution of each sample will be mixed in 96-wll microtiter plate follow: Control (A), DPPH 100 µL and solvent (MeOH) 100 µL; Blank control (B), solvent (MeOH) 200 µL; Test sample (C), DPPH 100 µL and sample 100 µL; Control sample (D), solvent (MeOH) 100 µLand sample 100 µL then kept in dark condition for 30 min at room temperature. The trapping effect will be assessed by measuring the absorbance of the solution at 517 nm against a 0.2 mM DPPH ethanolic solution after 30 min using a microplate reader. Ascorbic acid and BHT will be used as a positive control. The measurements will be performed at least in triplicate. The percentage of inhibition will be calculated following the equation below.

$$\%\text{inhibition} = \frac{(Abs_A - Abs_B) - (Abs_C - Abs_D)}{Abs_A - Abs_B} \times 100$$

3.6.2 Determination of 50% Inhibition Concentration (IC_{50}) of Crude Extracts and Isolated Compounds

The solution of DPPH (0.2 mM) will be mixed with the sample at various concentrations of a crude extract and isolated compound in mg/mL. The absorbances will be measured at 517 nm for 30 min. The concentration needed to decrease the % inhibition of DPPH solution to 50% inhibition (IC_{50}) will be obtained by analysis using GraphPad Prism software. The measurements will be performed at least in triplicate. The IC_{50} value of crude extract will be reported in µg/mL units, and the isolated compound will be reported in µM units by calculation of equivalent concentration from molar mass (MW).

3.7 Evaluation of Antioxidative Activity by ABTS Assay

A popular technique for assessing the antioxidant capacity of different natural extracts and compounds is the ABTS assay. According to the assay's premise, ABTS reacts with potassium persulfate to produce the ABTS radical cation ($ABTS^{\bullet+}$). When hydrogen-donating antioxidants are present, this persistent blue-green chromophore, which has an absorbance maximum at 734 nm, becomes decolorized. The test sample's antioxidant capacity is closely correlated with the degree of decolorization, which indicates the reduction of $ABTS^{\bullet+}$ to ABTS. IC_{50} values, or the concentration needed to block 50% of the $ABTS^{\bullet+}$ radicals, are a standard way to express the results (Xiao et al., 2019).

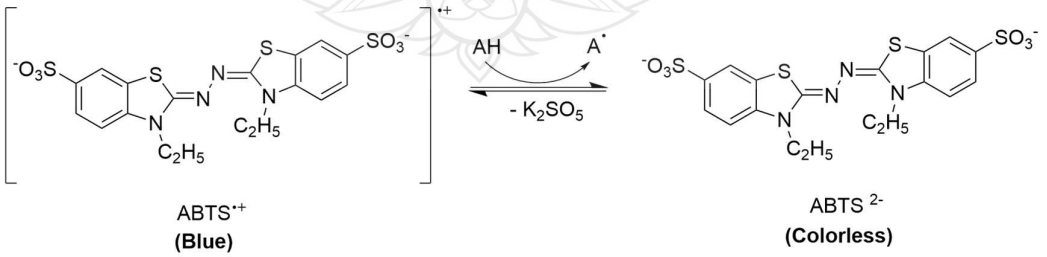

Figure 3.6 Reaction of the ABTS Radical in the Presence of the Antioxidant Compound during the ABTS Assay

3.7.1 Screening on the Free Radical Scavenging Activity of the Crude Extracts and Isolated Compounds

The radical cations of ABST will be mixed with 7 mM aqueous ABTS with 2.45 mM potassium persulphate, then the solution will be kept in dark conditions at room temperature for 16 hr. After incubation, ABTS will be utilized in the range of absorbance 0.700-0.020 at 734 nm by diluting with MeOH. 10% DMSO in MeOH will be used to dissolve the crude extracts and isolated chemicals, creating a solution with a concentration of 1.0 mg/mL. The 96-wll microtiter plate will be filled with each sample's solution as follows: Control (A), 160 µL of ABTS and 40 µL of solvent (MeOH); Blank control (B), 40 µL of solvent (MeOH); Test sample (C), 160 µL of ABTS and 40 µL of sample; Control sample (D), 160 µL of solvent (MeOH) and 40 µL of sample then incubated for 4 min in dark. The absorbance of the solution at 734 nm will be used to measure the radical-scavenging activity using a microplate reader. BHT and ascorbic acid will serve as positive controls. At least three duplicates of the measurements will be taken. The following equation, as the DPPH assay, will be used to determine the percentage of inhibition.

$$\%\text{inhibition} = \frac{(Abs_A - Abs_B) - (Abs_C - Abs_D)}{Abs_A - Abs_B} \times 100$$

3.7.2 Determination of 50% Inhibition Concentration (IC_{50}) of Crude Extracts and Isolated Compounds

The sample will be combined with the ABTS solution at different concentrations of crude extract and isolated compound in mg/mL. At 734 nm, the absorbances will be measured. GraphPad Prism software will be used for analysis in order to determine the concentration required to reduce the percentage inhibition of ABTS solution to 50% inhibition (IC_{50}). At least three duplicates of the measurements will be taken. By calculating the equivalent concentration from molar mass (MW), the isolated compound will be reported in µM units, while the crude extract's IC_{50} value will be reported in µg/mL units.

3.8 Evaluation of Antioxidative Activity by FRAP Assay

An established technique for assessing the reducing potential of antioxidants in biological materials is the Ferric Reducing Antioxidant Power (FRAP) assay. The idea behind the assay is that the test sample's antioxidants break down the Fe^{3+}-TPTZ (ferric-tripyridyltriazine) complex into its ferrous form, Fe^{2+}, which produces a vivid blue hue that can be measured at 593 nm. The sample's reducing power and, consequently, its antioxidant capacity are closely correlated with the increase in absorbance. To preserve iron solubility, the test is usually carried out in an acidic environment (pH 3.6) (Duangyod et al., 2014).

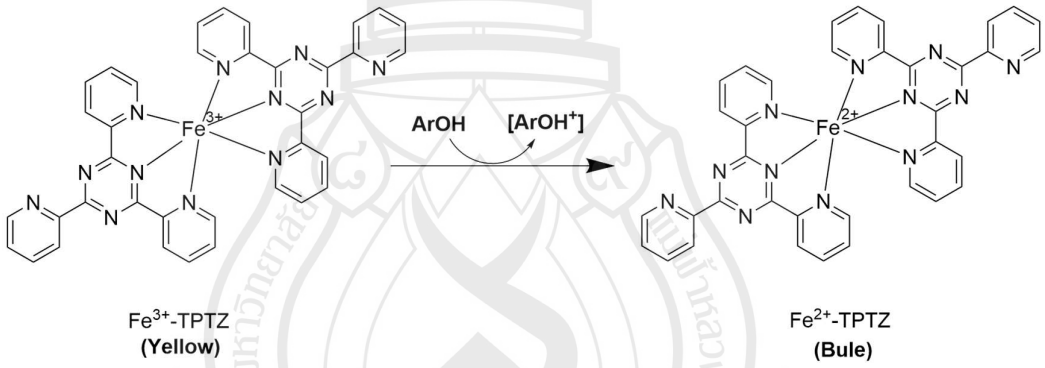

Figure 3.7 The Mechanism of Ferric Reducing Antioxidant Power (FRAP) Reaction

3.8.1 Screening on the Free Radical Scavenging Activity of the Crude Extracts and Isolated Compounds

Crude extracts and isolated compounds will be dissolved with 10% DMSO in MeOH. The FRAP solution will be prepared freshly before use by mixing the following: 100 mL of 300 mM acetate buffer (pH 3.6), 10 mL of 10 mM (TPTZ) solution prepared in 40 mM HCl, and 10 mL of 20 mM ferric chloride hexahydrate ($FeCl_3 \cdot 6H_2O$) solution. The freshly prepared FRAP reagent will be incubated in a water bath at 37 °C for 15 min before being use in the assay. The assay will be conducted in 96-well microplate format. Four sets of well will be prepared as follow: Control (A), 190 µL of FRAP reagent and 10 µL of solvent (MeOH); Blank control (B), 200 µL of

solvent (MeOH); Test sample (C), 190 µL of FRAP reagent and 10 µL of sample; Control sample (D), 190 µL of solvent (MeOH) and 10 µL of sample. All wells will be incubated at room temperature in the dark for 30 min. The absorbance will then be measured at 593 nm using a microplate reader. The measurements will be performed at least in triplicate. The percentage of inhibition will be calculated using the following equation:

$$\%\text{inhibition} = \frac{(Abs_C - Abs_D) - (Abs_A - Abs_B)}{Abs_C - Abs_D} \times 100$$

3.8.2 Determination of 50% Inhibition Concentration (IC_{50}) of Crude Extracts and Isolated Compounds

The sample will be combined with the FRAP reagent at different concentrations of crude extract and isolated compound in mg/mL. At 593 nm, the absorbances will be measured. The IC_{50} value, which represents the concentration of extract required to achieve 50% inhibition, was determined using linear regression analysis with GraphPad Prism software. At least three duplicates of the measurements will be taken. By calculating the equivalent concentration from molar mass (MW), the isolated compound will be reported in µM units, while the crude extract's IC_{50} value will be reported in µg/mL units. The IC_{50} value, which represents the concentration of extract required to achieve 50% inhibition, was determined using linear regression analysis with GraphPad Prism software.

3.9 Cytotoxicity Effect by MTT Assay

Anti-cancer effect of hexanes, dichloromethane, acetone and methanolic crude extract and isolated compound from G. xanthochymus will be studied based on the cytotoxicity against human cancer cell line from different origins including breast cancer cell line (MDA-MB-231 cells, ATCC ® HTB-26 ™), hepatocellular carcinoma cell line (Huh-7 cells, JCRB0403), colon cancer cell line (SW480 cells, ATCC-CCL-228) and non-small cell lung carcinoma cell line (A549 cells, ATCC CRM-CCL-185)

using standard 3-[4,5-dimethylthiazol-2-yl]-2,5 diphenyl tetrazolium bromide (MTT assay) with modification. (van Meerloo et al., 2011).

3.9.1 Determination of Cytotoxicity of Hexanes, Dichloromethane, Acetone and Methanolic Crude Extract and Isolated Compound from *G. xanthochymus* Against Four Human Cancer Cell Lines

Cells will be seeded into a 96-well culture plate at a density of 2×10^4 cells/well (in triplicate wells) with a total volume of 100 µL and incubated at 37 °C in a 5% CO_2 incubator for 24 hours. After incubation, the old medium will be aspirated, and the cells will be treated with 100 µL of complete medium containing either hexanes, dichloromethane, acetone and methanolic crude extract at final concentrations of 200, 100, 50, 25, and 12.5 µg/mL or isolated compounds at final concentrations of 100, 50, 25, 12.5, 6.25, 3.125, 1.5625, and 0.7812 µM. Complete medium without extract or compound and medium containing 1% v/v DMSO will be included as media and vehicle controls, respectively. The treatment will be carried out by incubating the cells for 72 hours at 37 °C in a 5% CO_2 incubator. Subsequently, 10 µL of MTT solution (5 mg/mL) will be added to each well, and the incubation will continue for 1 hour at 37 °C. The reaction mixture will then be aspirated, and the formazan crystals will be dissolved in 100 µL of DMSO. Cell cytotoxicity will be determined by measuring the optical density (OD) at 570 nm using a microplate reader. The cell viability for each treatment will be calculated relative to the OD of the media control, which will be set as 100%.

3.9.2 Determination of 50% Inhibition Concentration (IC_{50}) of Crude Extracts and Isolated Compounds

The cell viability will be presented as a bar graph, and the 50% inhibitory concentration (IC_{50}) will be calculated using linear regression analysis with GraphPad Prism software.

3.10 Apoptosis Assay

In this study, apoptosis was assessed using the Annexin V-FITC Apoptosis Detection Kit, which leverages the binding affinity of Annexin V for phosphatidylserine (PS) exposed on the outer leaflet of the plasma membrane during early apoptosis. This method allows for the reliable differentiation between apoptotic and non-apoptotic cells through flow cytometry and fluorescence microscopy.

The apoptosis assay was conducted using the Annexin V-FITC Apoptosis Staining/Detection Kit (ab14085, Abcam, Cambridge, UK) as described previously (Aluksanasuwan, Somsuan, Chiangjong, et al., 2024; Aluksanasuwan, Somsuan, Ngoenkam, et al., 2024). Briefly, MDA-MB-231, Huh-7, A549, and SW480 cells (2×10^5 cells/well) were seeded into 24-well culture plates and incubated for 24 h. Thereafter, the cells were treated with 100 μg/mL of GXBH for 96 h. After treatment, the cells were collected by trypsinization and washed with PBS. The cells were stained with annexin V-FITC and PI solution and analyzed using the DxFLEX flow cytometer (Beckman Coulter Inc., IN, USA). The percentages of viable cells (Annexin V^- / PI^-; Q4 quadrant), early apoptotic cells (Annexin V^+ / PI^-; Q3 quadrant), late apoptotic/necrotic cells (Annexin V^+ / PI^+; Q2 quadrant), and necrotic cells (Annexin V^- / PI^+; Q1 quadrant) were quantified using the CytExpert for Dxflex software (Beckman Coulter Inc.).

3.11 Colony-Forming Capability by Clonogenic Assay

MDA-MB-231, Huh-7, A549, and SW480 cells (2×10^4 cells/well) were seeded in 96-well plates and incubated for 24 h. Cells were treated with 100 μg/mL of GXBH for 96 h, followed by trypsinization and cell counting. Viable cells (1×10^3 for MDA-MB-231 and 5×10^3 for the other cell lines) were transferred to 12-well plates and incubated for colony formation (3 days for Huh-7 and 4 days for the other cell lines). The colonies were fixed with cool methanol, stained with 0.5% crystal violet overnight, photographed, and analyzed using ImageJ software (National Institutes of Health, Bethesda, USA).

CHAPTER 4

RESULTS AND DISCUSSION

4.1 Structural Elucidation of Isolated Compound from *G. xanthochymus*

The isolated compounds from *G. xanthochymus* were classified into five major groups, including xanthones, flavonoids, phenolic acids, anthraquinones, and other polyphenolic derivatives. Their structures were elucidated primarily by detailed interpretation of ^{1}H spectra, in combination with spectroscopic techniques such as circular dichroism (CD), which provided a major conformer of bioflavonoids essential for determining substitution patterns and interflavonoid linkages.

4.1.1 Xanthones and Derivatives

Xanthones represented the largest group of isolated compounds, including formoxanthone C (**GXBA-sm1**, (Boonsri et al., 2006)), euxanthone (**GXBA-sm2**, (Pinto et al., 2011)), pyranojacareubin (**GXBA-sm3**, (Shen et al., 2005)), 7-geranyloxy-1,3-dihydroxyxanthone (**GXBA-sm4**, Boonnak et al., 2009), and several hydroxylated and methoxylated analogues (**GXBA-sm7** (6-hydroxy-2,3-dimethoxyxanthone), **GXBA-sm8** (xanthone V1, Botta et al., 1986), **GXBA-sm10 (**morusignin I, Nomura et al., 1993), **GXBA-sm11** (dulxanthone B, Ito et al., 1997), **GXBA-sm12** (1,5-dihydroxy-3-methoxyxanthone, Iinuma et al., 1995), **GXTM-sm19** (2,5-dihydroxy-1-methoxyxanthone, Minami et al., 1996), **GXTM-sm20** (2,6-dihydroxy-1,5-dimethoxyxanthone, Minami et al., 1994), **GXTM-sm21** (1,2,5-trihydroxyxanthone, Wollenweber et al., 1994) , **GXTM-sm22** (1,2,5-trihydroxy-6-methoxyxanthone, F. F. Zhong et al., 2008)). The ^{1}H NMR data collectively confirm that all isolated compounds share the xanthone core structure and differ principally by substituent groups (prenyl/pyran, geranyl, methoxy and free hydroxyl) that predictably perturb chemical shifts and multiplicities. For example, formoxanthone C (**GXBA-sm1**) displays the classic chelated 1-OH singlet at δ 13.40 and two A-ring aromatic resonances (*ortho*-coupled pattern) together with resonances for isoprenyl methyl and allylic/methylene

protons, consistent with a prenylated xanthone framework; pyranojacareubin (**GXBA-sm3**) shows additional olefinic and downfield aromatic signals and distinct singlets in the δ 5–7 ppm region that are diagnostic of a fused pyran ring (pyran protons and associated deshielding of adjacent aromatic positions) (Table 4.1). Euxanthone (**GXBA-sm2**) and related derivatives (**GXBA-sm4**) retain the xanthone aromatic pattern but differ by an alkoxy/geranyloxy side chain (evidenced by olefinic protons at δ 5.47 (1H, *t*, *J* = 7.7 Hz, H-2′) and δ 5.09 (1H, *t*, *J* = 8.4 Hz, H-6′) ppm, multiple methylene/allylic signals and the characteristic *gem*-dimethyl singlets of geranyl units), while the heavily hydroxylated and methoxylated analogues (**GXBA-sm7, sm8, sm11, sm12** and **GXTM-sm19** to **GXTM-sm22**) show diagnostic phenolic OH resonances (broad singlets at δ 9–13 ppm) and signal of methoxy protons singlets near δ 3.8 ppm that track O-methylation sites (Table 4.2). Substitution pattern differences are reflected consistently across the series: *ortho*/*para* substitution on the xanthone rings gives rise to the observed *ortho J* value around 7.8–9.0 Hz aromatic as a doublet, *meta*-couplings ($J \approx 2$ Hz) (Table 4.3) for isolated A-ring protons, and broadened signals where exchangeable phenols engage in intramolecular hydrogen bonding. In summary, the NMR fingerprints establish a conserved xanthone scaffold diversified by prenyl/pyran formation, geranylation and O-methylation/hydroxylation, with each modification producing the expected chemical-shift shifts, multiplicity changes and OH exchange behavior that allow unambiguous differentiation among the isolated compounds.

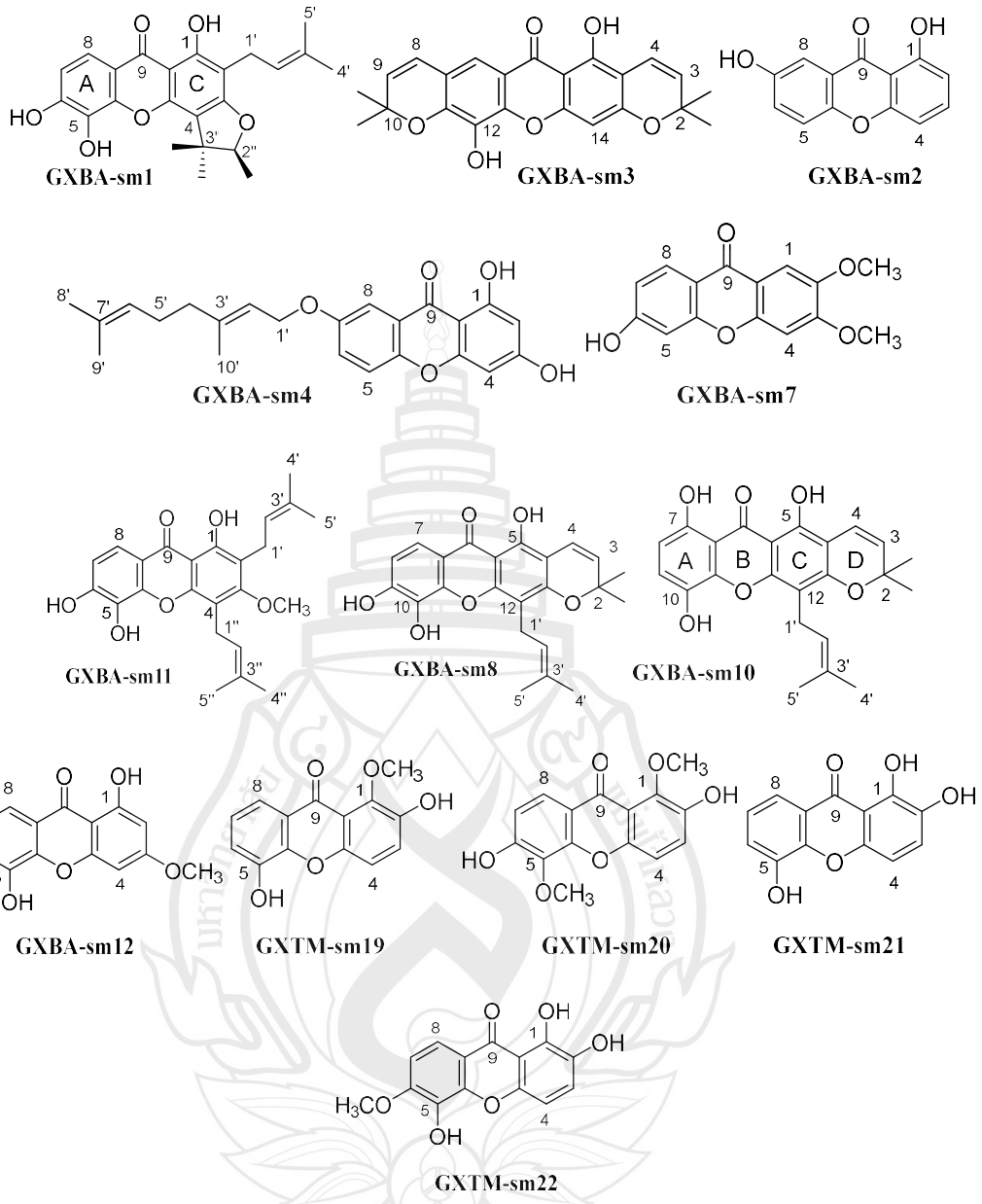

Figure 4.1 Compound Isolated from *G. xanthochymus* (xanthones)

Table 4.1 The ^{1}H NMR spectra data of **GXBA-sm1**, **GXBA-sm2**, **GXBA-sm3**, and **GXBA-sm4**

Position	δ in ppm and J value in Hz (300 MHz, $CDCl_3$)		Position	δ in ppm and J value in Hz (500 MHz, $(CD_3)_2CO$)	
	GXBA-sm1	GXBA-sm3		GXBA-sm2	GXBA-sm4
3	-	5.54 (1H, *d*, *J* = 10.0)	2	6.99 (1H, *d*, *J* = 8.5, 1.0)	6.24 (1H, *d*, *J* = 2.0)
4	-	6.82 (1H, *d*, *J* = 10.0)	3	7.69 (1H, *t*, *J* = 8.5)	-
7	6.92 (1H, *d*, *J* = 7.7)	7.41 (1H, *s*)	4	6.76 (1H, *d*, *J* = 8.5, 1.0)	6.36 (1H, *d*, *J* = 2.0)
8	7.74 (1H, *d*, *J* = 7.7)	6.38 (1H, *d*, *J* = 10.0)	5	7.51 (1H, *d*, *J* = 9.0)	7.34 (1H, *d*, *J* = 9.0)
9	-	5.67 (1H, *d*, *J* = 10.0)	6	7.42 (1H, *dd*, *J* = 9.0, 3.0)	7.40 (1H, *dd*, *J* = 9.0, 3.0)
14	-	6.19 (1H, *s*)	8	7.59 (1H, *d*, *J* = 3.0)	7.52 (1H, *d*, *J* = 3.0)
1′	3.31 (1H, *d*, *J* = 6.9)	-	1′	-	4.68 (2H, *d*, *J* = 7.7)
2′	5.29 (2H, *m*)	-	2′	-	5.47 (1H, *t*, *J* = 7.7)
4′	1.69 (3H, *s*)	-	4′	-	2.11 (2H, *m*)
5′	1.79 (3H, *s*)	-	5′	-	2.09 (2H, *m*)
2″	4.54 (1H, *q*, *J* = 6.3)	-	6′	-	5.09 (1H, *t*, *J* = 8.4)
1-OH	13.40 (1H, *s*)	-	8′	-	1.58 (3H, *s*)
5-OH	-	13.00 (1H, *s*)	9′	-	1.61 (3H, *s*)
2-$(CH_3)_2$	-	1.47 (6H, *s*)	10′	-	1.80 (3H, *s*)
10-$(CH_3)_2$	-	1.49 (6H, *s*)	1-OH	12.71 (1H, *s*)	12.92 (1H, *s*)
2″-CH_3	1.43 (3H, *d*, *J* = 6.3)	-	3-OH	-	9.85 (1H, *br s*)

Table 4.1 (continued)

Position	δ in ppm and J value in Hz (300 MHz, $CDCl_3$)		Position	δ in ppm and J value in Hz (500 MHz, $(CD_3)_2CO$)	
	GXBA-sm1	GXBA-sm3		GXBA-sm2	GXBA-sm4
3″-$(CH_3)_2$	1.32 (3H, *s*) 1.58 (3H, *s*)	-		-	-

Table 4.2 The ^{1}H NMR spectra data of **GXBA-sm7**, **GXBA-sm8**, **GXBA-sm11**, and **GXBA-sm10**

Position	δ in ppm and J value in Hz		Position	δ in ppm and J value in Hz (500 MHz, $(CD_3)_2CO$)	
	GXBA-sm7 (300 MHz, $(CD_3)_2CO$)	GXBA-sm11 (500 MHz, $CDCl_3$)		GXBA-sm8	GXBA-sm10
1	7.46 (1H, *s*)	-	3	5.73 (1H, *d*, *J* = 10.0)	5.65 (1H, *d*, *J* = 10.0 Hz)
4	7.16 (1H, *s*)	-	4	6.69 (1H, *d*, *J* = 10.0)	6.71 (1H, *d*, *J* = 10.0 Hz)
5	6.83 (1H, *d*, *J* = 2.0)	-	6	-	-
7	6.88 (1H, *dd*, *J* = 8.7, 2.0)	6.69 (1H, *d*, *J* = 8.8)	7	7.64 (1H, *d*, *J* = 8.7)	-
8	8.00 (1H, *d*, *J* = 8.7)	7.76 (1H, *d*, *J* = 8.8)	8	7.00 (1H, *d*, *J* = 8.7)	6.67 (1H, *d*, *J* = 9.0 Hz)
1′	-	3.41 (1H, *d*, *J* = 6.8)	9	-	7.23 (1H, *d*, *J* = 9.0 Hz)
2′	-	5.27 (2H, *m*)	1′	3.56 (1H, *d*, *J* = 7.4)	3.47 (2H, *d*, *J* = 7.0 Hz)
4′	-	1.70 (3H, *s*)	2′	5.30 (1H, *d*, *J* = 7.4)	5.21 (2H, *m*)
5′	-	1.81 (3H, *s*)	4′	1.65 (3H, *s*)	1.71 (3H, *br s*)
1″	-	3.56 (1H, d, *J* = 6.0)	5′	1.86 (3H, *s*)	1.86 (3H, *br* s)
2″	-	5.27 (2H, *m*)	2-$(CH_3)_2$	1.49 (6H, *s*)	1.49 (6H, *s*)
3″	-	1.70 (3H, *s*)	5-OH	13.55 (1H, *s*)	12.24 (1H, *s*)
4″	-	1.89 (3H, *s*)	7-OH	-	11.23 (1H, *s*)
1-OH	-	13.05 (1H, *s*)			

Table 4.2 (continued)

Position	δ in ppm and J value in Hz		Position	δ in ppm and J value in Hz (500 MHz, $(CD_3)_2CO$)	
	GXBA-sm7 (300 MHz, $(CD_3)_2CO$)	GXBA-sm11 (500 MHz, $CDCl_3$)		GXBA-sm8	GXBA-sm10
2-OMe	3.92 (3H, *s*)	-			
3-OMe	3.85 (3H, *s*)	3.80 (3H, *s*)			

Table 4.3 The ^{1}H NMR spectra data of **GXBA-sm12**, **GXTM-sm19**, **GXTM-sm20**, **GXTM-sm21** and **GXTM-sm22**

Position	**δ in ppm and J value in Hz (500 MHz, $(CD_3)_2CO$)**	**δ in ppm and J value in Hz (700 MHz, DMSO-d_6)**			
	GXBA-sm12	**GXTM-sm19**	**GXTM-sm20**	**GXTM-sm21**	**GXTM-sm22**
2	6.57 (1H, *d*, *J* = 2.2)	-	-	-	-
3	-	7.38 (1H, *d*, *J* = 9.0)	7.33 (1H, *d*, *J* = 9.0)	6.99 (1H, *d*, *J* = 8.9)	7.27 (1H, *d*, *J* = 8.9)
4	6.36 (1H, *d*, *J* = 2.2)	7.29 (1H, *d*, *J* = 9.0)	7.28 (1H, *d*, *J* = 9.0)	7.34 (1H, *d*, *J* = 8.9)	6.98 (1H, *d*, *J* = 8.9)
6	7.68 (1H, *dd*, *J* = 7.9, 1.6)	7.24 (1H, *dd*, *J* = 7.8, 1.6)	-	7.34 (1H, *dd*, *J* = 7.8, 1.5)	-
7	7.30 (1H, *t*, *J* = 7.9)	7.19 (1H, *t*, *J* = 7.8)	6.92 (1H, *d*, *J* = 8.8)	7.26 (1H, *t*, *J* = 7.8)	6.99 (1H, *d*, *J* = 8.9)
8	7.37 (1H, *dd*, *J* = 7.9, 1.6)	7.54 (1H, *dd*, *J* = 7.8, 1.6)	7.72 (1H, *d*, *J* = 8.8)	7.60 (1H, *dd*, *J* = 7.8, 1.5)	7.78 (1H, *d*, *J* = 8.9)
1-OH	12.92 (1H, *s*)	-	-	12.51 (1H, *s*)	12.72 (1H, *br s*)
2-OH	-	9.47 (1H, *s*)	10.57 (1H, *s*)	10.50 (1H, *s*)	-
5-OH	-	10.30 (1H, *s*)	-	9.36 (1H, *s*)	9.31 (1H, *br s*)
6-OH	-	-	9.43 (1H, *s*)	-	-
1-OMe	-	3.80 (3H, *s*)	3.78 (3H, *s*)	-	-
3-OMe	3.96 (3H, *s*)	-	-	-	-

Table 4.3 (continued)

Position	δ in ppm and J value in Hz (500 MHz, $(CD_3)_2CO$)	δ in ppm and J value in Hz (700 MHz, DMSO-d_6)			
	GXBA-sm12	**GXTM-sm19**	**GXTM-sm20**	**GXTM-sm21**	**GXTM-sm22**
5-OMe	-	-	3.88 (3H, *s*)	-	-
6-OMe	-	-	-	-	3.89 (3H, *s*)

4.1.2 Flavonoids & Biflavonoids

Three flavonoid-based compounds were identified: Kaempferol (**GXBA-sm6**, Milenković et al., 2019), *(2R,3S)*-morelloflavone (**GXBA-sm9**, Li et al., 2002), GB-2a (**GXTM-sm13**, Ansari et al., 1976), GB-1 (**GXTM-sm14**, Kapadia et al., 1994), and *(2S,2'S,3R)*-GB-1a (**GXTM-sm15**, Kapadia et al., 1994), and volkensiflavone (**GXTM-sm16**, Ansari et al., 1976). The ^{1}H NMR data (Table 4.4) support clear structural relationships among the three isolated flavonoids: **GXBA-sm6** (kaempferol) displays the diagnostic A-ring *meta*-coupled protons H-6 and H-8 at δ 6.27 (*d*, *J* = 2.1 Hz) and δ 6.53 (*d*, *J* = 2.1 Hz) together with an AA′BB′ pattern for a *para*-disubstituted B-ring at δ 8.15 (2H, *d*, *J* = 9.0 Hz) and δ 7.01 (2H, *d*, *J* = 9.0 Hz), and it lacks any H-2/H-3 resonances, consistent with a monomeric flavonol (no flavanone subunit) (Table 4.4). By contrast, **GXBA-sm9** (*(2R,3S)*-morelloflavone) and **GXTM-sm16** (volkensiflavone) both show the characteristic mutually coupled H-2/H-3 pair of a flavanone moiety (GXBA-sm9; δ 5.75, *d*, *J* = 12.0 Hz and 4.82, *d*, *J* = 12.0 Hz and GXTM-sm16; δ 5.66, *d*, *J* = 12.0 Hz and 5.48, *d*, *J* = 12.0 Hz), indicating a diastereomeric (*2R,3S*) flavanone subunit and confirming their biflavonoid nature. Each biflavonoid also contains at least one para-disubstituted aromatic system (AA′BB′ patterns near δ 7.10 (2H, *d*, *J* = 8.6 Hz), δ 6.43 (2H, *d*, *J* = 8.6 Hz) in sm9 and δ 7.06 (2H, *d*, *J* = 8.0 Hz), δ 6.66 (2H, *d*, *J* = 8.0 Hz) in sm16). In additional isolated aromatic singlets and 1,2,4-trisubstituted patterns arising from the second flavonoid unit; these extra aromatic signals and the downfield shifts relative to kaempferol reflect extended conjugation and differing points of interflavonoid linkage. The broader A-ring resonances observed in **GXTM-sm16** (broadened H-6/H-8) suggest stronger phenolic hydrogen-bonding or exchange compared with **GXBA-sm9**, accounting for subtle chemical-shift differences between the two biflavonoids. In contrast, **GXTM-sm13** to **GXTM-sm15** each show the mutual doublet pair at δ 5.4–5.7 and δ 4.6–5.2 (J ≈ 12.0 Hz), diagnostic of H-2/H-3 of a flavanone (saturated C-2/C-3) subunit and therefore indicate flavanone-type connectivity in these derivatives; their aromatic regions are highly substituted and congested (multiple overlapping *doublets* and *singlets* in the 6.0–7.5 ppm range), reflecting several *para*- and 1,2,4-substituted rings from two linked phenolic units (Table 4.5). Small systematic chemical-shift differences between **GXTM-sm13**, **GXTM-sm14** and **GXTM-sm15** (for example modest upfield or

downfield shifts of aromatic doublets and variations in the H-2/H-3 chemical shifts) correlate with changes in substitution pattern and stereochemistry (**GXTM-sm15**, assigned as *(2S,2'S,3R)*-GB-1a (CD spectrum in figure A17, Duddeck et al., 1978), shows the largest deviations), while broadened resonances in some A-ring positions indicate differing degrees of phenolic hydrogen-bonding or dynamic exchange. The NMR data collectively suggest that kaempferol may be regarded as a monomeric flavonol standard, while morelloflavone and volkensiflavone can be viewed as dimeric derivatives wherein one monomer consists of the kaempferol framework, and the other constitutes a flavanone unit, variations in linkage and hydrogen-bonding being responsible for the differing spectra.

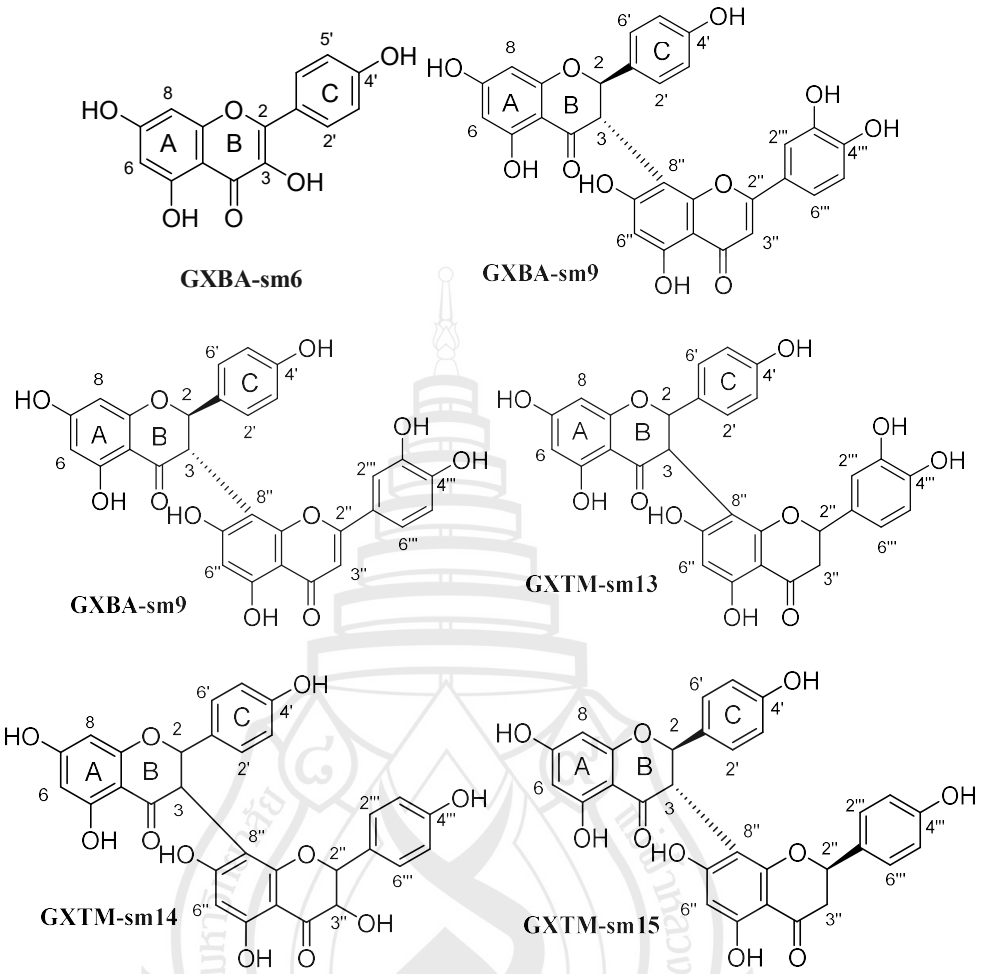

Figure 4.2 Compound Isolated from *G. xanthochymus* (flavonoids)

Table 4.4 The ^{1}H NMR spectra data of **GXBA-sm6**, **GXBA-sm9**, and **GXTM-sm16**

Position	δ in ppm and J value in Hz		
	GXBA-sm6 (500 MHz, $(CD_3)_2CO$)	**GXBA-sm9 (700 MHz, CD_3OD)**	**GXTM-sm16 (700 MHz, CD_3OD)**
2	-	5.75 (1H, *d*, *J* = 12.0)	5.66 (1H, *d*, *J* = 12.0)
3	-	4.82 (1H, *d*, *J* = 12.0)	5.48 (1H, *d*, *J* = 12.0)
6	6.27 (1H, *d*, *J* = 2.1)	5.97 (1H, *d*, *J* = 2.2)	5.83 (1H, *br s*)
8	6.53 (1H, *d*, *J* = 2.1)	5.99 (1H, *d*, *J* = 2.2)	5.77 (1H, *br s*)
2′, 6′	8.15 (2H, *d*, *J* = 9.0)	7.10 (2H, *d*, *J* = 8.6)	7.06 (2H, *d*, *J* = 8.0)
3′, 5′	7.01 (2H, *d*, *J* = 9.0)	6.43 (2H, *d*, *J* = 8.6)	6.66 (2H, *d*, *J* = 8.0)
3″	-	6.41 (1H, *s*)	6.07 (1H, *s*)
6″	-	6.26 (1H, *s*)	6.26 (1H, *s*)
2‴	-	7.35 (1H, *d*, *J* = 2.2)	7.17 (1H, *d*, *J* = 8.4)
3‴	-	-	6.84 (1H, *d*, *J* = 8.4)
5‴	-	6.91 (1H, *d*, *J* = 8.4)	6.84 (1H, *d*, *J* = 8.4)
6‴	-	7.29 (1H, *dd*, *J* = 8.4, 2.2)	7.17 (1H, *d*, *J* = 8.4)

Table 4.5 The ^{1}H NMR spectra data of **GXTM-sm13**, **GXTM-sm14**, and **GXTM-sm15**

Position	δ in ppm and J value in Hz (700 MHz, CD_3OD		
	GXTM-sm13	**GXTM-sm14**	**GXTM-sm15**
2	5.69 (1H, *d*, *J* = 12.0)	5.61 (1H, *d*, *J* = 12.0)	5.42 (1H, *d*, *J* = 12.0)
3	4.57 (1H, *d*, *J* = 12.0)	4.57 (1H, *d*, *J* = 12.0)	5.18 (1H, *d*, *J* = 12.0)
6	5.90 (1H, *d*, *J* = 2.2)	5.92 (1H, *br s*)	6.02 (1H, *d*, *J* = 2.2)
8	5.90 (1H, *d*, *J* = 2.2)	5.88 (1H, *br s*)	5.97 (1H, *d*, *J* = 2.2)
2′, 6′	6.72 (2H, *d*, *J* = 8.2)	6.99 (2H, *d*, *J* = 8.4)	7.07 (2H, *d*, *J* = 8.4)
3′, 5′	6.69 (2H, *d*, *J* = 8.2)	6.59 (2H, *d*, *J* = 8.4)	6.66 (2H, *d*, *J* = 8.4)
2″	5.47 (1H, *d*, *J* = 12.0)	5.84 (1H, *d*, *J* = 12.0)	5.33 (1H, *d*, *J* = 12.0)
3″	2.96 (1H, *m*)	4.38 (1H, *d*, *J* = 12.0)	2.66 (2H, *m*)
	2.66 (1H, *m*)		
6″	5.89 (1H, *s*)	5.94 (1H, *s*)	5.76 (1H, *s*)
2‴	7.11(2H, *m*)	6.72 (1H, *d*, *J* = 8.4)	7.14 (1H, *d*, *J* = 8.4)
3‴	-	6.83 (1H, *d*, *J* = 8.4)	6.70 (1H, *d*, *J* = 8.4)
5‴	6.67 (1H, *d*, *J* = 8.0)	6.83 (1H, *d*, *J* = 8.4)	6.70 (1H, *d*, *J* = 8.4)
6‴	7.11 (2H, *m*)	6.72 (1H, *d*, *J* = 8.4)	7.14 (1H, *d*, *J* = 8.4)

4.1.3 Other Phenolic Compounds

Two simple phenolic acids were obtained: 4-hydroxybenzoic acid (**GXTM-sm17**) and 4-hydroxy-3-methoxybenzoic acid (**GXTM-sm18**). Their structures were confirmed by diagnostic AB and ABX splitting patterns in the aromatic region of ^{1}H NMR (Table 4.6) (Cho et al., 1998). The methoxy substituent in **GXTM-sm18** was identified as a singlet at δ 3.80 ppm (^{1}H) (Chen et al., 2010). These results confirm the presence of low-molecular-weight phenolics that are commonly distributed in plants of the *Garcinia* family.

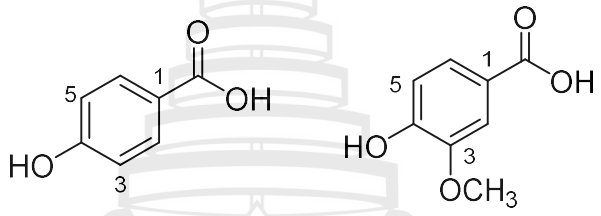

GXTM-sm17 **GXTM-sm18**

Figure 4.3 Compound Isolated from *G. xanthochymus* (phenolic compounds)

Table 4.6 The ^{1}H NMR spectra data of **GXTM-sm17** and **GXTM-sm18**

Position	δ in ppm and J value in Hz	
	GXTM-sm17 (700 MHz, DMSO-d_6)	**GXTM-sm18 (700 MHz, DMSO-d_6)**
2	7.78 (1H, *d*, *J* = 8.7)	7.43 (1H, *s*)
3	6.81 (1H, *d*, *J* = 8.7)	-
5	6.81 (1H, *d*, *J* = 8.7)	6.84 (1H, *d*, *J* = 8.0)
6	7.78 (1H, *d*, *J* = 8.7)	7.44 (1H, *dd*, *J* = 8.0, 1.8)
3-OMe	-	3.80 (3H, *s*)

4.1.4 Anthraquinones / Quinones

Damacanthal (**GXBA-sm5**, Akhtar et al., 2013) was the only anthraquinone derivative isolated. The ^{1}H-NMR spectral data showed signals of a hydroxyl group at δ 12.32 (*s*, 3-OH), a formyl proton at δ 10.50 (*s*, 2-CHO), methoxy protons at δ 4.16 (*s*, 1-CHO_3), an aromatic proton at δ 7.53 (*s*, H-4) and four aromatic protons at δ 8.22 (*dd*, *J* = 7.5, 1.5 Hz, H-5), δ 7.90 (*td*, *J* = 7.5, 1.5 Hz, H-6), δ 7.96 (*td*, *J* = 7.5, 1.5 Hz, H-7), and δ 8.28 (*dd*, *J* = 7.5, 1.5 Hz, H-8) (Table 4.7). These spectral data were identical to 2-formyl-3-hydroxy-1-methoxyanthraquinone, damnacanthal (Koumaglo et al., 1992).

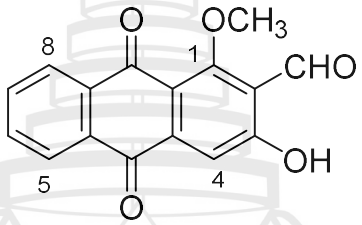

GXBA-sm5

Figure 4.4 Compound Isolated from *G. xanthochymus* (anthraquinones)

Table 4.7 The ^{1}H NMR spectra data of **GXBA-sm5**

Position	**δ in ppm and *J* value in Hz**
	GXBA-sm5 (500 MHz, $(CD_3)_2CO$)
4	7.53 (1H, *s*)
5	8.22 (1H, *dd*, *J* = 7.5, 1.5)
6	7.90 (1H, *td*, *J* = 7.5, 1.5)
7	7.96 (1H, *td*, *J* = 7.5, 1.5)
8	8.28 (1H, *dd*, *J* = 7.5, 1.5)
1-OMe	4.16 (3H, *s*)
2-CHO	10.50 (1H, *s*)
3-OH	12.32 (1H, *s*)

4.2 Evaluation of Antioxidant

The antioxidant activity of crude extracts from *G. xanthochymus* was evaluated using three in vitro assays, namely DPPH, ABTS, and FRAP. The percentage of inhibition and IC_{50} values are summarized in Tables 4.8 and 4.9. To further identify the bioactive constituents contributing to the antioxidant capacity of *G. xanthochymus*, isolated compounds were subjected to DPPH, ABTS, and FRAP assays. Their percentage of inhibition and IC_{50} values are presented in Tables 4.10 and 4.11.

4.2.1 Screening on Antioxidation Activity and Evaluation of 50% Inhibition Concentration (IC_{50}) of Crude Extracts

All extracts exhibited varying levels of radical scavenging activity. In the DPPH assay, the acetone extract of twig (GXTA) demonstrated the strongest inhibition (93.4 ± 5.6%), which was comparable to the positive controls, ascorbic acid (91.3 ± 0.3%) and BHT (85.6 ± 3.2%). Similarly, high inhibition was observed for the methanolic extract of bark (GXBH, 89.0 ± 4.8%), dichloromethane extract of twig (GXTD, 88.5 ± 1.9%), and bark (GXBD, 87.3 ± 0.9%), suggesting that phenolic constituents may contribute significantly to radical scavenging. In contrast, the hexane fraction of leaf extract (GXLH) showed the lowest activity (9.5 ± 3.0%), indicating that non-polar extracts possess fewer antioxidant compounds.

The ABTS assay revealed generally higher scavenging activity across extracts compared to DPPH. Most extracts exceeded 90% inhibition, with the highest activity recorded for GXBD (100.2 ± 2.0%). This broad effectiveness against ABTS radicals indicates that both hydrophilic and lipophilic antioxidants are present in *G. xanthochymus*. IC_{50} values confirmed these trends, where GXBD (30.3 ± 1.5 μg/mL) and GXBM (23.4 ± 1.0 μg/mL) were the most potent extracts in the DPPH assay, approaching the efficacy of ascorbic acid (7.8 ± 1.2 μg/mL). In the ABTS assay, GXBD also showed strong scavenging (133.7 ± 1.7 μg/mL), while GXTM exhibited weaker activity (292.2 ± 9.3 μg/mL). These findings suggest that bark and twig extracts contain high concentrations of potent antioxidant compounds.

The ferric reducing power of the extracts showed results consistent with the radical scavenging assays. GXBD again exhibited the highest reducing ability (94.0 ±

1.6%), followed by GXTD (93.9 ± 1.8%) and GXBM (93.2 ± 0.1%). The IC_{50} values further supported these observations, with GXBD (104.1 ± 3.2 μg/mL) and GXTD (106.2 ± 4.6 μg/mL) showing the strongest reducing capacities among the crude extracts. Interestingly, although BHT displayed strong radical scavenging in DPPH and ABTS, its FRAP value (79.1 ± 3.9% inhibition; IC_{50} = 256.1 ± 3.7 μg/mL) was weaker compared to the extracts. This suggests that the antioxidant constituents of *G. xanthochymus* may have better electron-donating capabilities than the synthetic antioxidant BHT.

Overall, dichloromethane bark extract (GXBD) and methanolic bark extract (GXBM) extracts consistently demonstrated the highest antioxidant activity across all assays, indicating that these plant parts are rich sources of phenolic or polyphenolic compounds with both hydrogen-donating and electron-transfer abilities. Leaf extracts (GXLA and GXLM) also showed moderate-to-strong activity, while hexane fractions (GXBH, GXLH and GXTH) generally exhibited the weakest performance, consistent with the poor solubility of phenolic antioxidants in non-polar solvents.

The findings suggest that *G. xanthochymus* possesses strong natural antioxidant potential, with certain extracts displaying activity comparable to standard antioxidants such as ascorbic acid and superior to BHT in FRAP. These results align with previous reports that members of the *Garcinia* genus are rich in xanthones and flavonoids, compounds known for their radical scavenging and reducing properties (Gunter et al., 2023; Ha et al., 2009; Tran et al., 2023).

Table 4.8 The percentage of inhibition of crude extracts from *G. xanthochymus*

Crude extracts	Antioxidation Activity (%Inhibition)		
	DPPH	ABTS	FRAP
GXBH	25.1 ± 3.7	38.1 ± 2.4	57.2 ± 9.2
GXLH	9.5 ± 3.0	5.4 ± 2.5	66.7 ± 15.1
GXTH	8.8 ± 2.4	20.1 ± 8.4	64.5 ± 9.9
GXBD	87.3 ± 0.9	100.2 ± 0.2	94.0 ± 1.6
GXLD	43.2 ± 1.7	61.1 ± 7.3	61.5 ± 11.1
GXTD	88.5 ± 1.9	99.7 ± 0.2	93.9 ± 1.8
GXLA	84.7 ± 2.1	98.9 ± 1.3	91.0 ± 2.4
GXTA	93.4 ± 5.6	99.7 ± 1.0	88.8 ± 0.4
GXBM	89.0 ± 4.8	99.6 ± 0.3	93.2 ± 0.1
GXLM	83.3 ± 2.7	99.9 ± 0.6	85.9 ± 1.0
GXTM	79.2 ± 1.4	98.7 ± 1.8	81.3 ± 2.0
Ascorbic Acid	91.3 ± 0.3	100.0 ± 0.5	98.3 ± 0.1
BHT	85.6 ± 3.2	100.6 ± 0.6	79.1 ± 3.9

Table 4.9 The IC_{50} value of crude extracts from *G. xanthochymus*

Crude extracts	Antioxidation Activity (IC_{50} - µg/mL)		
	DPPH	ABTS	FRAP
GXBD	30.3 ± 1.5	133.7 ± 1.7	104.1 ± 3.2
GXTD	41.9 ± 4.9	143.7 ± 4.5	106.2 ± 4.6
GXLA	66.1 ± 4.7	215.7 ± 7.6	230.8 ± 15.3
GXTA	41.5 ± 4.7	179.3 ± 8.4	201.9 ± 2.9
GXBM	23.4 ± 1.0	135.4 ± 3.9	108.9 ± 3.3
GXLM	63.2 ± 4.7	231.1 ± 11.4	373.9 ± 13.1
GXTM	97.1 ± 4.2	292.2 ± 9.3	401.3 ± 9.4
Ascorbic Acid	7.8 ± 1.2	22.8 ± 0.1	43.2 ± 1.5
BHT	91.3 ± 2.8	38.5 ± 0.8	256.1 ± 3.7

4.2.2 Screening on Antioxidation Activity and Evaluation of 50% Inhibition Concentration (IC_{50}) of Isolated Compounds

Among the isolated compounds, **GXBA-sm1**, **GXBA-sm9**, and **GXBA-sm6** exhibited the strongest radical scavenging effects. **GXBA-sm1** showed the highest DPPH inhibition (97.2 ± 6.6%), comparable to ascorbic acid (91.3 ± 0.3%), and significantly higher than the synthetic antioxidant BHT (85.6 ± 3.2%). Similarly, **GXBA-sm6** (94.3 ± 10.9%) and **GXBA-sm9** (96.3 ± 10.2%) demonstrated excellent activity, suggesting that these compounds possess highly reactive hydrogen-donating groups capable of stabilizing DPPH radicals.

The ABTS assay also supported these findings, where **GXBA-sm1** reached near-complete inhibition (100.5 ± 2.1%), on par with ascorbic acid and BHT. **GXBA-sm6** also exhibited strong activity (100.8 ± 0.9%). Interestingly, **GXBA-sm4** and **GXBA-sm5** were markedly less active (68.2 ± 3.5% and 4.4 ± 2.7%, respectively), suggesting structural differences in their substituents may reduce their electron-donating ability. IC_{50} values provided further confirmation. **GXBA-sm9** displayed relatively low IC_{50} values in the ABTS assay (298.7 ± 11.0 μM), though still higher than ascorbic acid (129.6± 0.8 μM), indicating that while these compounds are effective, they are less potent than the standard reference antioxidant. **GXBA-sm3** showed particularly weak activity (IC_{50} = 1026.5 ± 13.3 μM for ABTS), consistent with its moderate inhibition percentage.

The FRAP assay revealed that most isolated compounds had weaker reducing capacity compared to crude extracts. **GXBA-sm6** and **GXBA-sm9** showed the highest activity (96.7 ± 0.5% and 91.2 ± 1.7%), though their IC_{50} values (169.9 ± 1.9 μM and 92.2 ± 0.2 μM, respectively) were lower than ascorbic acid (254.4 ± 8.6 μM). This indicates that, these compounds can reduce Fe^{3+} ions and their reducing power is significantly higher compared to the standard antioxidant. Compounds such as **GXBA-sm5** exhibited very low FRAP activity (49.3 ± 9.5%) suggesting they may lack sufficient conjugated systems or hydroxy groups necessary for effective electron transfer.

Overall, **GXBA-sm1**, **GXBA-sm6**, and **GXBA-sm9** emerged as the most promising antioxidant compounds, with inhibition values comparable to ascorbic acid in DPPH and ABTS assays. Their higher IC_{50} values relative to the standard, however,

suggest that larger concentrations are required to achieve equivalent activity. This may indicate that these compounds act through different mechanisms, possibly involving stabilization of radical species via resonance rather than rapid hydrogen transfer. On the other hand, **GXBA-sm2**, **GXBA-sm5**, and **GXTM-sm15** showed poor antioxidant activity in all assays, which may be attributed to the absence of key functional groups (such as free hydroxy groups or prenylated side chains) known to enhance radical scavenging in xanthones and related phenolic compounds. When comparing isolated compounds to crude extracts, it is notable that crude extracts such as GXBD and GXBM exhibited stronger FRAP activity and lower IC_{50} values than the pure compounds. This suggests the possibility of synergistic effects among multiple constituents in the crude extracts, where combinations of phenolics, flavonoids, and xanthones may enhance overall antioxidant capacity.

The results highlight those specific compounds, particularly **GXBA-sm1**, **GXBA-sm6**, and **GXBA-sm9**, play key roles in the antioxidant potential of *G. xanthochymus*. These findings suggest that whole extracts, rather than isolated constituents, may provide superior antioxidant benefits, which is relevant for the development of nutraceuticals or functional food products.

Table 4.10 The percentage of inhibition of isolated compounds from *G. xanthochymus*

Compounds	Antioxidation Activity (%Inhibition)		
	DPPH	**ABTS**	**FRAP**
GXBA-sm1	97.2 ± 6.6	100.5 ± 2.1	88.0 ± 2.9
GXBA-sm2	0.5 ± 5.4	71.2 ± 3.8	60.1 ± 2.9
GXBA-sm3	93.9 ± 7.37	99.1 ± 0.8	85.3 ± 1.6
GXBA-sm4	1.4 ± 3.0	68.2 ± 3.5	86.5 ± 3.2
GXBA-sm5	7.9 ± 12.8	4.4 ± 7.2	49.3 ± 9.5
GXBA-sm6	94.3 ± 10.9	100.8 ± 0.9	96.7 ± 0.5
GXBA-sm9	96.3 ± 10.2	100.3 ± 1.2	91.2 ± 1.7
GXTM-sm15	23.6 ± 9.5	49.5 ± 8.0	78.0 ± 1.5
Ascorbic Acid	91.3 ± 0.3	100.0 ± 0.5	98.3 ± 0.1
BHT	85.6 ± 3.2	100.6 ± 0.6	79.1 ± 3.9

Table 4.11 The IC_{50} value of isolated compounds from *G. xanthochymus*

Compounds	Antioxidation Activity (IC_{50} - µM)		
	DPPH	**ABTS**	**FRAP**
GXBA-sm1	514.9 ± 8.6	495.7 ± 15.7	1653.4 ± 20.5
GXBA-sm3	556.6 ± 9.8	1026.5 ± 13.3	1365.2 ± 14.1
GXBA-sm6	66.2 ± 0.5	469.6 ± 19.2	169.9 ± 1.9
GXBA-sm9	34.4 ± 0.7	298.7 ± 11.0	92.2 ± 0.2
Ascorbic Acid	44.1 ± 6.6	129.6 ± 0.8	245.4 ± 8.6
BHT	414.3 ± 12.6	174.7 ± 3.4	1162.1 ± 16.8

4.3 Anticancer Activity of *Gracinia xanthoxhymus* Crude Extract Against Human Cancer Cells: *in vitro* Evaluation in MDA-MB-231, Huh-7, A549, and SW480 Cell Lines

4.3.1 Metabolites in Different Parts of *G. xanthochymus*

The metabolite profiles of crude extracts from different parts of *G. xanthochymus* are presented in a bar graph (Figure 4.1). The major compound groups identified include xanthones, flavonoids, and other classes such as benzophenones, phloroglucinols, polyphenols, coumarins, and organic acids. In total, 73 compounds were identified across all extracts, comprising 36 xanthones, 37 flavonoids, and 29 compounds from other compound groups (Table A1). Xanthones were unevenly distributed among the extracts. Notably, compounds 45, 50, and 55 were highly abundant in GXBM and GXTA, while GXTM also exhibited a high xanthone content but with a distinct profile compared to the other extracts. This variation suggests that GXBM and GXTA possess a greater capacity for xanthone biosynthesis, potentially influenced by genetic factors or environmental conditions. Flavonoids, represented by 37 identified metabolites, were more uniformly distributed across the extracts than xanthones. Extracts such as GXLA, GXLD, and GXTH contained moderate to high levels of various flavonoids. However, none of the extracts exhibited flavonoid levels as high as those observed for xanthones, suggesting that flavonoid production in *G. xanthochymus* may be more consistent and less variable. The remaining 29 metabolites—including benzophenones, phloroglucinols, polyphenols, coumarins, and organic acids—were generally present in lower abundance. Nonetheless, GXLD and GXTA showed elevated levels of certain metabolites, indicating selective accumulation. This selectivity may reflect specialized metabolic processes or be influenced by external factors such as environmental conditions. These findings are consistent with previous reports indicating that *Garcinia* species are prolific producers of xanthones and flavonoids. The observed patterns of metabolite accumulation are likely regulated by both genetic and environmental factors (Che Hassan et al., 2018; Kumatso & Sigge, 2024; Pailee et al., 2017; Reutrakul et al., 2006). Regarding bioavailability, *G. xanthochymus* is recognized for its pharmacological potential due to

xanthones, benzophenones, and flavonoids, with further research needed on their bioavailability and mechanisms of action (Che Hassan et al., 2018). Janhavi et al. (2020) reported that polyphenols such as epicatechin and catechin from *G. xanthochymus* fruit exhibited high bioaccessibility and bioavailability, with in vivo studies in mice showing peak plasma concentrations (Cmax) approximately 2 hours after oral administration. These findings suggest that *G. xanthochymus* is a promising source of bioavailable antioxidant compounds for functional food or pharmaceutical applications (Janhavi et al., 2020).

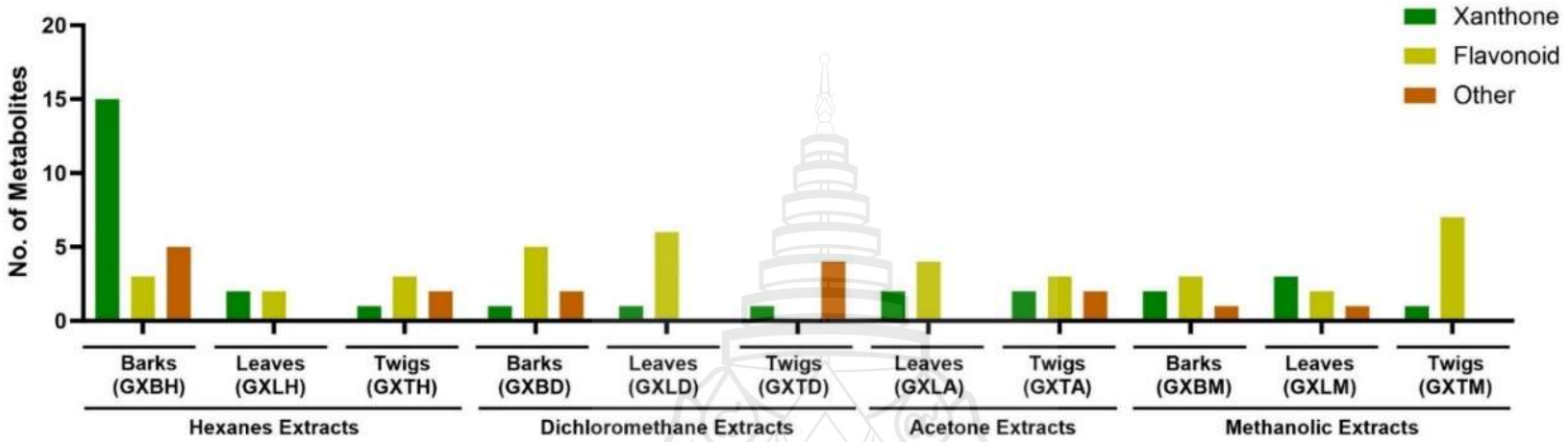

Figure 4.5 Metabolite distribution in *G. xanthochymus* crude extracts. A bar graph shows the number of xanthone, flavonoid, and other compounds identified in crude extracts from each part in different solvents.

4.3.2 Cytotoxicity Effect of *G. Xanthochymus* Crude Extract on Cancer Cell Lines

The cytotoxic activities of *G. xanthochymus* crude extracts—prepared using hexanes, dichloromethane, acetone, and methanol—were evaluated against four human cancer cell lines: MDA-MB-231 (breast cancer), Huh-7 (liver cancer), A549 (lung cancer), and SW480 (colon cancer). As shown in the bar graphs (Figure 4.2A, 4.2C, 4.2E, and 4.2G), the hexanes and dichloromethane extracts exhibited strong cytotoxic effects, particularly against MDA-MB-231 and SW480 cells. In contrast, extracts prepared with acetone and methanol demonstrated comparatively lower cytotoxicity. A dose-dependent reduction in cell viability was observed across all tested cell lines.

The heat maps (Figure 4.2B, 4.2D, 4.2F, and 4.2H) revealed distinct cytotoxic response patterns for each cell line, suggesting that differences in extract composition may influence cellular sensitivity. These cytotoxic effects are likely attributable to bioactive secondary metabolites such as xanthones, flavonoids, and benzophenones found in *G. xanthochymus* (Baggett et al., 2005; Che Hassan et al., 2018; Chen et al., 2008; He et al., 2021; Hemshekhar et al., 2011). The IC_{50} values for each extract are summarized in Table 4.12. Among all extracts, the hexane extract (GXBH) demonstrated the highest cytotoxic activity, with IC_{50} values of 66.9 ± 5.1 µg/mL for MDA-MB-231, 64.7 ± 14.9 µg/mL for Huh-7, 80.0 ± 11.9 µg/mL for A549, and 65.4 ± 7.8 µg/mL for SW480 cells. Based on these results, GXBH was selected for further studies to investigate its effects on apoptosis and colony-forming ability.

Table 4.12 Anti-cancer effect of hexanes, dichloromethane, acetone, and methanolic crude extract of *G. xanthochymus* against four human cancer cells

Crude	Cell lines (IC_{50} - µg/mL)			
	MDA-MB-231	**HuH-7**	**A549**	**SW480**
GXBH	66.9 ± 5.1	64.7 ± 14.9	80.0 ± 11.9	65.4 ± 7.8
GXLH	51.7 ± 2.8	71.1 ± 11.6	76.9 ± 3.9	75.0 ± 3.8
GXTH	162.6 ± 6.2	109.6 ± 38.8	143.7 ± 18.8	212.5 ± 27.6
GXBD	154.4 ± 2.0	228.2 ± 12.9	89.0 ± 22.1	Inactive
GXLD	80.2 ± 10.1	188.0 ± 25.7	92.9 ± 27.2	297.6 ± 19.0
GXTD	77.4 ± 3.5	76.3 ± 6.8	69.5 ± 9.9	Inactive
GXLA	148.0 ± 2.0	118.4 ± 14.5	210.3 ± 39.6	524.0± 12.8
GXTA	539.0 ± 27.8	Inactive	Inactive	323.0 ± 20.5
GXBM	482.4 ± 19.0	Inactive	Inactive	323.5 ± 21.2
GXLM	173.7 ± 11.6	259.4 ± 41.5	137.8 ± 17.3	73.7 ± 3.7
GXTM	Inactive	Inactive	Inactive	130.6 ± 7.3

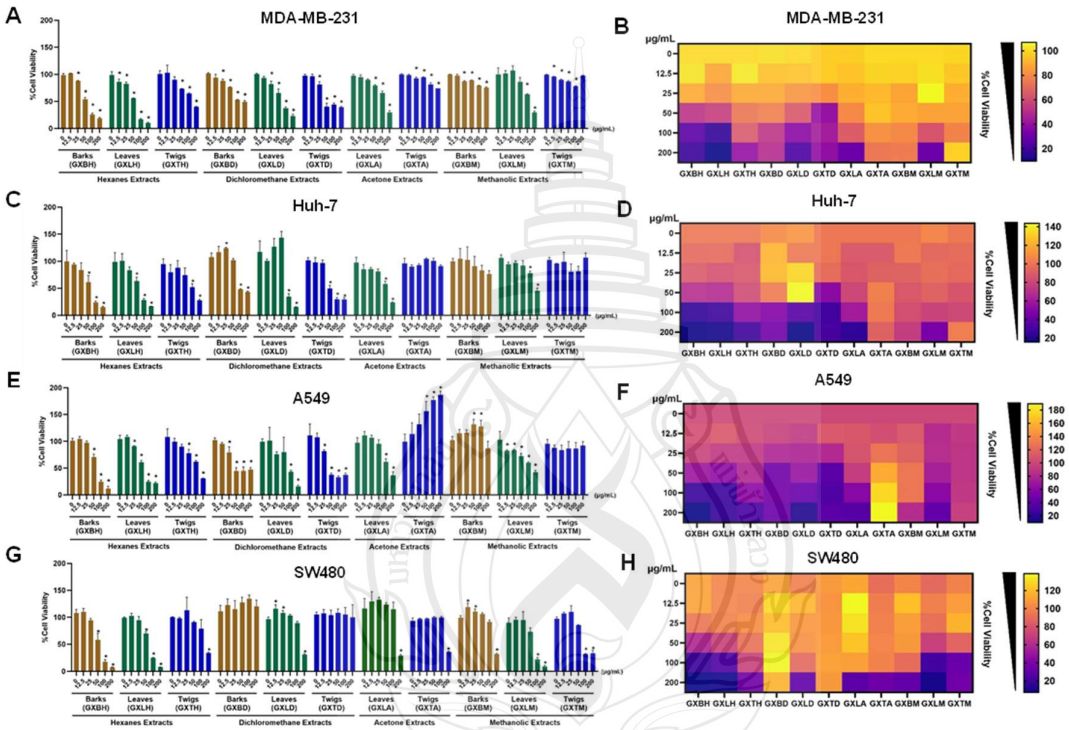

Figure 4.6 Cytotoxicity assay of human cancer cell lines after treatment with *G. xanthochymus* crude extracts for 72 h. Bar graphs show the percentage of cell viability of MDA-MB-231 (A), Huh-7 (C), A549 (E), and SW480 (G). Data represent mean ± SD from three independent experiments. *$P < 0.05$ vs. equivalent concentrations of vehicle solvent (DMSO). Heat maps illustrate the percentage of cell viability in MDA-MB-231 (B), Huh-7 (D), A549 (F), and SW480 (H).

4.3.3 Effect of GXBH Extract on Apoptosis of Cancer Cells

Apoptosis is a fundamental process in the elimination of cancer cells and a key target in anticancer therapy (Elmore, 2007). To assess the pro-apoptotic effects of the GXBH extract, annexin V and propidium iodide (PI) staining were performed on four cancer cell lines. The experiment initially used IC50 concentrations and time points from cytotoxicity assays. However, annexin V/PI staining detected <10% apoptosis under these conditions (data not shown). To enhance apoptotic detection, the concentration was increased to 100 μg/mL, inducing ~90% cell death, and incubation extended to 96 h. Our results revealed a significant increase in the proportion of apoptotic cells in all cell lines treated with GXBH compared to untreated controls (figure 4.3A–H). Notably, the SW480 cell line exhibited a marked elevation in early apoptotic cells (figure 4.3G and 4.3H), highlighting the potential of GXBH to trigger apoptosis in cancer cells.

The varying ratios of early and late apoptotic populations across different cell lines may be attributed to differential expression of key apoptosis-regulating proteins, such as Bcl-2, Bax, and members of the caspase family (Papaliagkas et al., 2007; Qian et al., 2022). These proteins play central roles in the intrinsic and extrinsic apoptotic pathways and may modulate the cellular response to GXBH treatment. Xanthones have long been recognized as natural anti-cancer agents (Kurniawan et al., 2021). Mechanistically, they promote apoptosis primarily through activation of the mitochondrial pathway, characterized by reduced intracellular ATP levels, release of cytochrome c and AIF, activation of caspase-9 and caspase-3, and endonuclease G translocation. Additionally, xanthones modulate apoptosis via the miR-143/ERK5/c-Myc axis, inhibit nitric oxide production, induce cell cycle arrest, inhibit sarco-endoplasmic reticulum Ca^{2+}-ATPase, and promote intracellular ROS accumulation (Shan et al., 2011). Nevertheless, further mechanistic studies are required to elucidate the specific molecular pathways by which GXBH induces apoptosis in cancer cells.

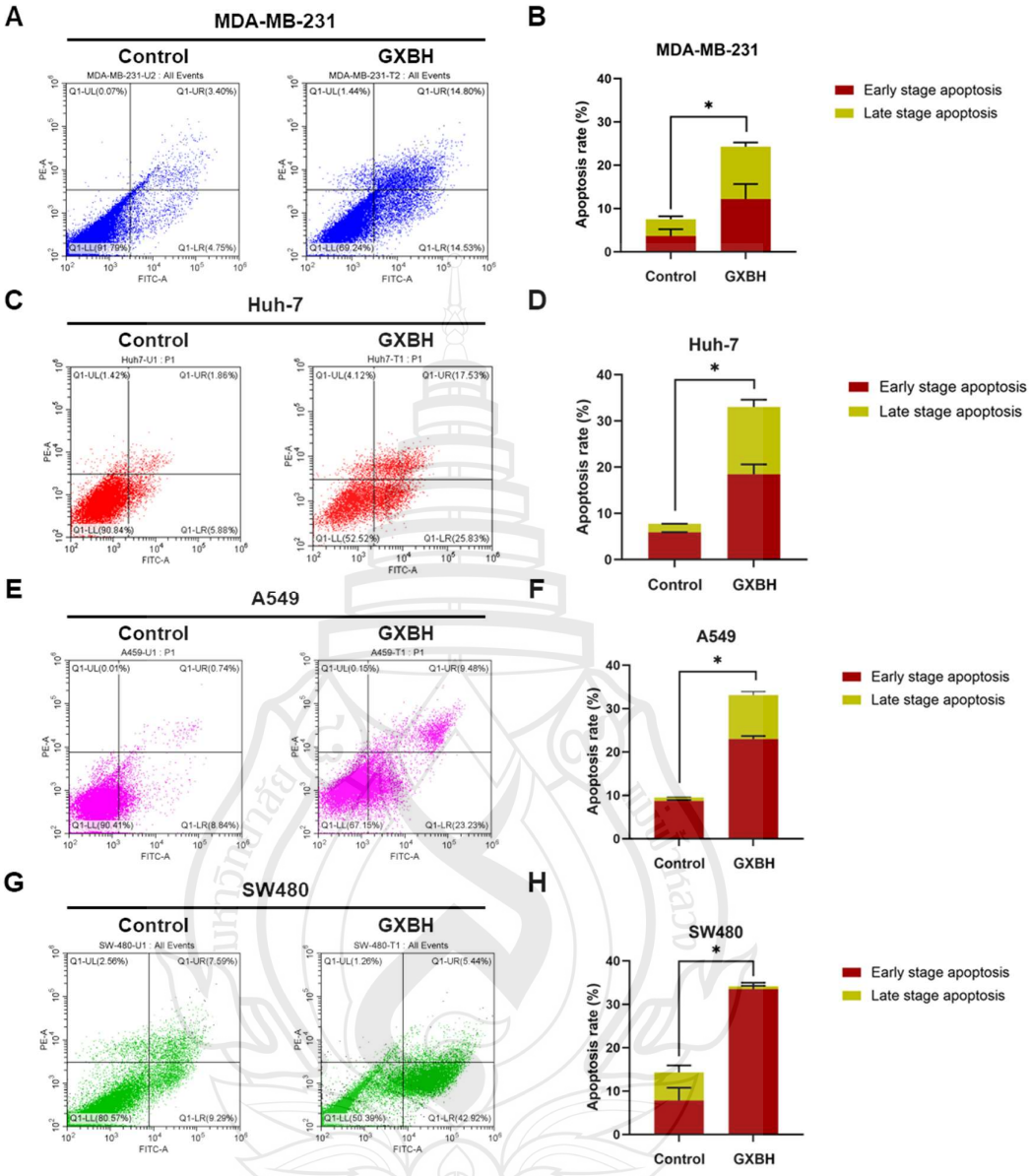

Figure 4.7 Annexin V and PI staining assay of human cancer cell lines after treatment with GXBH for 96 h. Representative flow cytometric dot plots of annexin V and PI-stained cells in MDA-MB-231 (A), Huh-7 (C), A549 (E), and SW480 (G). Bar graphs show the percentage of apoptotic cells in MDA-MB-231 (B), Huh-7 (D), A549 (F), and SW480 (H). Data represent mean ± SD from three independent experiments. *$P < 0.05$ vs. control (0 μg/mL).

4.3.4 Effect of GXBH Extract on Colony-Forming Capability

Colony-forming capability is a hallmark of cancer, reflecting the uncontrolled proliferative potential of cancer cells (Hanahan & Weinberg, 2011). The anti-colony-forming effect of GXBH was assessed across four cancer cell lines by quantifying the percentage of colony area intensity. Compared to the untreated control, GXBH significantly inhibited colony formation, particularly in A549 and MDA-MB-231 cells (Figure 4.4A and 4.4B), suggesting a possible selectivity of GXBH toward specific cancer types. The observed reduction in colony-forming ability indicates the potential of GXBH to suppress long-term cancer cell growth, correlating with its pro-apoptotic effects. GXBH not only induces apoptosis but also exhibits anti-proliferative activity. The significant decrease in colony-forming ability may be attributed to the inhibition of cyclin-dependent kinases (CDKs), which regulate the S and M phases of the cell cycle, or to the upregulation of CDK inhibitors such as p21 and p27 (Patel et al., 2016; Zhang et al., 2019). Previous studies have reported that compounds isolated from *Garcinia* species exhibit diverse biological activities, including the inhibition of multiple signaling pathways. GXBH may similarly suppress cancer cell growth by targeting PI3K/Akt/mTOR or MAPK/ERK signaling pathways (Patil & Appaiah, 2015; Paul & Zaman, 2022; Xu et al., 2020).

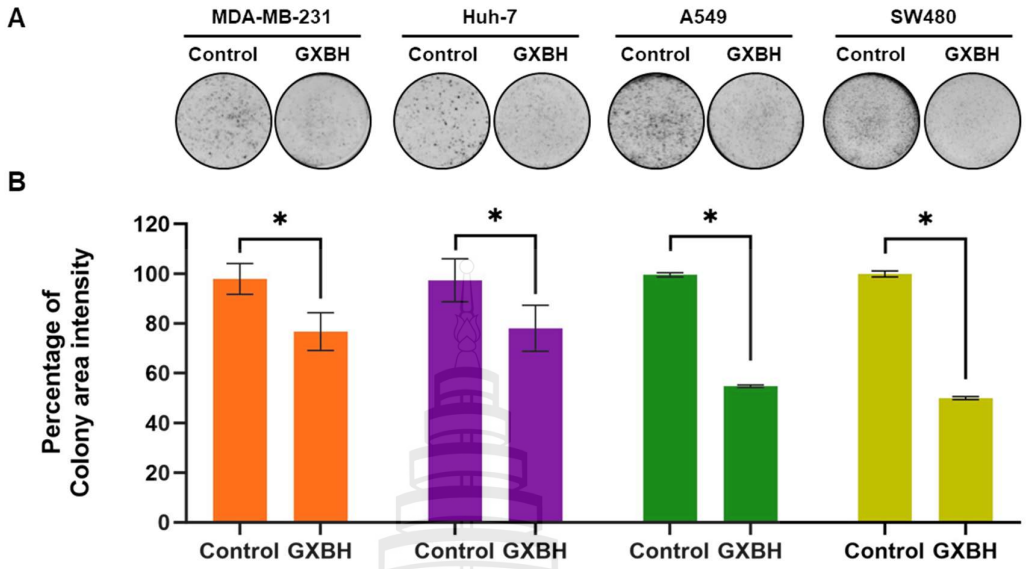

Figure 4.8 Clonogenic assay of human cancer cell lines after treatment with GXBH for 96 h. (A) Representative images of formed colonies of MDA-MB-231, Huh-7, A549, and SW480. (B) Bar graphs show the percentage of colony area intensity of MDA-MB-231, Huh-7, A549, and SW480. Data represent mean ± SD from three independent experiments. *$P < 0.05$ vs. control (0 µg/mL).

4.4 Evaluation of Anticancer Activity of Isolated Compound from *G. xanthochymus*

The cytotoxic effect of selected isolated compounds from *G. xanthochymus* (**GXBA-sm1**, **GXBA-sm2**, and **GXBA-sm4**) was investigated against the human triple-negative breast cancer cell line MDA-MB-231. Cell viability was determined after 72 hours of treatment with increasing concentrations of the compounds, and IC_{50} values were calculated (Figure 4.5 and Table 4.13).

4.4.1 Screening on Anticancer Activity and Evaluation of 50% Inhibition Concentration (IC_{50}) of Isolated Compounds

The results revealed differential cytotoxic activity among the tested compounds. **GXBA-sm1** (formoxanthone C) showed no detectable inhibitory effect on MDA-MB-231 cells within the tested concentration range (0.78125–100 μM), as cell viability remained above 90%. This indicates that **GXBA-sm1** does not possess significant cytotoxic potential against this cancer cell line. **GXBA-sm2** (euxanthone) exhibited weak cytotoxicity, with a high IC_{50} value of 338.63 ± 10.70 μM. Although cell viability gradually decreased with increasing concentration, substantial inhibition was not observed until higher doses (>50 μM), suggesting limited anticancer potential.

In contrast, **GXBA-sm4** (7-geranyloxy-1,3-dihydroxyxanthone) demonstrated strong dose-dependent cytotoxicity, with significant reductions in cell viability observed at concentrations ≥12.5 μM. The IC_{50} value of **GXBA-sm4** was determined to be 24.51 ± 2.31 μM, indicating potent cytotoxicity compared to **GXBA-sm1** and **GXBA-sm2**. This suggests that structural modifications, such as the presence of a geranyloxy side chain, may play a crucial role in enhancing anticancer activity.

Table 4.13 Anti-cancer effect of isolated compounds from *G. xanthochymus* against the human triple-negative breast cancer cell line MDA-MB-231.

Isolated Compounds	Cell lines (IC_{50} - µM)
	MDA-MB-231
GXBA-sm1	Non-Detectable
GXBA-sm2	338.6 ± 10.7
GXBA-sm4	24.5 ± 2.3

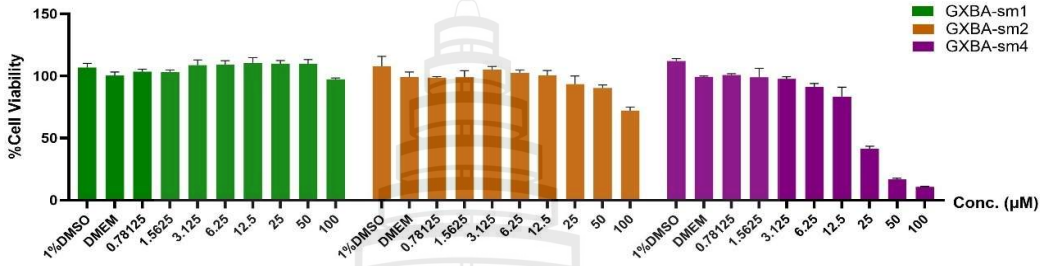

Figure 4.9 Cytotoxic Effect of Isolated Compounds from *G. xanthochymus* on MDA-MB-231 Cells

4.4.2 Structure–activity Relationship

The contrasting activities among the tested compounds highlight the importance of substituent groups in modulating the cytotoxicity of xanthones. **GXBA-sm1** and **GXBA-sm2**, both lacking bulky lipophilic substitutions, exhibited little to weak activity. **GXBA-sm4**, however, contained a geranyloxy moiety which may increase lipophilicity, improve cell membrane permeability, and facilitate interactions with cellular targets involved in apoptosis or growth inhibition. This finding is consistent with previous studies reporting that prenylated and geranylated xanthones often show stronger anticancer activity compared to non-substituted analogues (Gunter et al., 2023; Ha et al., 2009; Tran et al., 2023).

Among the tested compounds, **GXBA-sm4** was clearly the most effective against MDA-MB-231 cells, with an IC_{50} in the low micromolar range. Such potency suggests that **GXBA-sm4** could serve as a promising lead compound for further anticancer drug development. In contrast, **GXBA-sm1** and **GXBA-sm2** exhibited poor cytotoxicity, there for, and therefore may contribute more to other biological activities, such as antioxidant or anti-inflammatory effects, rather than direct anticancer potential. The marked difference in activity also underscores the importance of structure–activity relationship (SAR) studies for xanthones, as slight modifications to the core structure can drastically alter biological activity. Future work should therefore include mechanistic studies to clarify whether **GXBA-sm4** induces apoptosis, cell cycle arrest, or other anticancer pathways in triple-negative breast cancer cells.

These results demonstrate that not all xanthones isolated from *G. xanthochymus* possess anticancer potential. **GXBA-sm4** emerged as the most active compound against MDA-MB-231 cells, while **GXBA-sm1** and **GXBA-sm2** showed negligible to weak effects. The strong cytotoxicity of **GXBA-sm4** highlights the therapeutic potential of prenylated/geranylated xanthones as anticancer agents, warranting further investigation into their mechanism of action and selectivity against cancer versus normal cells.

CHAPTER 5

CONCLUSIONS

This study presents a comprehensive investigation of *Garcinia xanthochymus* through an integrated approach that encompasses a literature review, extraction methodologies, compound isolation, and biological evaluation. The literature survey highlighted the plant's rich repository of xanthones, benzophenones, and flavonoids, emphasizing its long-standing ethnomedicinal relevance and pharmacological potential. Guided by this evidence, systematic extraction and fractionation were performed using appropriate solvents, yielding crude extracts and partially purified fractions that were elucidated in structure and characterized using spectroscopic methodologies. These analytical efforts supported the identification of key secondary metabolites consistent with previously reported constituents, thereby reinforcing the scientific basis for selecting *G. xanthochymus* as a viable source of bioactive compounds. Twenty-two compounds are isolated from the bark and twig of *G. xanthochymus*, which include 13 xanthones (**GXBA-sm1** (formoxanthone C), **GXBA-sm2** (euxanthone), **GXBA-sm3** (pyranojacreubin), **GXBA-sm4** (7-geranyloxy-1,3-dihydroxyxanthone), **GXBA-sm7** (6-hydroxy-2,3-dimethoxy xanthone), **GXBA-sm8** (Xanthone V1), **GXBA-sm10** (morusignin I), **GXBA-sm11** (dulxanthone B), **GXBA-sm12** (1,5-dihydroxy-3-methoxyxanthone), **GXTM-sm19** (2,5-dihydroxy-1-methoxyxanthone), **GXTM-sm20** (2,6-dihydroxy-1,5-dimethoxyxanthone), **GXTM-sm21** (1,2,5-trihydroxyxanthone), and **GXTM-sm22** (1,2,5-trihydroxy-6-methoxyxanthone)), six of flavonoid scaffolds (**GXBA-sm6** (kaempferol), **GXBA-sm9** ((*2R,3S*)-morelloflavone), **GXTM-sm13** (GB-2a), **GXTM-sm14** (GB-1), **GXTM-sm15** (*(2S,2'S,3R)*-GB-1a), and **GXTM-sm16** (volkensiflavone)), two of benzene derivatives (**GXTM-sm17** (4-hydroxybenzoic acid) and **GXTM-sm18** (4-hydroxy-3-methoxybenzoic acid)), and one anthraquinone (**GXBA-sm5** (damnacanthal)) (Figure 5.1).

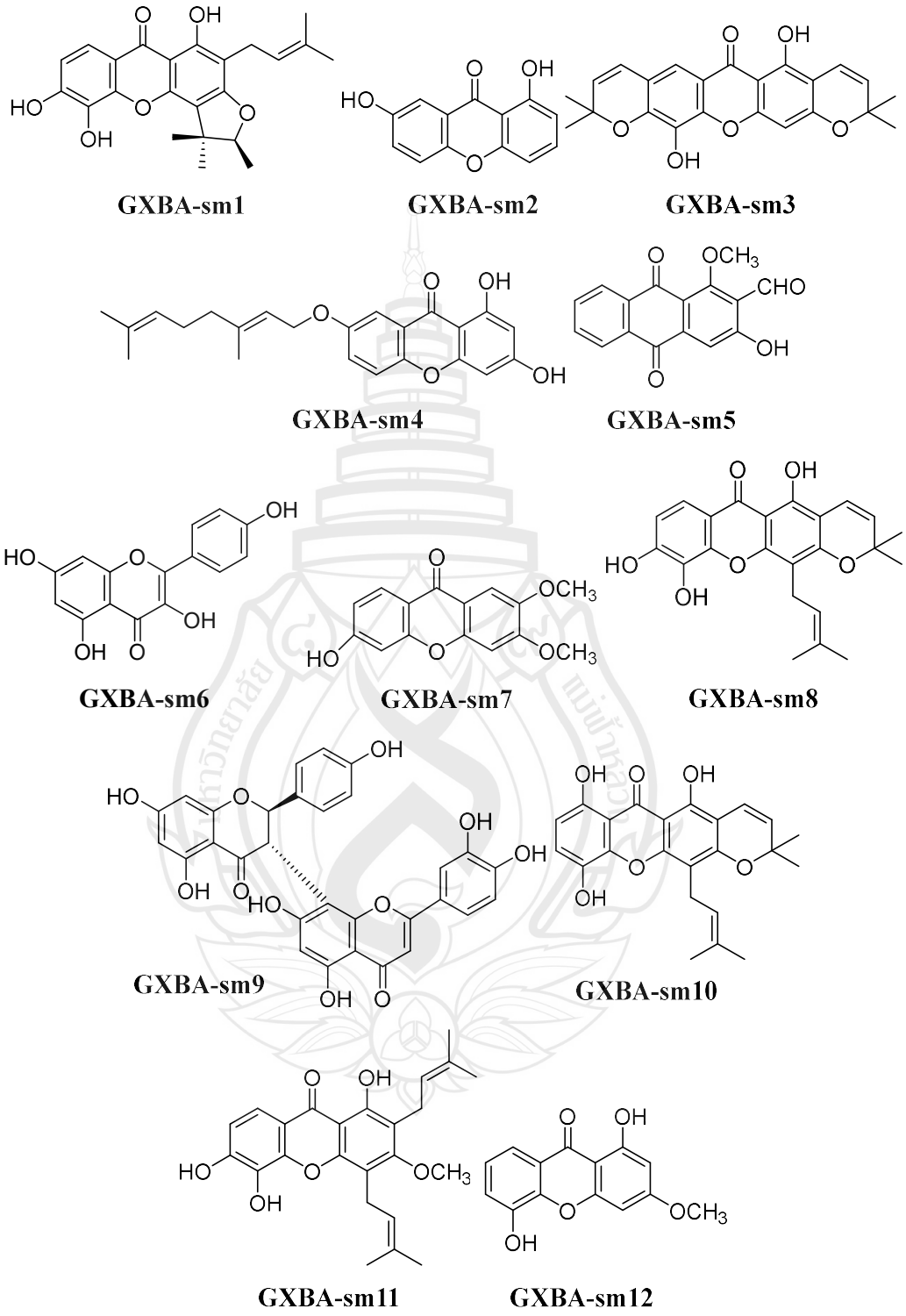

Figure 5.1 Compound Isolated from *G. xanthochymus*

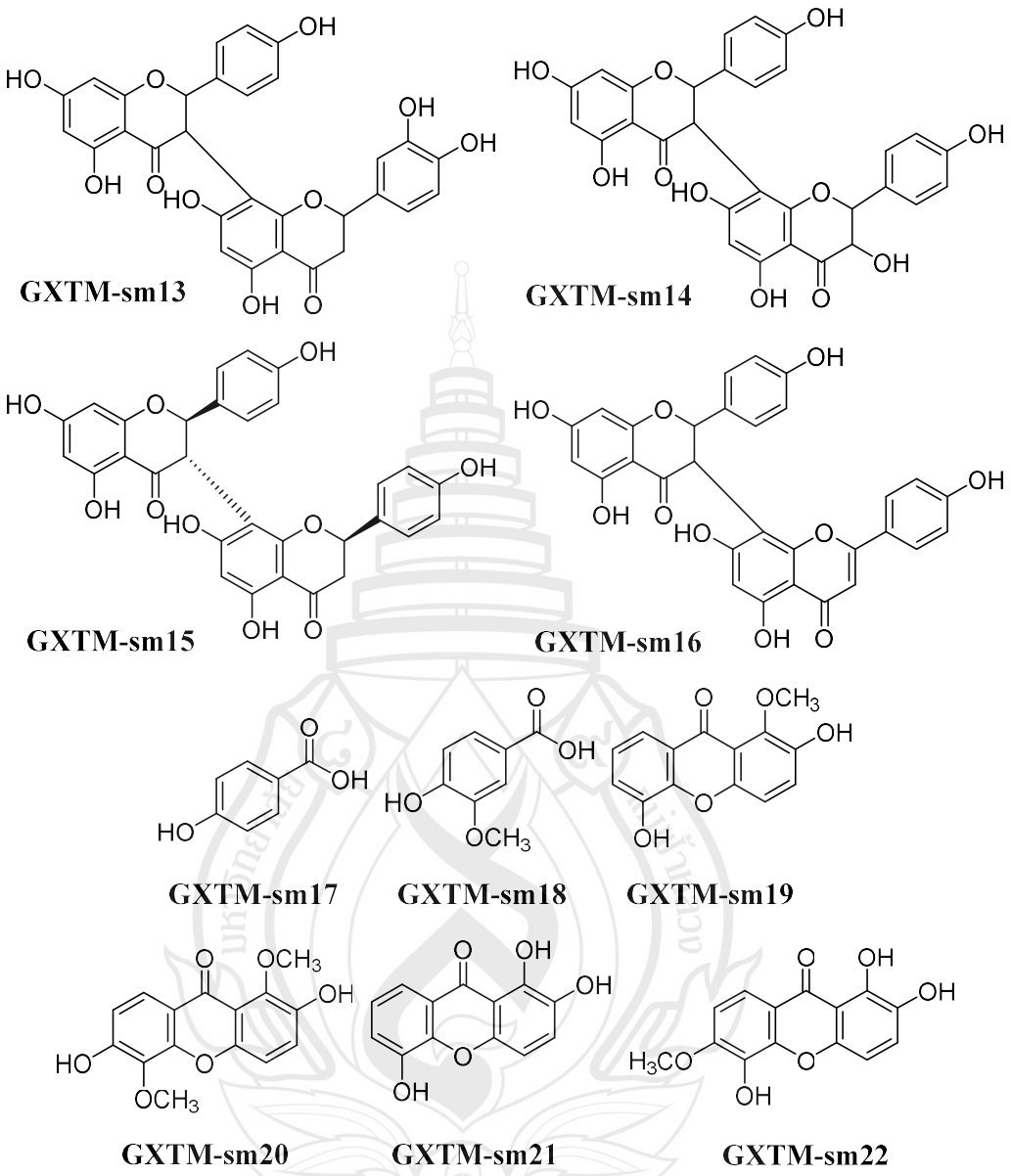

Figure 5.1 (continued)

The biological assessments demonstrated that the crude extracts possessed notable antioxidant and anticancer activities, particularly against selected human cancer cell lines. The antioxidant potential supported the hypothesis that phenolic and xanthone constituents contribute significantly to free radical scavenging, which dichloromethane bark extract (GXBD) and methanolic bark extract (GXBM) consistently demonstrated the highest antioxidant activity across all assays. GXBD

shows potential as an antioxidant with an IC_{50} value of 133.7 ± 1.7 μg/mL and 104.1 ± 3.2 μg/mL in ABTS and FRAP assays, respectively, and GXBM shows the highest potential in the DPPH assay with an IC_{50} value of 23.4 ± 1.0 μg/mL. Furthermore, the isolated compound, GXBA-sm9, exhibits the best potential across all assays with the lowest IC_{50} value of 44.1 ± 6.6 μM, 129.6 ± 0.8 μM, and 92.2 ± 0.2 μM in DPPH, ABTS, and FRAP assays, respectively. While in vitro cytotoxicity results indicated promising anticancer effects. GXBH crude extract shows the potential to be a natural anticancer agent, which shows the lowest IC_{50} value of 66.9 ± 5.1 μg/mL for MDA-MB-231, 64.7 ± 14.9 μg/mL for Huh-7, 80.0 ± 11.9 μg/mL for A549, and 65.4 ± 7.8 μg/mL for SW480 cells. In addition, GXBH exhibits the ability to induce apoptosis in cancer cells by increasing the number of apoptotic cells after treatment and can reduce the colony-forming capability of cancer cells. The investigation of the anticancer activity of the isolated compound shows that GXBA-sm4 shows the potential to be an anticancer agent to provide an IC_{50} value of 24.5 ± 2.3 μM in MDA-MB-231 cells, but the molecular mechanism needs further investigation.

Overall, the findings of this work not only validate the traditional use of *G. xanthochymus* but also provide a foundation for future research aimed at compound isolation, structural modification, and targeted therapeutic applications. Continued investigation into bioavailability, safety profiling, and formulation strategies may further advance the development of this plant as a source of novel pharmacological agents.

REFERENCES

Akhtar, M. N., Zareen, S., Yeap, S. K., Ho, W. Y., Lo, K. M., Hasan, A., & Alitheen, N. B. (2013). Total synthesis, cytotoxic effects of damnacanthal, nordamnacanthal and related anthraquinone analogues. *Molecules*, 18(8). https://doi.org/10.3390/molecules180810042

All.Can international. (2025). *Cancer Anywhere in Thailand*. https://www.hfocus.org/content/2024/05/30453

Aluksanasuwan, S., Somsuan, K., Chiangjong, W., Rongjumnong, A., Jaidee, W., Rujanapun, N., … Charoensup, R. (2024). SWATH-proteomics reveals Mathurameha, a traditional anti-diabetic herbal formula, attenuates high glucose-induced endothelial dysfunction through the EGF/NO/IL-1β regulatory axis. *Journal of Proteomics*, *306*, 105263. https://doi.org/10.1016/j.jprot.2024.105263

Aluksanasuwan, S., Somsuan, K., Ngoenkam, J., Chiangjong, W., Rongjumnong, A., Morchang, A., … Pongcharoen, S. (2024). Knockdown of heat shock protein family D member 1 (HSPD1) in lung cancer cell altered secretome profile and cancer-associated fibroblast induction. *Biochimica et Biophysica Acta (BBA) - Molecular Cell Research*, *1871*(5), 119736. https://doi.org/10.1016/j.bbamcr.2024.119736

Ansari, W. H., Rahman, W., Barraclough, D., Maynard, R., & Scheinmann, F. (1976). Biflavanoids and a flavanone-chromone from the leaves of *Garcinia dulcis* (Roxb.) Kurz. *Journal of the Chemical Society*, *Perkin Transactions 1*, 13. https://doi.org/10.1039/p19760001458

Asma, S. T., Acaroz, U., Imre, K., Morar, A., Shah, S. R. A., Hussain, S. Z., Arslan-Acaroz, D., … Ince, S. (2022). Natural Products/Bioactive Compounds as a Source of Anticancer Drugs. *Cancers*, *14*(24). https://doi.org/10.3390/cancers14246203

Baggett, S., Protiva, P., Mazzola, E. P., Yang, H., Ressler, E. T., Basile, M. J., … Kennelly, E. J. (2005). Bioactive Benzophenones from *Garcinia xanthochymus* Fruits. *Journal of Natural Products*, *68*(3), 354–360. https://doi.org/10.1021/np0497595

Begg, A. C., Stewart, F. A., & Vens, C. (2011). Strategies to improve radiotherapy with targeted drugs. *Nature Reviews Cancer*, *11*(4). https://doi.org/10.1038/nrc3007

Bizuayehu, H. M., Ahmed, K. Y., Kibret, G. D., Dadi, A. F., Belachew, S. A., Bagade, T., … Ross, A. G. (2024). Global Disparities of Cancer and Its Projected Burden in 2050. *JAMA Network Open*, *7*(11), e2443198. https://doi.org/10.1001/jamanetworkopen.2024.43198

Blois, M. S. (1958). Antioxidant determinations by the use of a stable free radical. *Nature*, *181*(4617). https://doi.org/10.1038/1811199a0

Boonnak, N., Karalai, C., Chantrapromma, S., Ponglimanont, C., Fun, H. K., Kanjana-Opas, A., ... & Kato, S. (2009). Anti-*Pseudomonas aeruginosa* xanthones from the resin and green fruits of *Cratoxylum cochinchinense*. *Tetrahedron*, *65*(15). https://doi.org/10.1016/j.tet.2009.01.083

Boonsri, S., Karalai, C., Ponglimanont, C., Kanjana-Opas, A., & Chantrapromma, K. (2006). Antibacterial and cytotoxic xanthones from the roots of *Cratoxylum formosum*. *Phytochemistry*, *67*(7). https://doi.org/10.1016/j.phytochem.2006.01.007

Botta, B., Delle Monache, G., Delle Monache, F., Bettolo, G. B. M., & Menichini, F. (1986). Vismione H and prenylated xanthones from *vismia guineensis*. *Phytochemistry*, *25*(5). https://doi.org/10.1016/S0031-9422(00)81583-6

Chanmahasathien, W., Li, Y., Satake, M., Oshima, Y., Ruangrungsi, N., & Ohizumi, Y. (2003). Prenylated xanthones with NGF-potentiating activity from *Garcinia xanthochymus*. *Phytochemistry*, *64*(5). https://doi.org/10.1016/S0031-9422(03)00431-X

Chantree, P., Martviset, P., Thongsepee, N., Sangpairoj, K., & Sornchuer, P. (2023). Anti-Inflammatory Effect of Garcinol Extracted from *Garcinia dulcis* via Modulating NF-κB Signaling Pathway. *Nutrients*, *15*(3). https://doi.org/10.3390/nu15030575

Che Hassan, N. K. N., Taher, M., & Susanti, D. (2018). Phytochemical constituents and pharmacological properties of *Garcinia xanthochymus* - A review. In *Biomedicine and Pharmacotherapy* (Vol. 106, pp. 1378–1389). Elsevier Masson SAS. https://doi.org/10.1016/j.biopha.2018.07.087

Chen, G. Y., Dai, C. Y., Wang, T. S., Jiang, C. W., Han, C. R., & Songa, X. P. (2010). A new flavonol from the stem bark of *Premna fulva*. *Arkivoc*, *2010*(2). https://doi.org/10.3998/ark.5550190.0011.213

Chen, M., Li, Z., Sun, G., Jin, S., Hao, X., Zhang, C., … Yunsheng, X. (2023). Theoretical study on the free radical scavenging potency and mechanism of natural coumestans: Roles of substituent, noncovalent interaction and solvent. *Phytochemistry*, *207*. https://doi.org/10.1016/j.phytochem.2022.113580

Chen, T. H., Tsai, M. J., Fu, Y. S., & Weng, C. F. (2019). The exploration of natural compounds for anti-diabetes from distinctive species *Garcinia linii* with comprehensive review of the garcinia family. *Biomolecules* ,*9*(11). https://doi.org/10.3390/biom9110641

Chen, Y., Fan, H., Yang, G. Z., Jiang, Y., Zhong, F. F., & He, H. W. (2010). Prenylated xanthones from the bark of *Garcinia xanthochymus* and their 1,1-diphenyl-2-picrylhydrazyl (DPPH) radical scavenging activities. *Molecules*, *15*(10). https://doi.org/10.3390/molecules15107438

Chen, Y., Fan, H., Yang, G.-Z., Jiang, Y., Zhong, F.-F., & He, H.-W. (2011). Two Unusual Xanthones from the Bark of *Garcinia xanthochymus*. *Helvetica Chimica Acta*, *94*(4), 662–668. https://doi.org/10.1002/hlca.201000287

Chen, Y., Gan, F., Jin, S., Liu, H., Wu, S., Yang, W., & Yang, G. (2017). Adamantyl derivatives and rearranged benzophenones from *Garcinia xanthochymus* fruits. *RSC Advances*, *7*(28). https://doi.org/10.1039/c7ra01543g

Chen, Y., Zhong, F., He, H., Hu, Y., Zhu, D., & Yang, G. (2008). Structure elucidation and NMR spectral assignment of five new xanthones from the bark of *Garcinia xanthochymus*. *Magnetic Resonance in Chemistry*, *46*(12), 1180–1184. https://doi.org/10.1002/mrc.2317

Cho, J. Y., Moon, J. H., Seong, K. Y., & Park, K. H. (1998). Antimicrobial activity of 4-hydroxybenzoic acid and trans 4-hydroxycinnamic acid isolated and identified from rice hull. *Bioscience, Biotechnology and Biochemistry*, *62*(11). https://doi.org/10.1271/bbb.62.2273

Duangyod, T., Palanuvej, C., & Ruangrungsi, N. (2014). Catechins contents and *in vitro* antioxidant activities of *Pentace burmanica* stem bark. *Journal of Chemical and Pharmaceutical Research*, *6*(12), 137–142. www.jocpr.com

Duddeck, H., Snatzke, G., & Yemul, S. S. (1978). 13C NMR and CD of some 3,8″-biflavanoids from *Garcinia* species and of related flavanones. *Phytochemistry*, *17*(8). https://doi.org/10.1016/S0031-9422(00)94591-6

Elmore, S. (2007). Apoptosis: A Review of Programmed Cell Death. *Toxicologic Pathology*, *35*(4), 495–516. https://doi.org/10.1080/01926230701320337

Francenia Santos-Sánchez, N., Salas-Coronado, R., Villanueva-Cañongo, C., & Hernández-Carlos, B. (2019). *Antioxidant Compounds and Their Antioxidant Mechanism*. IntechOpen. https://doi.org/10.5772/intechopen.85270

Fu, M., Hu, X., Xu, J., Chen, Y., & Yang, G. (2014). In Vitro Assessment of Antidiabetic Activities of *Garcinia Xanthochymus* Leaf,Root and Fruit Extracts. *Natural Product Research and Development*, *26*(2), 255–259.

García, M. C., Rossen, L. M., Matthews, K., Guy, G., Trivers, K. F., Thomas, C. C., … Iademarco, M. F. (2024). Preventable Premature Deaths from the Five Leading Causes of Death in Nonmetropolitan and Metropolitan Counties, United States, 2010–2022. *MMWR. Surveillance Summaries*, *73*(2), 1–11. https://doi.org/10.15585/mmwr.ss7302a1

Gogoi, N., Gogoi, A., & Neog, B. (2015). Free radical scavenging activities of *Garcinia xanthochymus* hook. F. and *Garcinia lanceaefolia* roxb. using various *in vitro* assay models. *Asian Journal of Pharmaceutical and Clinical Research*, *8*(3). 138-141.

Gulcin, İ. (2020). Antioxidants and antioxidant methods: An updated overview. *Archives of Toxicology*, *94*(3). https://doi.org/10.1007/s00204-020-02689-3

Gunter, N. V., Teh, S. S., Jantan, I., Cespedes-Acuña, C. L., & Mah, S. H. (2023). The mechanisms of action of prenylated xanthones against breast, colon, and lung cancers, and their potential application against drug resistance. *Phytochemistry Reviews*, *22*(3). https://doi.org/10.1007/s11101-022-09846-9

Ha, L. D., Hansen, P. E., Vang, O., Duus, F., Pham, H. D., & Nguyen, L. H. D. (2009). Cytotoxic geranylated xanthones and O-alkylated derivatives of α-mangostin. *Chemical and Pharmaceutical Bulletin*, *57*(8). https://doi.org/10.1248/cpb.57.830

Hamidon, H., Taher, M., Jaffri, J. M., Tg Zakaria, T. M., Sulaiman, W. M., Susanti, D., … Zakaria, Z. A. (2016). Cytotoxic and Anti-Inflammatory Activities of *Garcinia xanthochymus* Extracts on Cell Lines. *Makara Journal of Health Research*, *20*(1). https://doi.org/10.7454/msk.v20i1.5599

Han, Q. B., Qiao, C. F., Song, J. Z., Yang, N. Y., Cao, X. W., Peng, Y., Yang, D. J., Chen, S. L., & Xu, H. X. (2007). Cytotoxic prenylated phenolic compounds from the Twig Bark of *Garcinia xanthochymus*. *Chemistry and Biodiversity*, *4*(5). https://doi.org/10.1002/cbdv.200790083

Hanahan, D., & Weinberg, R. A. (2011). Hallmarks of Cancer: *The Next Generation. Cell*, *144*(5), 646–674. https://doi.org/10.1016/j.cell.2011.02.013

He, X., Yang, F., & Huang, X. (2021). Proceedings of Chemistry, Pharmacology, Pharmacokinetics and Synthesis of Biflavonoids. *Molecules*, *26*(19), 6088. https://doi.org/10.3390/molecules26196088

Hemshekhar, M., Sunitha, K., Santhosh, M. S., Devaraja, S., Kemparaju, K., Vishwanath, B. S., … Girish, K. S. (2011). An overview on genus garcinia: Phytochemical and therapeutical aspects. *Phytochemistry Reviews*, *10*(3), 325–351. https://doi.org/10.1007/s11101-011-9207-3

Iinuma, M., Tosa, H., Tanaka, T., Asai, F., & Shimano, R. (1995). Three xanthones from root bark of *Garcinia subelliptica*. *Phytochemistry*, *38*(1). https://doi.org/10.1016/0031-9422(94)00595-K

Ito, C., Miyamoto, Y., Nakayama, M., Kawai, Y., Rao, K. S., & Furukawa, H. (1997). A novel depsidone and some new xanthones from *Garcinia species*. *Chemical and Pharmaceutical Bulletin*, *45*(9). https://doi.org/10.1248/cpb.45.1403

Jackson, D. N., Yang, L., Wu, S. B., Kennelly, E. J., & Lipke, P. N. (2015). *Garcinia xanthochymus* benzophenones promote hyphal apoptosis and potentiate activity of fluconazole against Candida albicans biofilms. *Antimicrobial Agents and Chemotherapy*, *59*(10). https://doi.org/10.1128/AAC.00820-15

Janhavi, P., Sindhoora, S., & Muthukumar, S. P. (2020). Bioaccessibility and bioavailability of polyphenols from sour mangosteen (*Garcinia xanthochymus*) fruit. *Journal of Food Measurement and Characterization*, *14*(5). https://doi.org/10.1007/s11694-020-00488-z

Ji, F., Li, Z., Liu, G., Niu, S., Zhao, N., Liu, X., & Hua, H. (2012). Xanthones with Antiproliferative Effects on Prostate Cancer Cells from the Stem Bark of *Garcinia xanthochymus*. *Natural Product Communications*, *7*(1), 53–56. https://doi.org/10.1177/1934578X1200700119

Jin, S., Shi, K., Liu, L., Chen, Y., & Yang, G. (2019). Xanthones from the bark of *Garcinia xanthochymus* and the mechanism of induced apoptosis in human hepatocellular carcinoma HepG2 cells via the mitochondrial pathway. *International Journal of Molecular Sciences*, *20*(19). https://doi.org/10.3390/ijms20194803

Brahma, J., Ray, S., Islary, A., & Saikia, B. (2025). Sustainable valorization of endemic Garcinia species namely Garcinia pedunculata, Garcinia morella and Garcinia xanthochymus of Bodoland Territorial Regions of Assam, India: physicochemical and biofunctional characterization. *Food Science and Applied Biotechnology*, *8*(1), 75-88. https://doi.org/10.30721/fsab2025.v8.i1.478

Joseph, K. S., Dandin, V. S., & Murthy Hosakatte, N. (2016). Chemistry and Biological Activity of *Garcinia xanthochymus*: A Review. *In Journal of Biologically Active Products from Nature*, *6*(3). https://doi.org/10.1080/22311866.2016.1199285

Kapadia, G. J., Oguntimein, B., & Shukla, Y. N. (1994). High-speed counter-current chromatographic separation of biflavanoids from *Garcinia kola* seeds. *Journal of Chromatography A*, *673*(1). https://doi.org/10.1016/0021-9673(94)87067-5

Khan, T., Ali, M., Khan, A., Nisar, P., Jan, S. A., Afridi, S., & Shinwari, Z. K. (2020). Anticancer plants: A review of the active phytochemicals, applications in animal models, and regulatory aspects. *Biomolecules*, *10*(1). https://doi.org/10.3390/biom10010047

Kim, H. P., Park, H., Son, K. H., Chang, H. W., & Kang, S. S. (2008). Biochemical pharmacology of biflavonoids: Implications for anti-inflammatory action. *Archives of Pharmacal Research*, *31*(3). https://doi.org/10.1007/s12272-001-1151-3

Koumaglo, K., Gbeassor, M., Nikabu, O., De Souza, C., & Werner, W. (1992). Effects of three compounds extracted from *Morinda lucida* on *Plasmodium falciparum*. *Planta Medica*, *58*(6). https://doi.org/10.1055/s-2006-961543

Kumatso, J. M., & Sigge, G. (2024). Nutritional Benefits, Phytoconstituents, and Pharmacological Properties of *Garcinia* Fruits: A Review. *Biointerface Research in Applied Chemistry*, *14*(5), 102. https://doi.org/10.33263/BRIAC144.102

Kurniawan, Y. S., Priyangga, K. T. A., Jumina, Pranowo, H. D., Sholikhah, E. N., Zulkarnain, A. K., Fatimi, H. A., & Julianus, J. (2021). An update on the anticancer activity of xanthone derivatives: A review. *Pharmaceuticals*, *14*(11). https://doi.org/10.3390/ph14111144

Li, X. C., Joshi, A. S., Tan, B., ElSohly, H. N., Walker, L. A., Zjawiony, J. K., & Ferreira, D. (2002). Absolute configuration, conformation, and chiral properties of flavanone-(3→8″)-flavone biflavonoids from Rheedia acuminata. *Tetrahedron*, *58*(43). https://doi.org/10.1016/S0040-4020(02)01096-7

Li, Y., & Ohizumi, Y. (2004). Search for constituents with neurotrophic factor-potentiating activity from the medicinal plants of Paraguay and Thailand. *In Yakugaku Zasshi*, *124*(7). https://doi.org/10.1248/yakushi.124.417

Li, Y., Zhao, P., Chen, Y., Fu, Y., Shi, K., Liu, L., … Xiao, Y. (2017). Depsidone and xanthones from *Garcinia xanthochymus* with hypoglycemic activity and the mechanism of promoting glucose uptake in L6 myotubes. *Bioorganic and Medicinal Chemistry*, *25*(24). https://doi.org/10.1016/j.bmc.2017.10.043

Milenković, D., Dimitrić Marković, J. M., Dimić, D., Jeremić, S., Amić, D., Pirković, M. S., & Marković, Z. S. (2019). Structural characterization of kaempferol: A spectroscopic and computational study. *Macedonian Journal of Chemistry and Chemical Engineering*, *38*(1). https://doi.org/10.20450/mjcce.2019.1333

Minami, H., Kinoshita, M., Fukuyama, Y., Kodama, M., Yoshizawa, T., Sugiura, M., … Tago, H. (1994). Antioxidant xanthones from *Garcinia subelliptica*. *Phytochemistry*, *36*(2). https://doi.org/10.1016/S0031-9422(00)97103-6

Minami, H., Takahashi, E., Kodama, M., & Fukuyama, Y. (1996). Three xanthones from *Garcinia Subelliptica*. *Phytochemistry*, *41*(2). https://doi.org/10.1016/0031-9422(95)00567-6

More, S. V., Koppula, S., Kim, I. S., Kumar, H., Kim, B. W., & Choi, D. K. (2012). The role of bioactive compounds on the promotion of neurite outgrowth. *Molecules*, *17*(6). https://doi.org/10.3390/molecules17066754

National Cancer Institute. (2024). Hospital-based cancer registry 2022. http://www.nci.go.th

Nguyen, C. N., Trinh, B. T. D., Tran, T. B., Nguyen, L. T. T., Jäger, A. K., & Nguyen, L. H. D. (2017). Anti-diabetic xanthones from the bark of *Garcinia xanthochymus*. *Bioorganic and Medicinal Chemistry Letters*, *27*(15). https://doi.org/10.1016/j.bmcl.2017.06.021

Nomura, T., Hano, Y., Okamoto, T., Suzuki, K., & Negishi, M. (1993). Components of the Root Bark of Morus insignis Bur. 3. Structures of Three New Isoprenylated Xanthones Morusignins I, J, and K and an Isoprenylated Flavone Morusignin L. *HETEROCYCLES*, *36*(6), 1359. https://doi.org/10.3987/COM-92-6320

Pailee, P., Kruahong, T., Hongthong, S., Kuhakarn, C., Jaipetch, T., Pohmakotr, M., … Reutrakul, V. (2017). Cytotoxic, anti-HIV–1 and anti-inflammatory activities of lanostanes from fruits of *Garcinia speciosa*. *Phytochemistry Letters*, *20*, 111–118. https://doi.org/10.1016/j.phytol.2017.04.007

Papaliagkas, V., Anogianaki, A., Anogianakis, G., & Ilonidis, G. (2007). The proteins and the mechanisms of apoptosis: A mini-review of the fundamentals. *Hippokratia*, *11*(3), 108.

Patel, J., Wong, H. Y., Wang, W., Alexis, J., Shafiee, A., Stevenson, A. J., Gabrielli, … Khosrotehrani, K. (2016). Self-Renewal and High Proliferative Colony Forming Capacity of Late-Outgrowth Endothelial Progenitors Is Regulated by Cyclin-Dependent Kinase Inhibitors Driven by Notch Signaling. *Stem Cells*, *34*(4), 902–912. https://doi.org/10.1002/stem.2262

Patil, M., & Appaiah, K. (2015). *Garcinia*: Bioactive compounds and health benefits. *Introduction to Functional Food Science*, *1*(January 2013), 110–125.

Paul, A., & Zaman, Md. K. (2022). A comprehensive review on ethnobotany, nutritional values, phytochemistry and pharmacological attributes of ten *Garcinia* species of South-east Asia. *South African Journal of Botany*, *148*, 39–59. https://doi.org/10.1016/j.sajb.2022.03.032

Payamalle, S., Joseph, K. S., Bijjaragi, S. C., Aware, C., Jadhav, J. P., & Murthy, H. N. (2017). Anti-diabetic activity of *Garcinia xanthochymus* seeds. *Comparative Clinical Pathology*, *26*(2). https://doi.org/10.1007/s00580-016-2396-9

Payamalle, S., & Murthy, H. N. (2015). Atomic force microscopic study for the antibacterial study of *Garcinia Xanthochymus* hook. F. leaf extract. *International Journal of Pharmacy and Pharmaceutical Sciences*, *7*(11).

Pinto, E., Afonso, C., Duarte, S., Vale-Silva, L., Costa, E., Sousa, E., & Pinto, M. (2011). Antifungal Activity of Xanthones: Evaluation of their Effect on Ergosterol Biosynthesis by High-performance Liquid Chromatography. *Chemical Biology and Drug Design*, *77*(3). https://doi.org/10.1111/j.1747-0285.2010.01072.x

Prakash, J., Sallaram, S., Martin, A., Veeranna, R. P., & Peddha, M. S. (2022). Phytochemical and Functional Characterization of Different Parts of the *Garcinia xanthochymus* Fruit. *ACS Omega*, *7*(24), 21172–21182. https://doi.org/10.1021/acsomega.2c01966

Pruksakorn, P., Lertru, S., Wachisunthon, D., Wanpen, K., Panyajai, P., & Prasertvaree, P. (2024). Antibacterial Activity of Benzophenones Derived from the Ripe Fruit Extract of *Garcinia xanthochymus* against *Streptococcus mutans. South Asian Research Journal of Natural Products*, *7*(3), 394–400.

Qian, S., Wei, Z., Yang, W., Huang, J., Yang, Y., & Wang, J. (2022). The role of BCL-2 family proteins in regulating apoptosis and cancer therapy. *Frontiers in Oncology*, *12*, 01–16. https://doi.org/10.3389/fonc.2022.985363

Quan, F., Luan, X., Zhang, J., Gao, W., Yan, J., & Li, P. (2023). Cytotoxic Isopentenyl Phloroglucinol Compounds from *Garcinia xanthochymus* Using LC-MS-Based Metabolomics. *Metabolites*, *13*(2). https://doi.org/10.3390/metabo13020258

Rahminiwati, M., Iswantini, D., Trivadila, Sianipar, R. N. R., Sukma, R. M., Indariani, S., & Murni, A. (2025). The Strong Inhibition of Pancreatic Lipase by Selected Indonesian Medicinal Plants as Anti-Obesity Agents. In *Current Issues in Molecular Biology*, *47*(1), 29. Multidisciplinary Digital Publishing Institute (MDPI). https://doi.org/10.3390/cimb47010039

Reutrakul, V., Anantachoke, N., Pohmakotr, M., Jaipetch, T., Sophasan, S., Yoosook, C., … Tuchinda, P. (2006). Cytotoxic and Anti-HIV-1 Caged Xanthones from the Resin and Fruits of *Garcinia hanburyi*. *Planta Medica*, *73*(01), 33–40. https://doi.org/10.1055/s-2006-951748

Rob, M. M., Hossen, K., Khatun, M. R., Iwasaki, K., Iwasaki, A., Suenaga, K., & Kato-Noguchi, H. (2021). Identification and application of bioactive compounds from *Garcinia xanthochymus* Hook. f. For weed management. *Applied Sciences (Switzerland)*, *11*(5). https://doi.org/10.3390/app11052264

Rob, M. M., Iwasaki, A., Suzuki, R., Suenaga, K., & Kato-Noguchi, H. (2019). Garcienone, a novel compound involved in allelopathic activity of *Garcinia xanthochymus* Hook.f.. *Plants*, *8*(9). https://doi.org/10.3390/plants8090301

Safe, S. (2024). Natural products as anticancer agents and enhancing their efficacy by a mechanism-based precision approach. *Exploration of Drug Science*, 408–427. https://doi.org/10.37349/eds.2024.00054

Sangchan, A., Bootdee, A., & Chanroj, S. (2016). Inhibitory Effects of Cinnamon and Garcinia Crude Extracts on Alpha-amylase, Lipase, Trypsin and Alcohol Dehydrogenase. *Burapha Science Journal*, *21*(3), 268–278.

Seifried, H. E., McDonald, S. S., Anderson, D. E., Greenwald, P., & Milner, J. A. (2003). The antioxidant conundrum in cancer. *Cancer research*, *63*(15), 4295-4298.

Shan, T., Ma, Q., Guo, K., Liu, J., Li, W., Wang, F., & Wu, E. (2011). Xanthones from Mangosteen Extracts as Natural Chemopreventive Agents: Potential Anticancer Drugs. *Current Molecular Medicine*, *11*(8). https://doi.org/10.2174/156652411797536679

Shen, Y. C., Wang, L. T., Khalil, A. T., Chiang, L. C., & Cheng, P. W. (2005). Bioactive pyranoxanthones from the roots of *Calophyllum blancoi*. *Chemical and Pharmaceutical Bulletin*, *53*(2). https://doi.org/10.1248/cpb.53.244

Sripan, P., Sriplung, H., Pongnikorn, D., Virani, S., Bilheem, S., Chaisaengkhaum, U., … Chitapanarux, I. (2017). Trends in female breast cancer by age group in the Chiang Mai population. *Asian Pacific Journal of Cancer Prevention*, *18*(5). https://doi.org/10.22034/APJCP.2017.18.5.1411

Sunkar, S., & Nachiyar, C. V. (2012). Biogenesis of antibacterial silver nanoparticles using the endophytic bacterium Bacillus cereus isolated *from Garcinia xanthochymus*. *Asian Pacific Journal of Tropical Biomedicine*, *2*(12). https://doi.org/10.1016/S2221-1691(13)60006-4

Tourinho-Barbosa, R. R., Pompeo, A. C. L., & Glina, S. (2016). Prostate cancer in Brazil and Latin America: epidemiology and screening. *International Braz j Urol*, *42*(6), 1081–1090. https://doi.org/10.1590/s1677-5538.ibju.2015.0690

Tran, N., Nguyen, M., Le, K. P. B., Nguyen, N., Tran, Q., & Le, L. (2020). Screening of antibacterial activity, antioxidant activity, and anticancer activity of *Euphorbia hirta* linn. Extracts. *Applied Sciences (Switzerland)*, *10*(23). https://doi.org/10.3390/app10238408

Tran, T. T. T., Le, P. M., Nguyen, T. K. A., Hoang, T. M. N., Do, T. Q. A., Martel, A. L., … Le, H. T. (2023). Novel human STING activation by hydrated-prenylated xanthones from *Garcinia cowa. Journal of Pharmacy and Pharmacology*, *75*(8). https://doi.org/10.1093/jpp/rgad038

Trisuwan, K., Boonyaketgoson, S., Rukachaisirikul, V., & Phongpaichit, S. (2014). Oxygenated xanthones and biflavanoids from the twigs of *Garcinia xanthochymus*. *Tetrahedron Letters*, *55*(26). https://doi.org/10.1016/j.tetlet.2014.04.105

Van Meerloo, J., Kaspers, G. J., & Cloos, J. (2011). Cell sensitivity assays: the MTT assay. In *Cancer cell culture: methods and protocols* (pp. 237-245). Totowa, NJ: Humana press. https://doi.org/10.1007/978-1-61779-080-5_20

Winata, H. S., Hafiz, I., Kartika, Y., & Sihombing, D. (2021). Inflammatory Activity Test of N-Hexant Extract of Kandis Acid (*Garcinia xanthochymus*) Against Male White Mice (*Rattus norvegicus*). *Budapest International Research and Critics Institute-Journal (BIRCI-Journal)*, *4*(3), 5034-5042.

Wollenweber, E., Dörr, M., Roitman, J. N., & Arriaga-Giner, F. J. (1994). Triterpenes and a novel natural xanthone as lipophilic glandular products in hypericum balearicum. *Zeitschrift Fur Naturforschung - Section C Journal of Biosciences*, 49(5–6). https://doi.org/10.1515/znc-1994-5-617

World Health Organization (WHO). (2024). *Global cancer burden growing, amidst mounting need for services*. WHO.

Xiao, X., Ren, W., Zhang, N., Bing, T., Liu, X., Zhao, Z., & Shangguan, D. (2019). Comparative Study of the Chemical Constituents and Bioactivities of the Extracts from Fruits, Leaves and Root Barks of *Lycium barbarum*. *Molecules*, *24*(8). https://doi.org/10.3390/molecules24081585

Xu, J., Gan, S., Li, J., Wand, D. B., Chen, Y., Hu, X., & Yang, G. Z. (2017). *Garcinia xanthochymus* extract protects PC12 cells from H 2 O 2-induced apoptosis through modulation of PI3K/AKT and NRF2/HO-1 pathways. *Chinese Journal of Natural Medicines*, *15*(11), 825-833. https://doi.org/10.1016/S1875-5364(18)30016-5

Xu, J., Jin, S., Gan, F., Xiong, H., Mei, Z., Chen, Y., & Yang, G. (2020). Polycyclic polyprenylated acylphloroglucinols from *Garcinia xanthochymus* fruits exhibit antitumor effects through inhibition of the STAT3 signaling pathway. *Food & Function*, *11*(12), 10568–10579. https://doi.org/10.1039/D0FO02535F

Xu, Z. H., Grossman, R. B., Qiu, Y. F., Luo, Y., Lan, T., & Yang, X. W. (2022). Polycyclic Polyprenylated Acylphloroglucinols Bearing a Lavandulyl-Derived Substituent from *Garcinia xanthochymus* Fruits. *Journal of Natural Products*, *85*(12). https://doi.org/10.1021/acs.jnatprod.2c00888

Xu, Z. H., Luo, Y., Qiu, Y. F., Yang, X. W., & Lan, T. (2023). Prenylated acylphloroglucinols from the fruits of *Garcinia xanthochymus*. *Fitoterapia*, *165*. https://doi.org/10.1016/j.fitote.2023.105427

Zehiroglu, C., & Ozturk Sarikaya, S. B. (2019). The importance of antioxidants and place in today's scientific and technological studies. *In Journal of Food Science and Technology*, *56*(11). https://doi.org/10.1007/s13197-019-03952-x

Zhang, J., Su, G., Lin, Y., Meng, W., Lai, J. K. L., Qiao, L., … Xie, X. (2019). Targeting cyclin-dependent kinases in gastrointestinal cancer therapy. *Discovery Medicine*, *27*(146), 27–36.

Zhong, F., Chen, Y., Wang, P., Feng, H., & Yang, G. (2009). Xanthones from the bark of *Garcinia xanthochymus* and their 1,1-diphenyl-2-picrylhydrazyl radical-scavenging activity. *Chinese Journal of Chemistry*, *27*(1). https://doi.org/10.1002/cjoc.200990029

Zhong, F. F., Chen, Y., Song, F. J., & Yang, G. Z. (2008). Three new xanthones from *Garcinia xanthochymus*. *Yaoxue Xuebao*, *43*(9).

APPENDIX A

^{1}H NMR AND CD SPECTRUM OF ISOLATED COMPOUND FROM *Garcinia xanthochymus* Hook. f.

The ^{1}H NMR spectrum of GXBAsm-1 to GXTM-sm22 and CD spectrum of GXBA-sm9 and GXTM-sm15 was how in the figureA1 to A24.

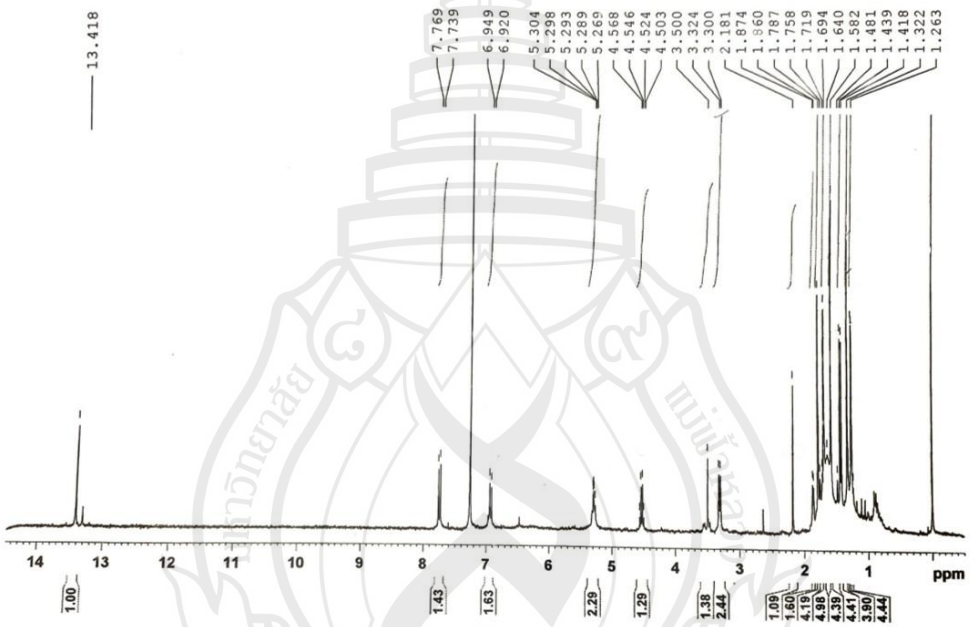

Figure A1 ^{1}H NMR spectrum of GXBA-sm1

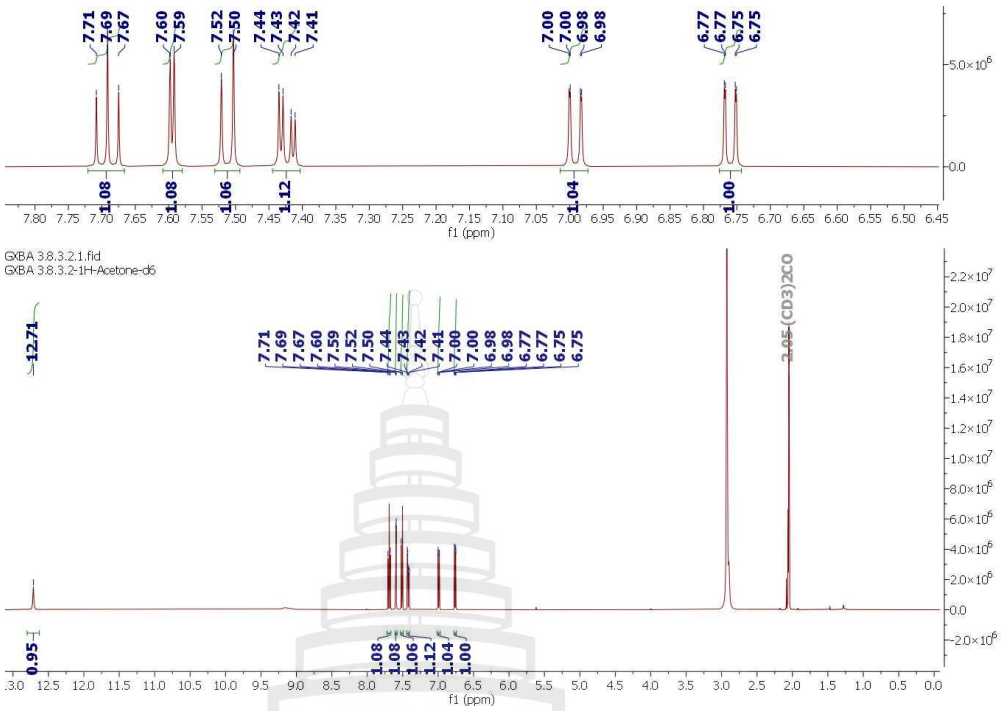

Figure A2 ^{1}H NMR spectrum of GXBA-sm2

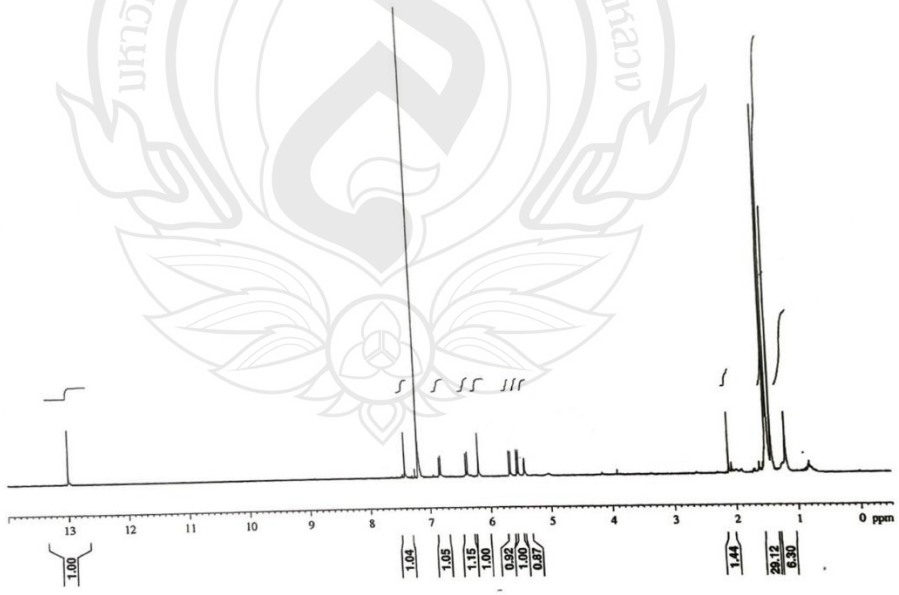

Figure A3 ^{1}H NMR spectrum of GXBA-sm3

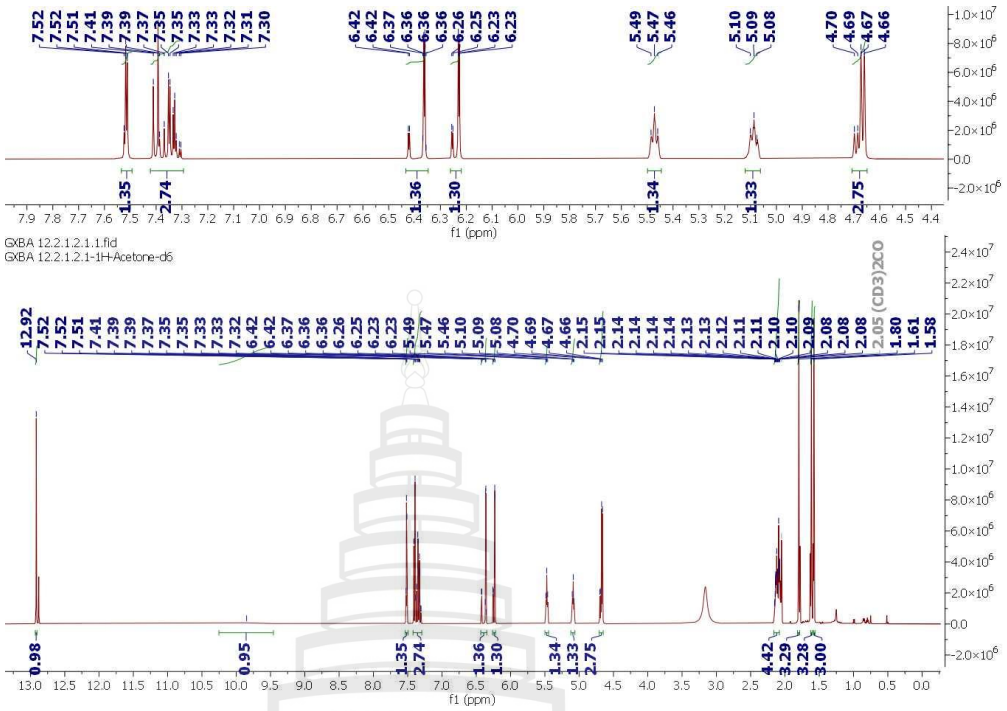

Figure A4 ^{1}H NMR spectrum of GXBA-sm4

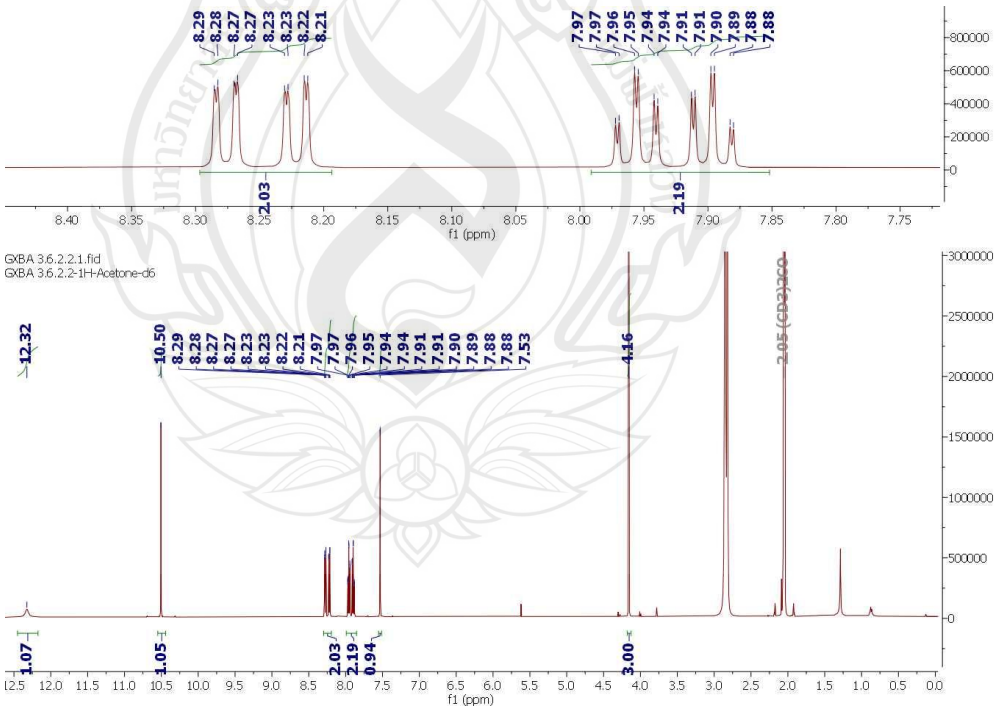

Figure A5 ^{1}H NMR spectrum of GXBA-sm5

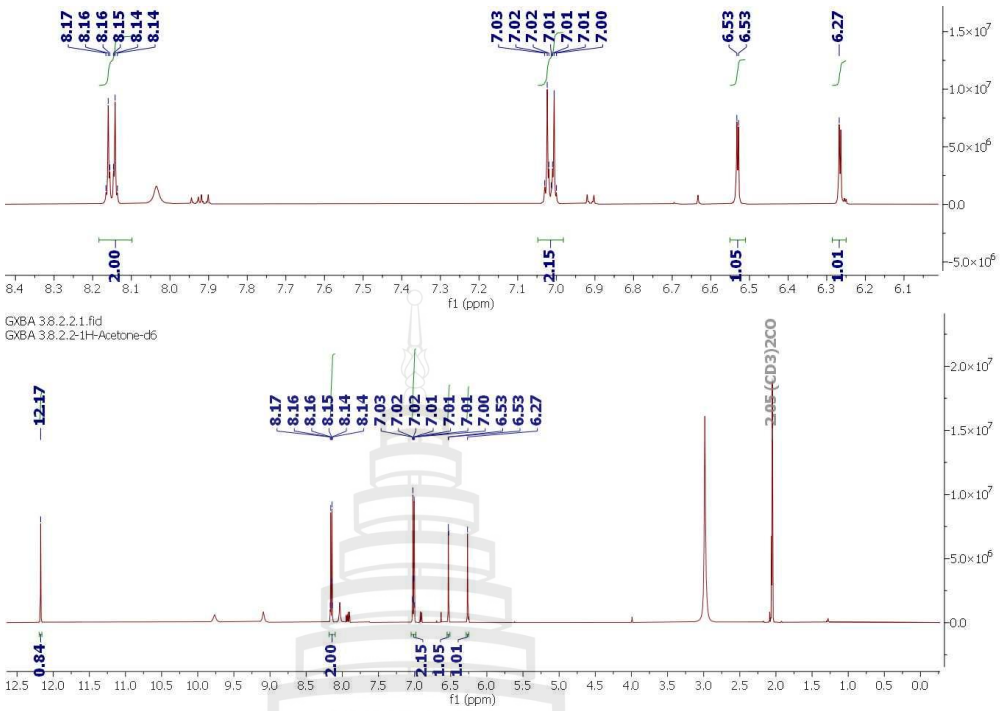

Figure A6 ^{1}H NMR spectrum of GXBA-sm6

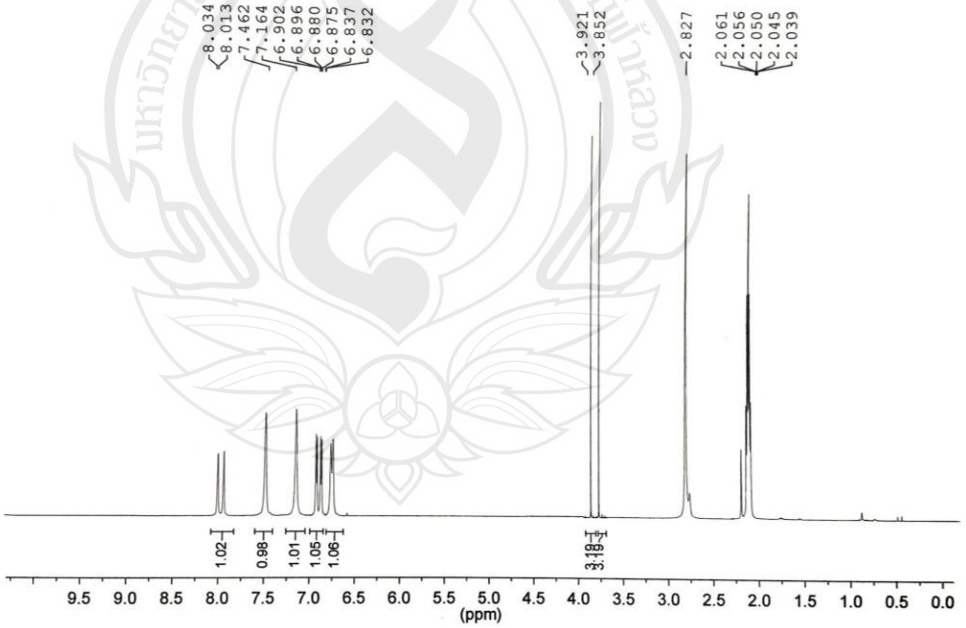

Figure A7 ^{1}H NMR spectrum of GXBA-sm7

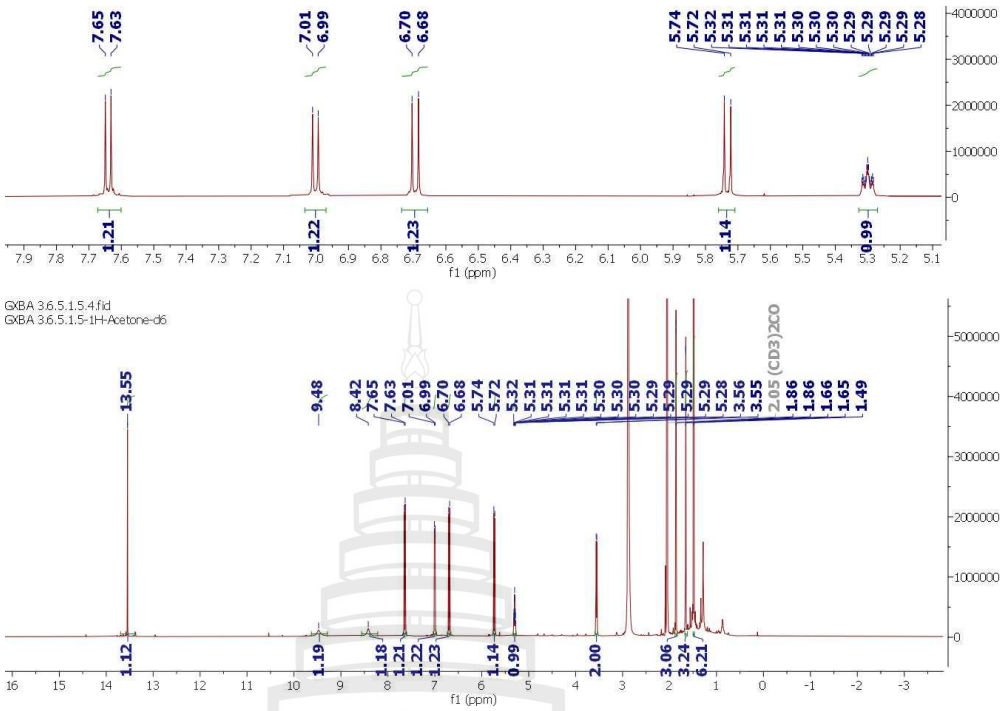

Figure A8 ^{1}H NMR spectrum of GXBA-sm8

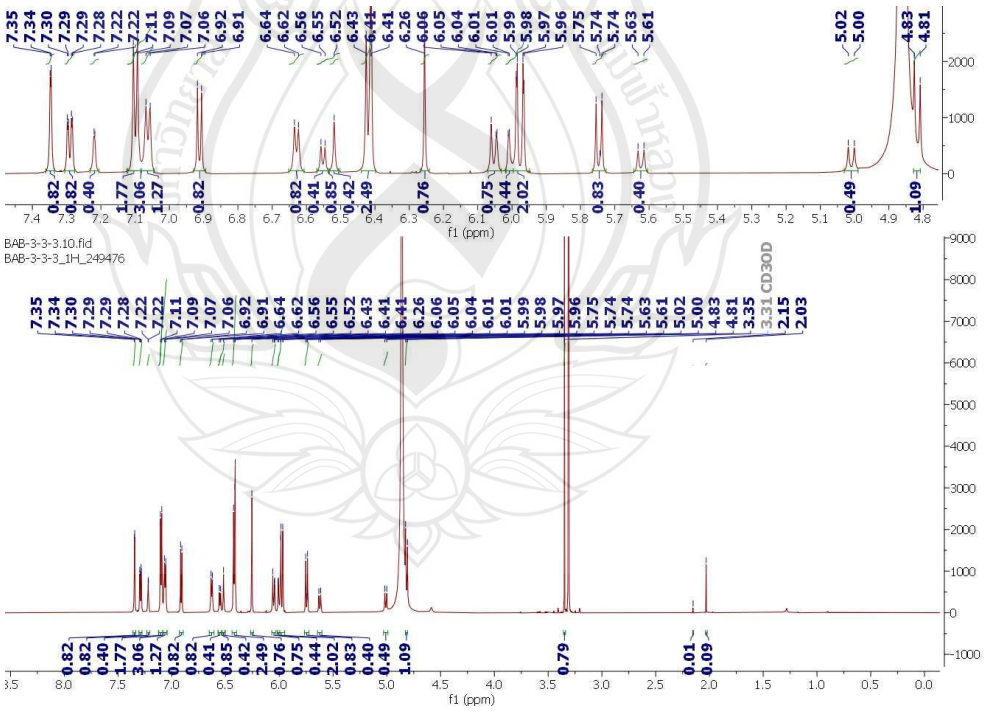

Figure A9 ^{1}H NMR spectrum of GXBA-sm9

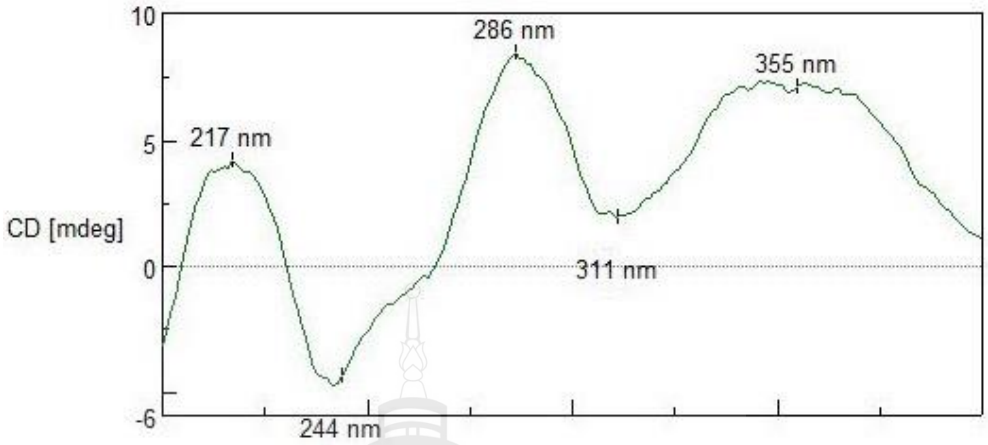

Figure A10 CD spectrum of GXBA-sm9

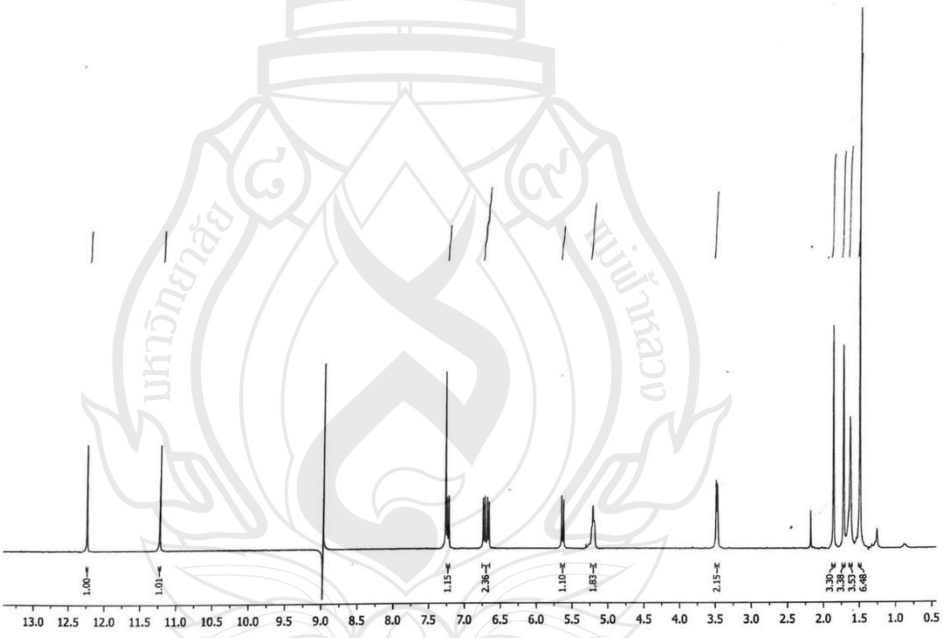

Figure A11 ^{1}H NMR spectrum of GXBA-sm10

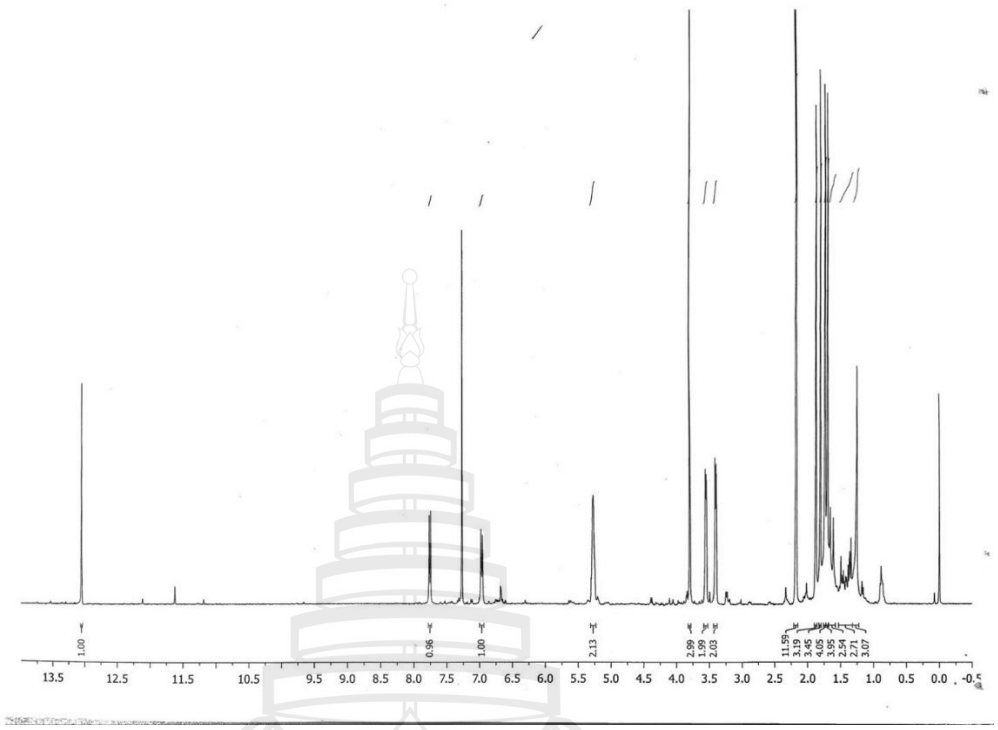

Figure A12 ^{1}H NMR spectrum of GXBA-sm11

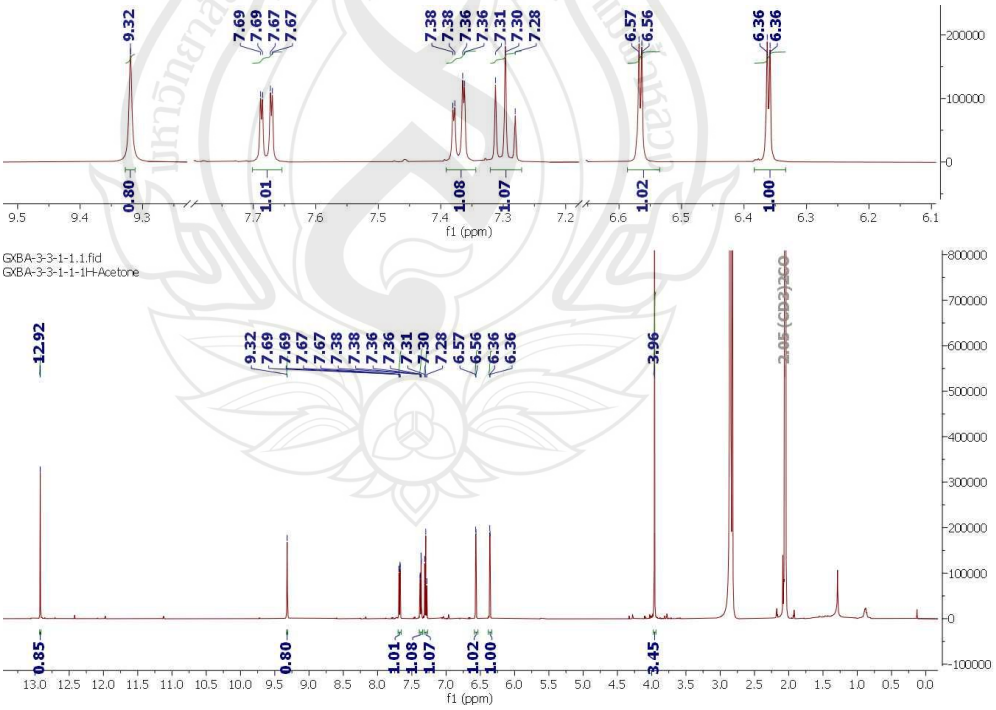

Figure A13 ^{1}H NMR spectrum of GXBA-sm12

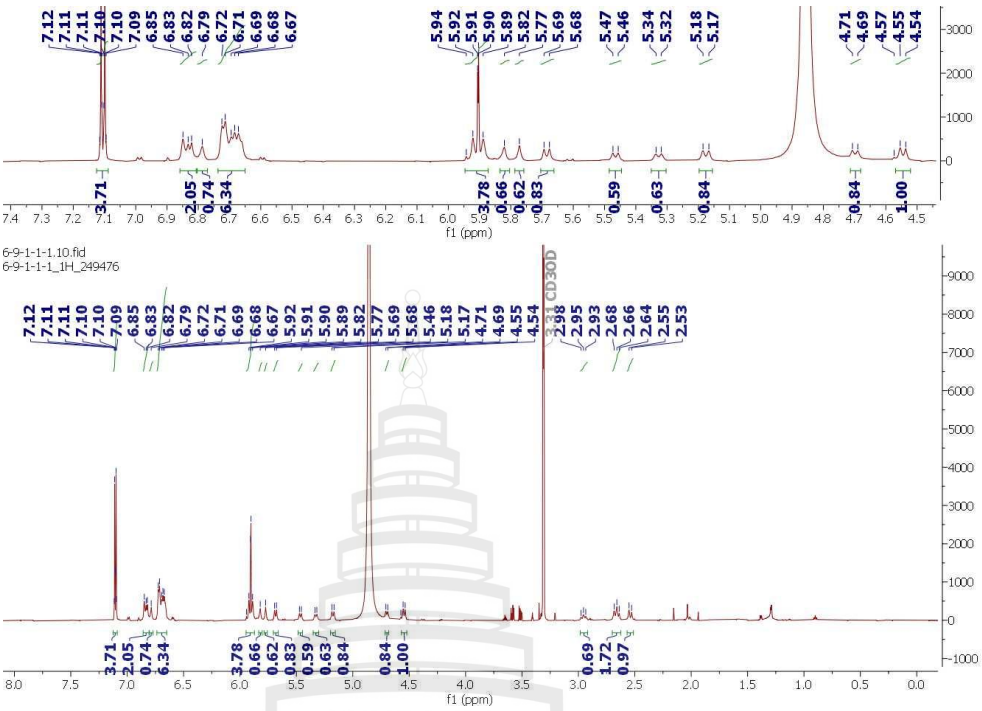

Figure A14 ^{1}H NMR spectrum of GXTM-sm13

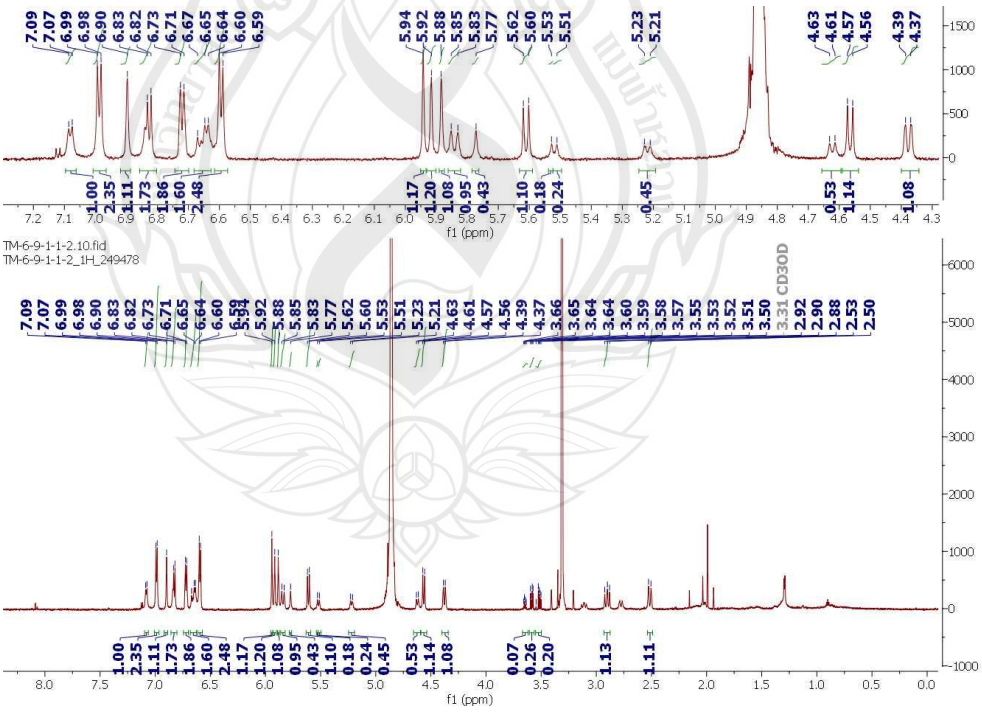

Figure A15 ^{1}H NMR spectrum of GXTM-sm14

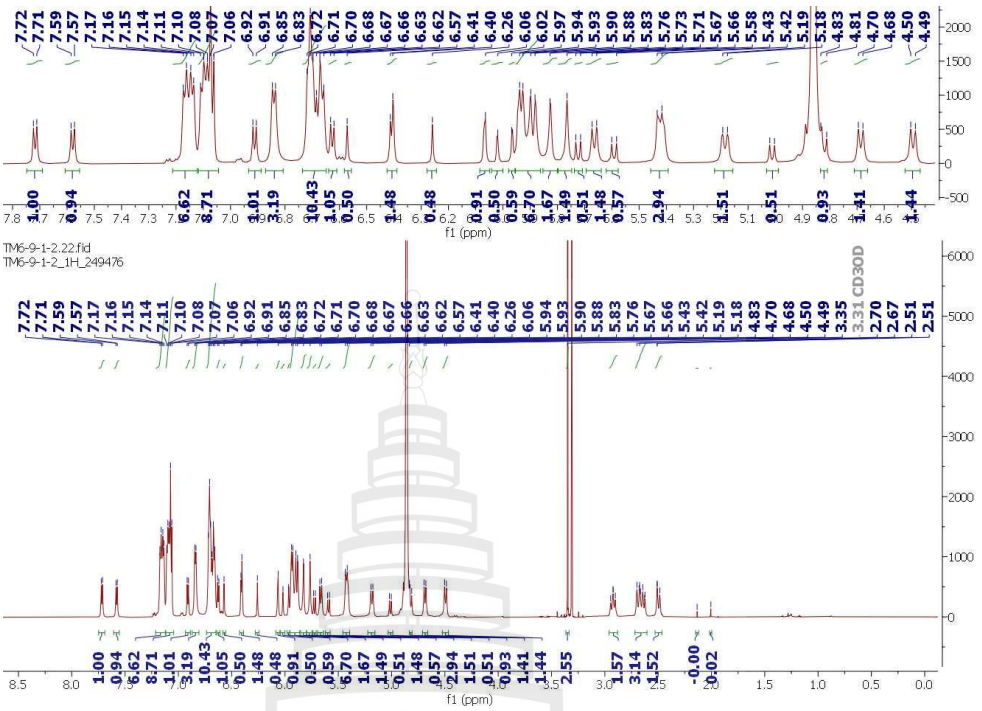

Figure A16 ^{1}H NMR spectrum of GXTM-sm15

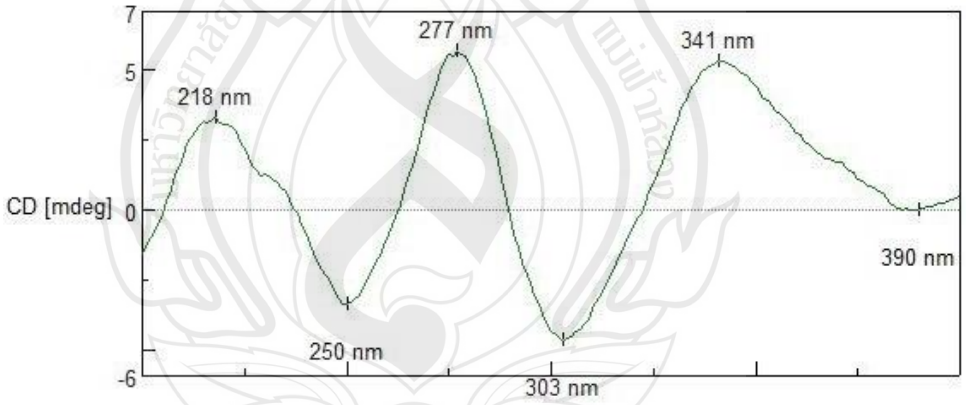

Figure A17 CD spectrum of GXTM-sm15

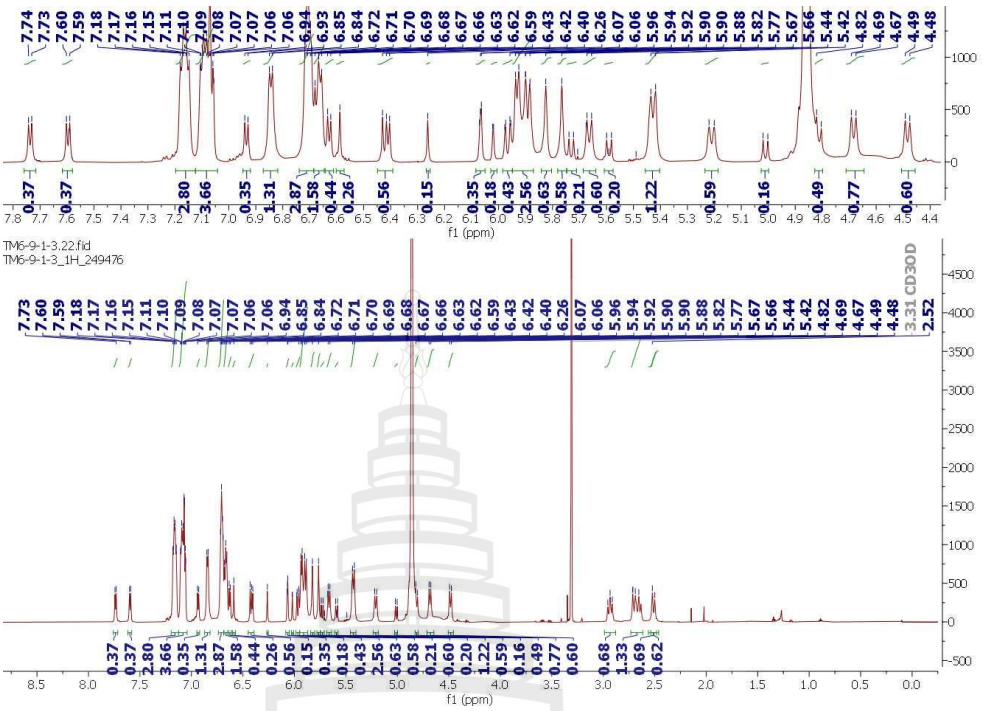

Figure A18 ^{1}H NMR spectrum of GXTM-sm16

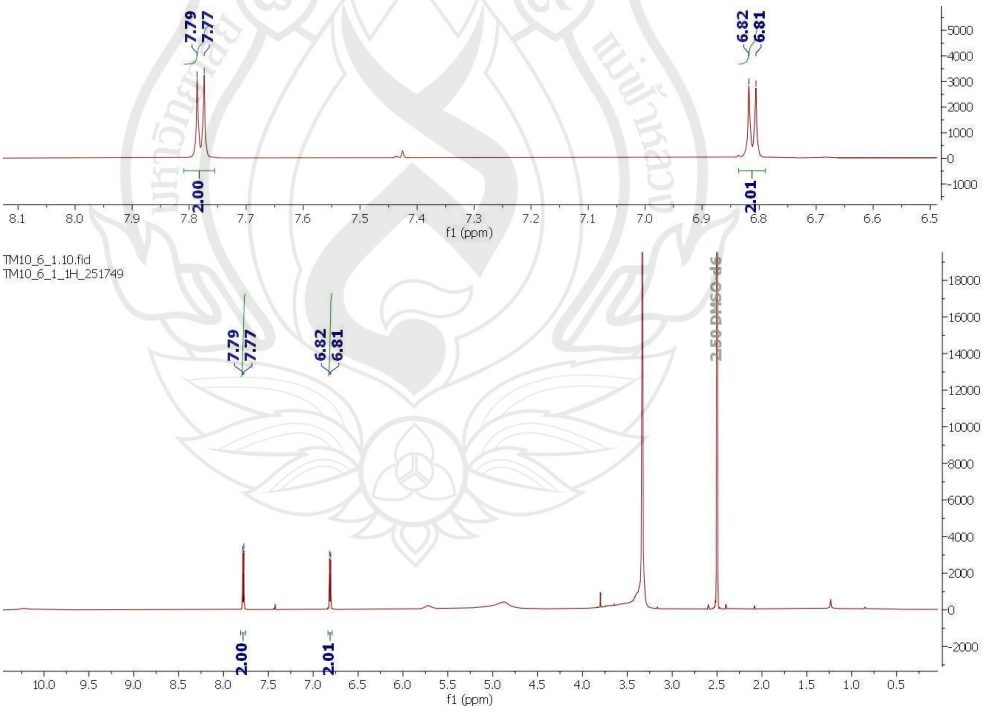

Figure A19 ^{1}H NMR spectrum of GXTM-sm17

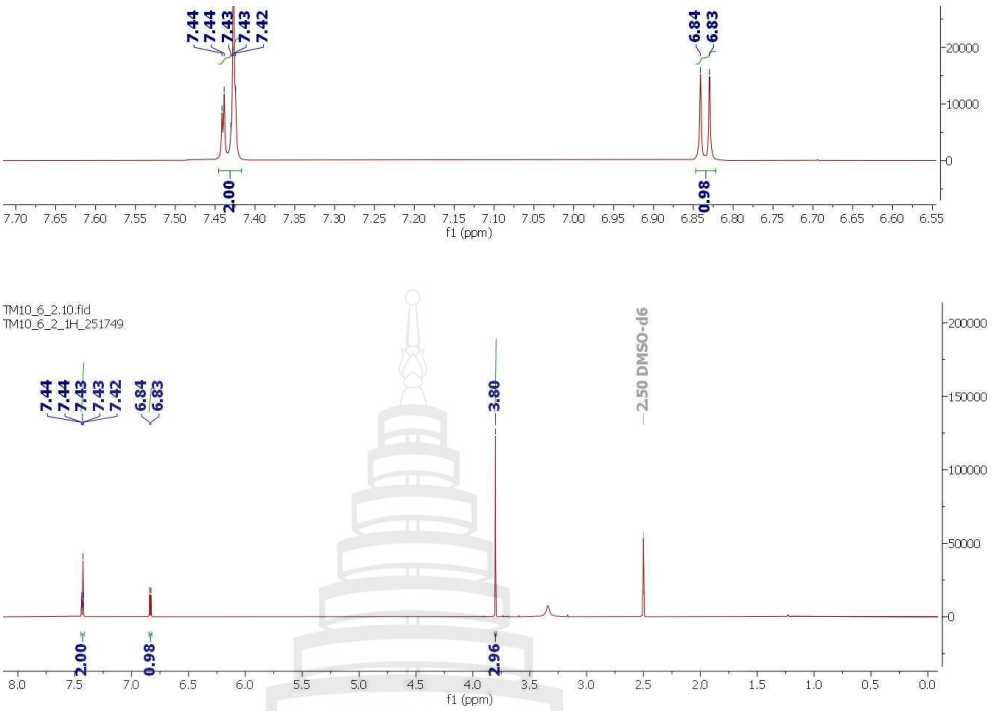

Figure A20 ^{1}H NMR spectrum of GXTM-sm18

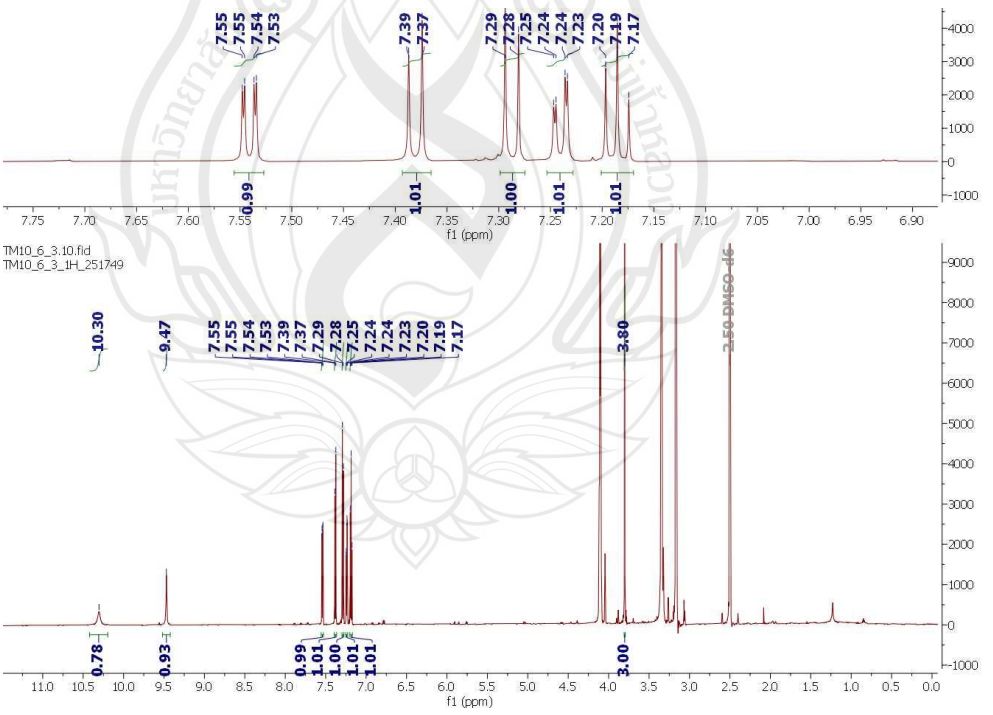

Figure A21 ^{1}H NMR spectrum of GXTM-sm19

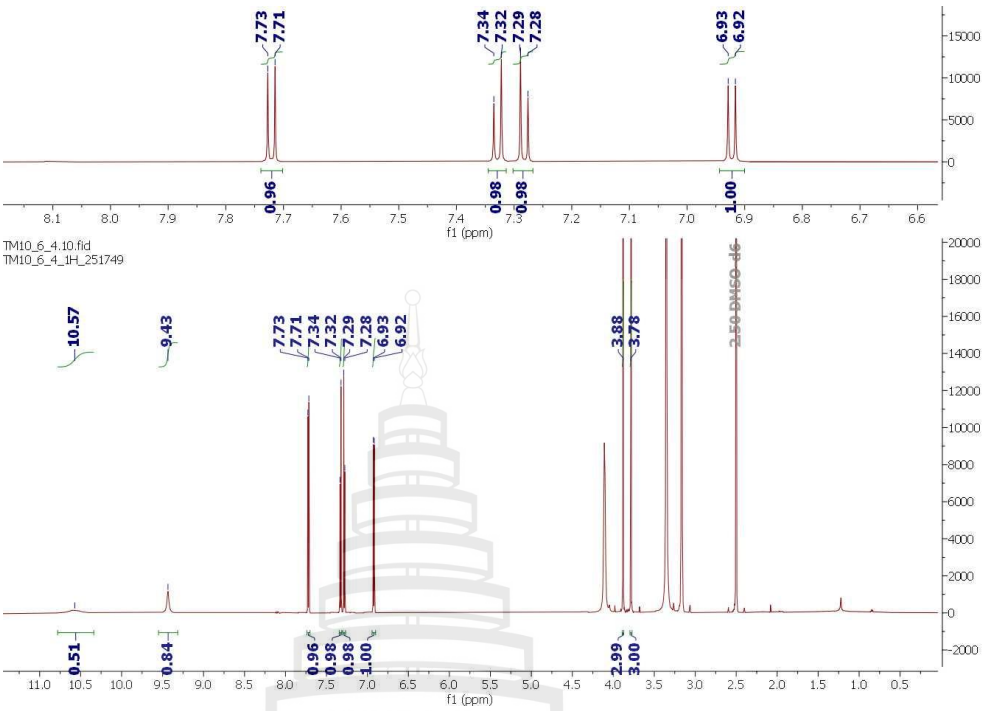

Figure A22 ^{1}H NMR spectrum of GXTM-sm20

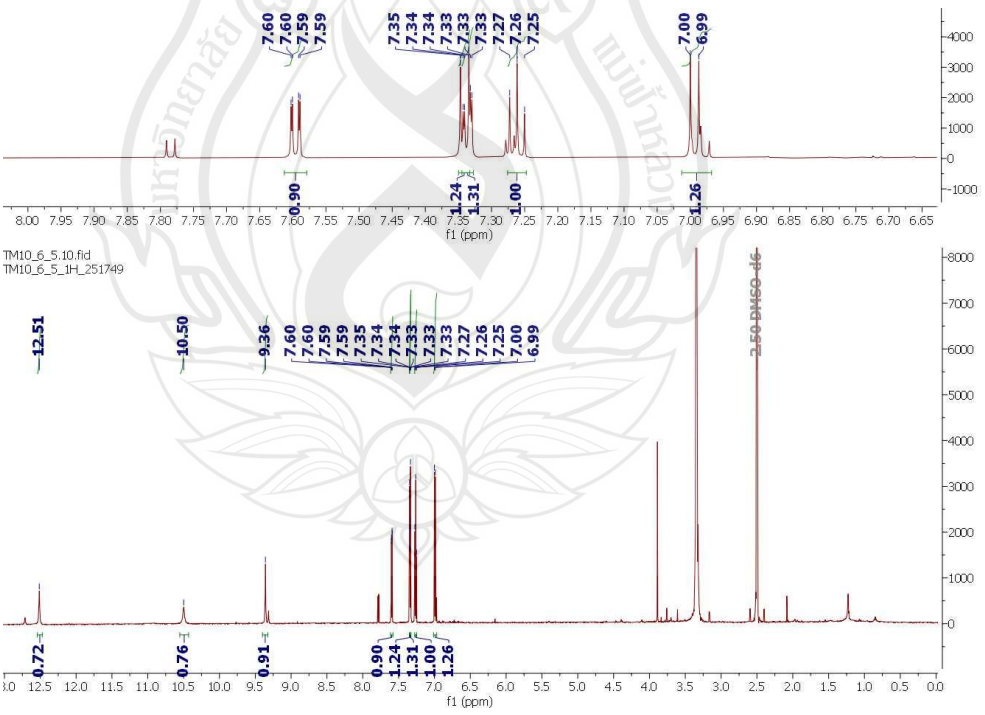

Figure A23 ^{1}H NMR spectrum of GXTM-sm21

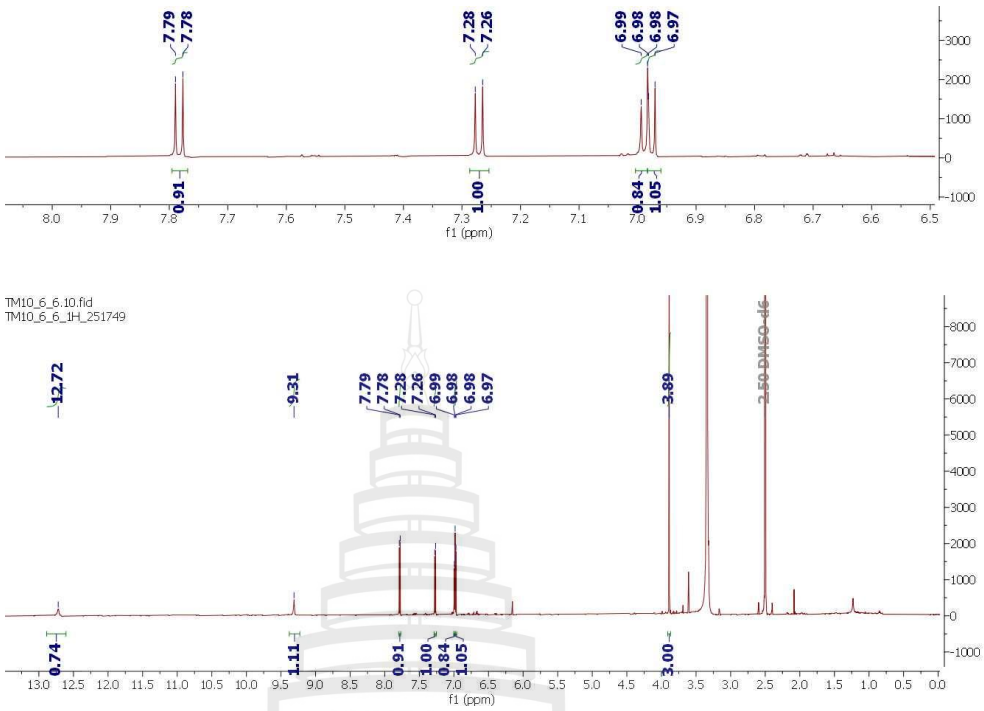

Figure A24 ^{1}H NMR spectrum of GXTM-sm22

APPENDIX B

LIST OF SECONDARY MARTABOLITES AND CHROMATOGRAM FROM UHPLC-QTOF

The secondary metabolite in crude extract of *G. xanthochymus* was analyzed by UHPLC-QTOF, which show in Table A1 and the chromatogram in both of positive and negative was show in figureA25-A46.

Table A1 Metabolite identification in extracts from different parts of *G. xanthochymus*

No.	RT	Type of ion	Mass	Formular	Score	Identification	Class	Extract parts
1	1.497	[M-H] $^-$	243.94	$C_8H_5BrO_4$	67.62	4-Bromoisophthalic acid	Other	BH
2	1.634	[M-H] $^-$	311.94	$C_8H_4F_3IN_2$	83.24	3-(Trifluoromethyl)-3-(3-iodophenyl) diazirine	Other	BH
3	1.739	[M+H] +	163.08	$C_6H_{13}NO_4$	77.97	4-Amino-4,6-dideoxy-D-mannose	Flavonoid	LA
4	1.806	[M+H] +	706.26	$C_{38}H_{42}O_{13}$	67.78	unknow	Flavonoid	BH, TH, TM
5	1.892	[M-H] $^-$	194.00	$C_7H_2F_4O_2$	59.54	2,3,4,5-Tetrafluorobenzoic acid	Other	BH
6	2.469	[M-H] $^-$	192.03	$C_6H_8O_7$	95.53	Citric acid	Flavonoid	TH
7	6.151	[M+H] +	230.16	$C_{11}H_{22}N_2O_3$	81.27	D-Leucyl-D-valine	Flavonoid	LM
8	7.161	[M-H] $^-$	112.02	$C_5H_4O_3$	86.45	Pyromeconic acid	Other	BH
9	7.998	[M+H] +	394.15	$C_{16}H_{26}O_{11}$	92.78	3-Methylbut-2-enoyl-1-O-β-D-glucopyranosyl-β-D-apiofuranoside	Other	BM
10	8.024	[M+H] +	432.11	$C_{21}H_{20}O_{10}$	86.56	Vitexin	Flavonoid	BM
11	8.809	[M+H] +	168.04	$C_8H_8O_4$	45.62	4-Methoxysalicylic acid	Flavonoid	LA
12	10.624	[M-H] $^-$	166.03	$C_8H_6O_4$	99.66	Terephthalic acid	Benzophenone	TH
13	10.663	[M-H] $^-$	122.04	$C_7H_6O_2$	86.76	2-Hydroxybenzaldehyde	Flavonoid	BD
14	10.669	[M-H] $^-$	166.03	$C_8H_6O_4$	92.85	Terephthalic acid	Flavonoid	BD
15	11.321	[M-H] $^-$	154.03	$C_7H_6O_4$	88.23	Gentisic acid	Flavonoid	BD
16	11.616	[M+H] +	420.16	$C_{25}H_{24}O_6$	64.82	Pomiferin	Flavonoid	LH, LD
17	12.059	[M+H] +	652.25	$C_{35}H_{40}O_{12}$	91.84	Triptofordin F4	Flavonoid	BH
18	12.114	[M-H] $^-$	178.03	$C_9H_6O_4$	85.11	3,5-Dihydroxybenzoic acid	Phloroglucinol	BD
19	12.431	[M+H] +	414.24	$C_{14}H_{34}N_6O_8$	91.98	2,2'-Azobis[n-(2-carboxyethyl)-2-methylpropionamidine]	Flavonoid	LA
20	12.947	[M-H] $^-$	198.05	$C_9H_{10}O_5$	80.55	Syringic acid	Flavonoid	BD
21	13.604	[M-H] $^-$	166.06	$C_9H_{10}O_3$	83.83	Tropic acid	Other	TD
22	13.604	[M-H] $^-$	182.06	$C_9H_{10}O_4$	80.00	Hydroxy tropic acid	Other	TD
23	13.606	[M+H] +	508.21	$C_{29}H_{32}O_8$	75.22	Gomisin G	Flavonoid	BD
24	14.451	[M+H] +	596.42	$C_{41}H_{56}O_3$	94.12	Bacteriorubixanthinal	Carotenoid	LM
25	14.494	[M+H] +	596.42	$C_{41}H_{56}O_3$	91.09	Bacteriorubixanthinal	Polyphenol	BD
26	16.147	[M+H] +	252.12	$C_{11}H_{16}N_4O_3$	85.90	Histidylproline	Flavonoid	LD
27	16.329	[M+H] +	602.36	$C_{38}H_{50}O_6$	94.79	(-)-Guttiferone E	Xanthone	BD, LM, TH, TA, TM

Table A1 Metabolite identification in extracts from different parts of *G. xanthochymus*

No.	RT	Type of ion	Mass	Formular	Score	Identification	Class	Extract parts
28	16.341	[M+H] +	602.36	$C_{38}H_{50}O_6$	85.00	Guttiferone F	Xanthone	TA
29	16.713	[M-H] $^-$	286.10	$C_{20}H_{14}O_2$	61.31	1,2-Dibenzoylbenzene	Benzophenone	TH
30	16.718	[M+H] +	740.47	$C_{40}H_{68}O_{12}$	69.17	Gypenoside LXXVII	Flavonoid	LD
31	17.108	[M-H] $^-$	374.10	$C_{19}H_{18}O_8$	99.43	1,5,8-Trihydroxy-3-methyl-6-prenylxanthone	Xanthone	BM, LH, LM
32	17.181	[M-H] $^-$	718.15	$C_{36}H_{30}O_{16}$	78.81	Fukugiside	Flavonoid	TA
33	17.221	[M+H] +	354.11	$C_{20}H_{18}O_6$	80.95	Curcumin derivative	Flavonoid	LD
34	17.556	[M+H] +	288.06	$C_{15}H_{12}O_6$	72.35	3',4',5,7-Tetrahydroxyisoflavanone	Flavonoid	TA
35	17.601	[M-H] $^-$	704.17	$C_{36}H_{32}O_{15}$	67.47	Occidentoside	Flavonoid	TA
36	18.221	[M+H] +	532.30	$C_{30}H_{44}O_8$	43.07	Ganoderic acid	Flavonoid	TH
37	18.247	[M-H] $^-$	556.10	$C_{30}H_{20}O_{11}$	81.04	Morelloflavone	Flavonoid	TM
38	18.248	[M+H] +	556.10	$C_{30}H_{20}O_{11}$	77.02	Ephedrannin A	Other	TA, TD
39	18.552	[M-H] $^-$	358.07	$C_{18}H_{14}O_8$	80.75	Psoromic acid	Xanthone	BH, LD, LA, TD
40	18.581	[M-H] $^-$	540.11	$C_{30}H_{20}O_{10}$	73.51	Volkensiflavone	Flavonoid	TM
41	18.590	[M+H] +	518.12	$C_{28}H_{22}O_{10}$	71.78	Xanosporolactone	Other	TA, TD
42	18.595	[M-H] $^-$	402.10	$C_{20}H_{18}O_9$	96.88	4-O-Demethyl-13-dihydroadriamycinone	Flavonoid	BH
43	18.600	[M-H] $^-$	224.10	$C_{12}H_{16}O_4$	70.95	Aspidinol	Other	BH
44	18.618	[M-H] $^-$	542.12	$C_{30}H_{22}O_{10}$	97.39	Neochamaejasmin A	Flavonoid	TM
45	18.808	[M-H] $^-$	396.16	C_{23} H_{24} O_6	94.48	4-(1,1-Dimethyl-2-propenyl)-1,3,5,6 tetrahydroxy-7-prenylxanthone	Xanthone	BH
46	18.811	[M+H] +	396.16	$C_{23}H_{24}O_6$	77.26	4-(1,1-Dimethyl-2-propenyl)-1,3,5,6-tetrahydroxy-7-prenylxanthone	Xanthone	BH
47	18.887	[M-H] $^-$	478.05	$C_{24}H_{14}O_{11}$	55.55	Fucofuroeckol B	Flavonoid	TM
48	19.273	[M-H] $^-$	372.08	$C_{19}H_{16}O_8$	87.36	7-Hydroxy-3,5,8-trimethoxy-3',4'-methylenedioxyflavone	Flavonoid	BM, LH, LD, LA, LM, TM
49	19.375	[M+H] +	394.14	C_{23} H_{22} O_6	79.87	Garcinone B	Xanthone	BH
50	19.538	[M-H] $^-$	320.05	C_{15} H_{12} O_8	76.20	2,7-Dimethoxy-1,3,6,8 tetrahydroxyxanthone	Xanthone	BH
51	19.708	[M-H] $^-$	326.08	C_{18} H_{14} O_6	68.17	O-Demethylforbexanthone	Xanthone	BH
52	19.712	[M-H] $^-$	594.14	$C_{30}H_{26}O_{13}$	79.58	Tiliroside	Flavonoid	TM

Table A1 Metabolite identification in extracts from different parts of *G. xanthochymus*

No.	RT	Type of ion	Mass	Formular	Score	Identification	Class	Extract parts
53	20.480	[M-H] $^-$	326.08	C_{18} H_{14} O_6	80.76	Globulixanthone C	Xanthone	BH
54	20.619	[M-H] $^-$	566.12	$C_{32}H_{22}O_{10}$	74.23	Podocarpusflavone B	Flavonoid	BM, LD
55	20.672	[M-H] $^-$	412.15	C_{23} H_{24} O_7	76.78	1,3,8-Trihydroxy-2-(3-methyl-2 butenyl)-4-(3-hydroxy-3 methylbutanoyl)-xanthone	Xanthone	BH
56	20.845	[M-H] $^-$	342.11	$C_{19}H_{18}O_6$	99.02	1,5,8-Trihydroxy-3-methyl-2-prenylxanthone	Xanthone	BM, LH, LA, LM
57	20.848	[M-H] $^-$	342.11	C_{19} H_{18} O_6	83.17	1,5,8-Trihydroxy-3-methyl-2 prenylxanthone	Xanthone	BH
58	20.848	[M-H] $^-$	342.11	C_{19} H_{18} O_6	83.17	Dulxanthone D	Xanthone	BH
59	20.958	[M-H] $^-$	396.16	C_{23} H_{24} O_6	82.71	Formoxanthone C	Xanthone	BH
60	20.964	[M+H] +	396.16	$C_{23}H_{24}O_6$	77.54	Formoxanthone C	Xanthone	BH
61	21.225	[M-H] $^-$	394.14	C_{23} H_{22} O_6	81.93	Formoxanthone A	Xanthone	BH
62	21.693	[M-H] $^-$	380.16	C_{23} H_{24} O_5	71.89	7-Geranyloxy-1,3 dihydroxyxanthone	Xanthone	BH
63	21.712	[M-H] $^-$	396.16	C_{23} H_{24} O_6	81.99	Isoalvaxanthone	Xanthone	BH
64	21.950	[M+H] +	394.14	C_{23} H_{22} O_6	73.15	Formoxanthone A	Xanthone	BH
65	22.315	[M-H] $^-$	438.20	C_{26} H_{30} O_6	53.05	Hydroxy-8-(2-hydroxy-3 methylbut-3-enyl)-3,6,7 trimethoxy-2-(3-methylbut-2 enyl)-xanthone	Xanthone	BH
66	22.756	[M-H] $^-$	464.22	C_{28} H_{32} O_6	51.58	1,3,5,6-Tetrahydroxy-4,7,8-tri (3 methyl-2-butenyl) xanthone	Xanthone	BH
67	23.345	[M-H] $^-$	378.15	C_{23} H_{22} O_5	88.03	Blancoxanthone	Xanthone	BH
68	23.651	[M-H] $^-$	394.18	C_{24} H_{26} O_5	47.43	1,3,8-Trihydroxy-4-methyl-2,7 diprenylxanthone	Xanthone	BH
69	24.003	[M-H] $^-$	408.16	C_{24} H_{24} O_6	87.15	6,8-Dihydroxy-1,7 diprenylxanthone-2-carboxylic acid	Xanthone	BH
70	24.395	[M-H] $^-$	408.19	C_{25} H_{28} O_5	79.20	1-Hydroxy-3,5-dimethoxy-2,4 diprenylxanthone	Xanthone	BH
71	24.856	[M-H] $^-$	462.20	C_{28} H_{30} O_6	97.33	Virgataxanthone B	Xanthone	BH
72	24.866	[M+H] +	462.20	C_{28} H_{30} O_6	92.63	Virgataxanthone B	Xanthone	BH
73	25.336	[M+H] +	328.17	C_{20} H_{24} O_4	93.68	7-Geranyloxy-5-methoxycoumarin	Coumarin	BH

Note B: Bark, **L**: Leave, **T**: Twig, **H**: Hexanes, **D**: Dichloromethane, **A**: Acetone, **M**: Methanol

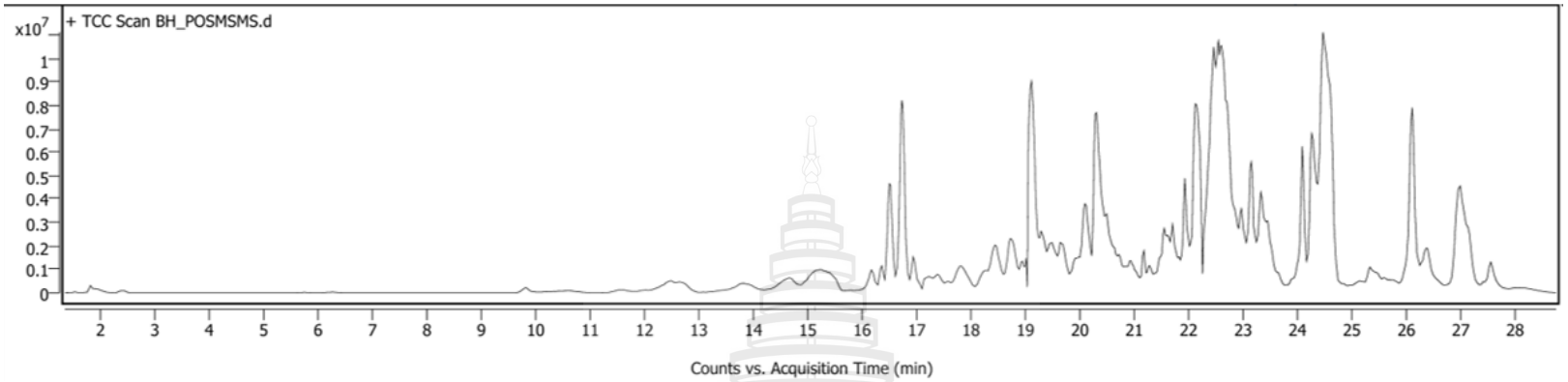

Figure A25 Total compound chromatogram of UHPLC-QTOF of *G. xanthochymus* bark extract with hexanes (POS)

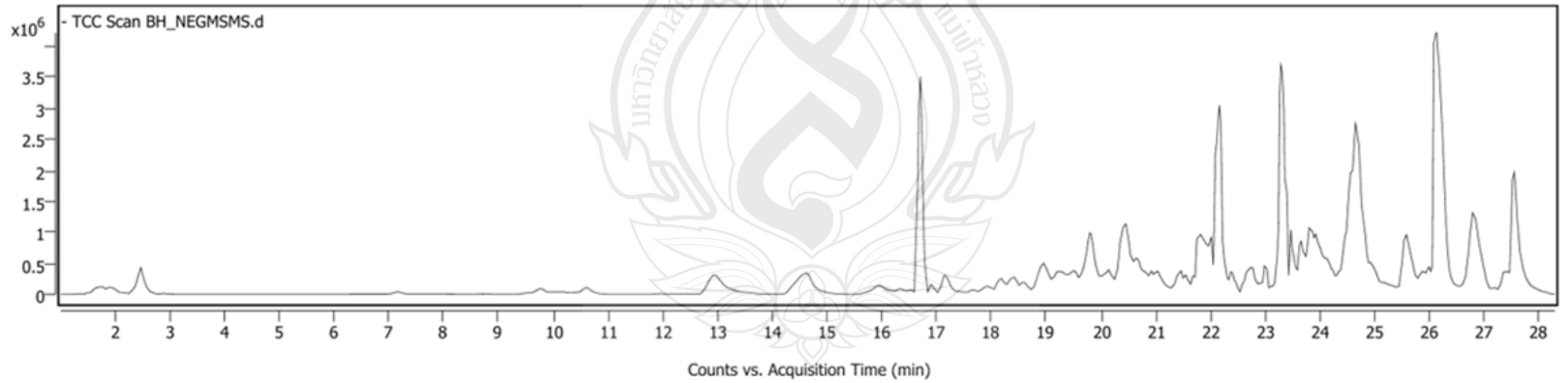

Figure A26 Total compound chromatogram of UHPLC-QTOF of *G. xanthochymus* bark extract with hexanes (NEG)

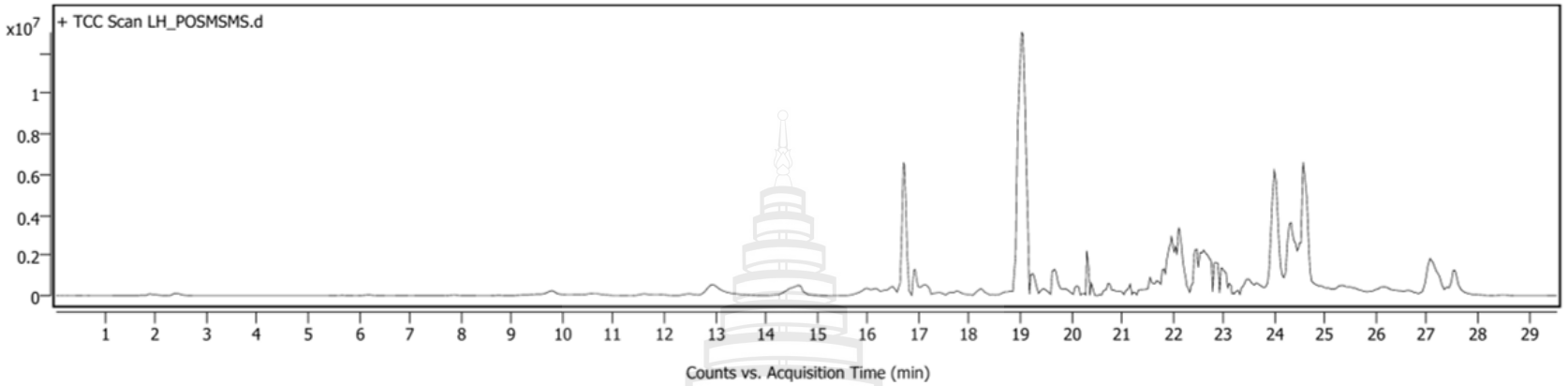

Figure A27 Total compound chromatogram of UHPLC-QTOF of *G. xanthochymus* leave extract with hexanes (POS)

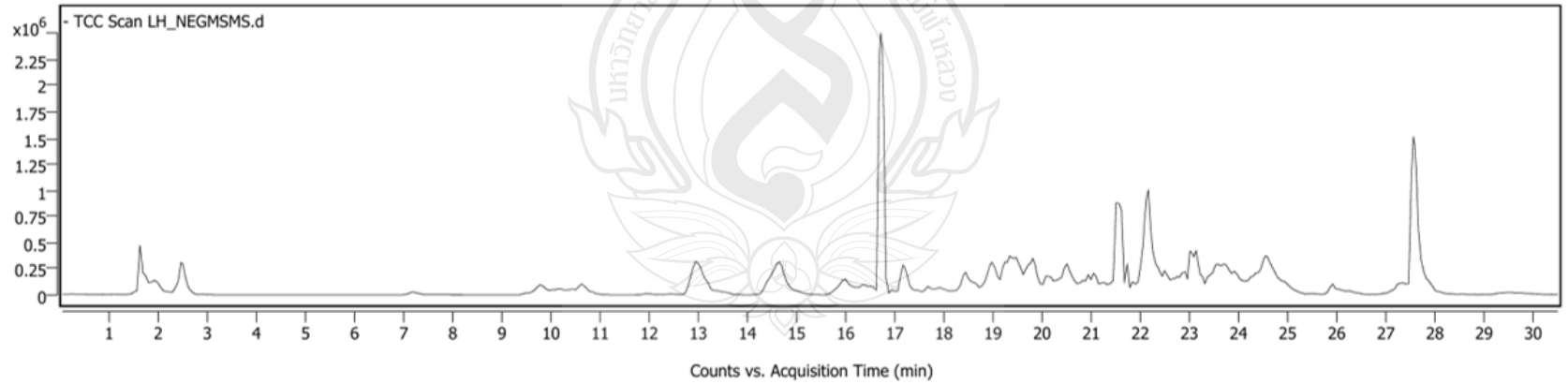

Figure A28 Total compound chromatogram of UHPLC-QTOF of *G. xanthochymus* leave extract with hexanes (NEG)

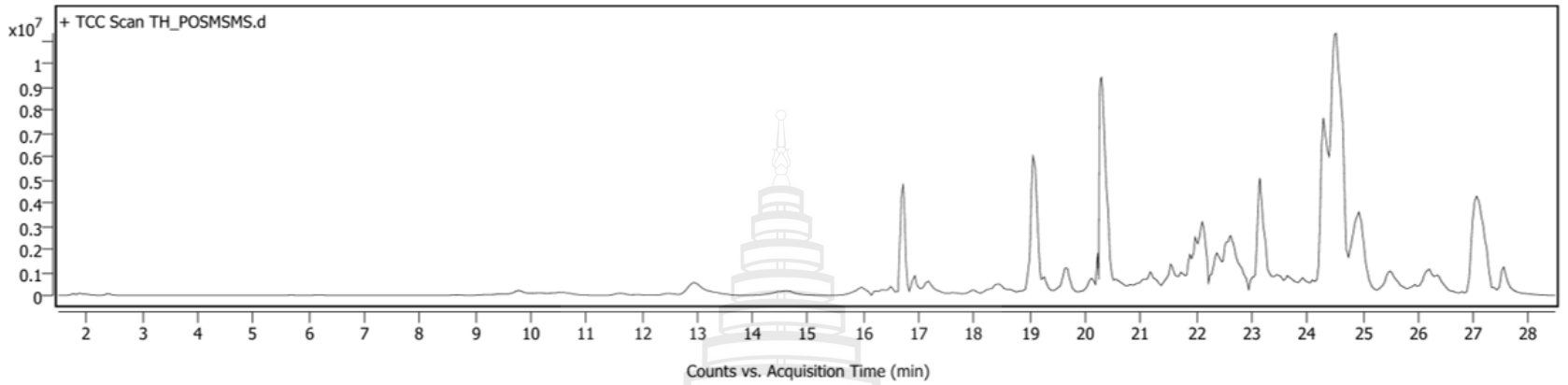

Figure A29 Total compound chromatogram of UHPLC-QTOF of *G. xanthochymus* twig extract with hexanes (POS)

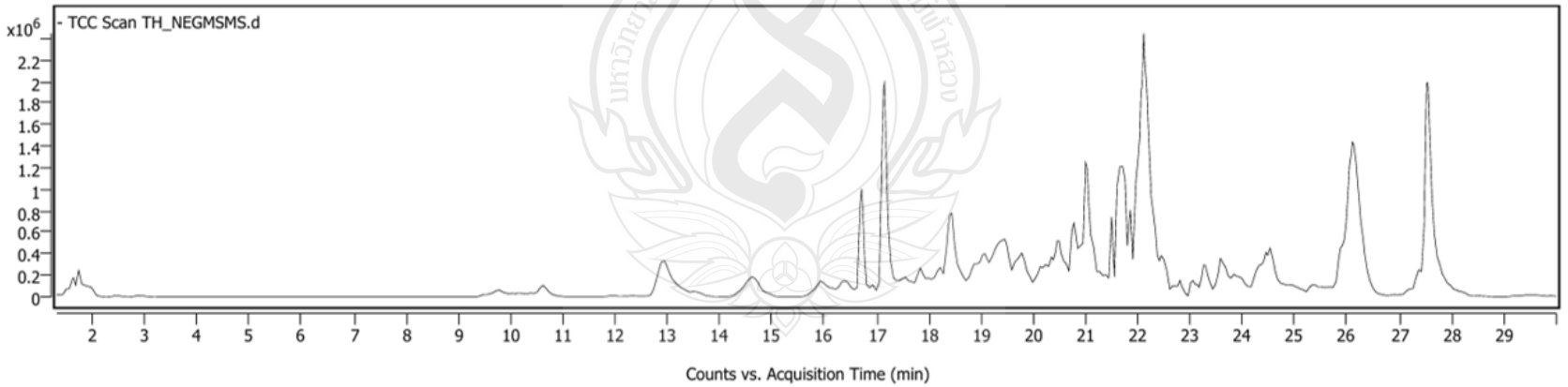

Figure A30 Total compound chromatogram of UHPLC-QTOF of *G. xanthochymus* twig extract with hexanes (NEG)

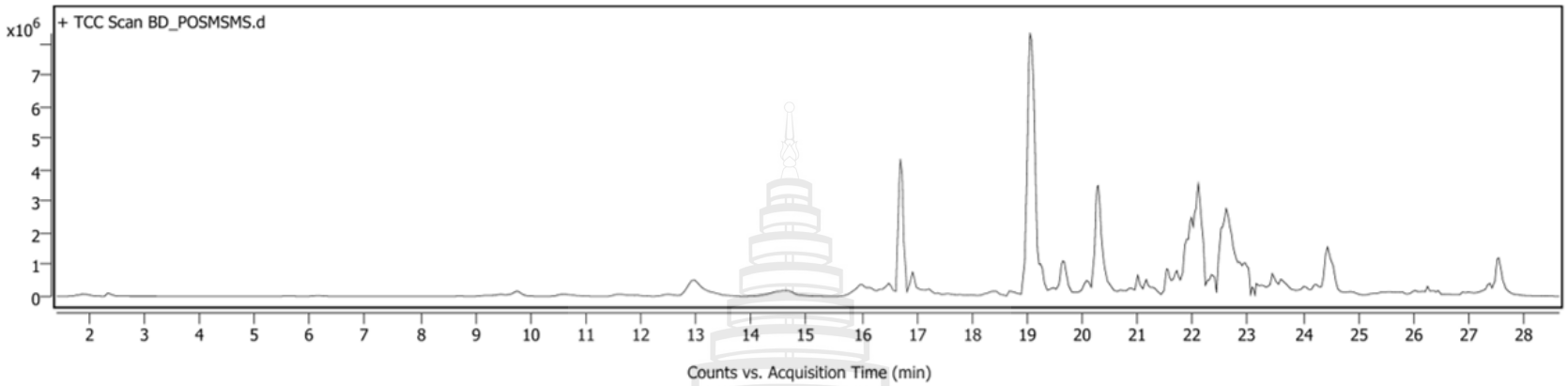

Figure A31 Total compound chromatogram of UHPLC-QTOF of *G. xanthochymus* bark extract with dichloromethane (POS)

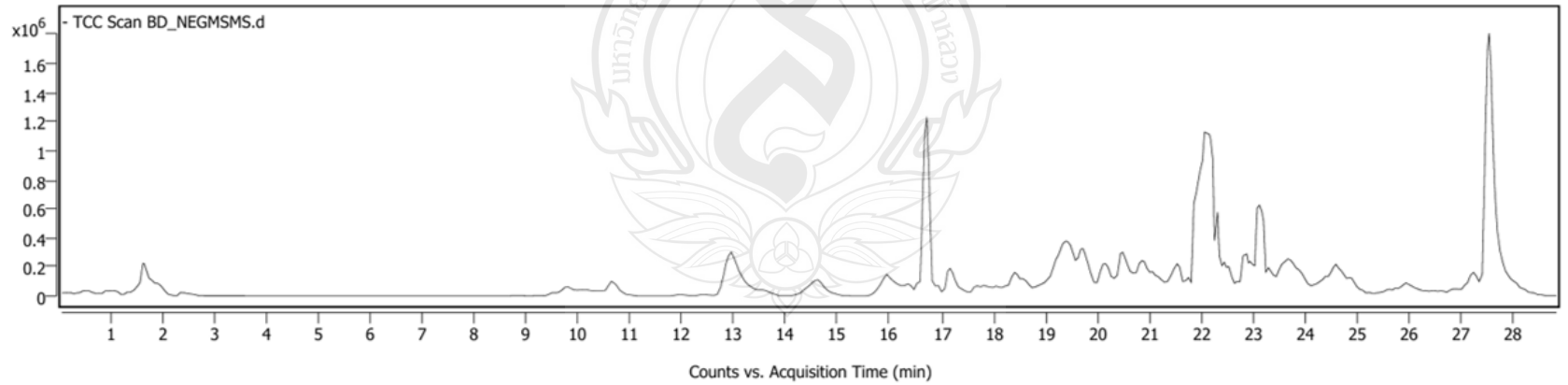

Figure A32 Total compound chromatogram of UHPLC-QTOF of *G. xanthochymus* bark extract with dichloromethane (NEG)

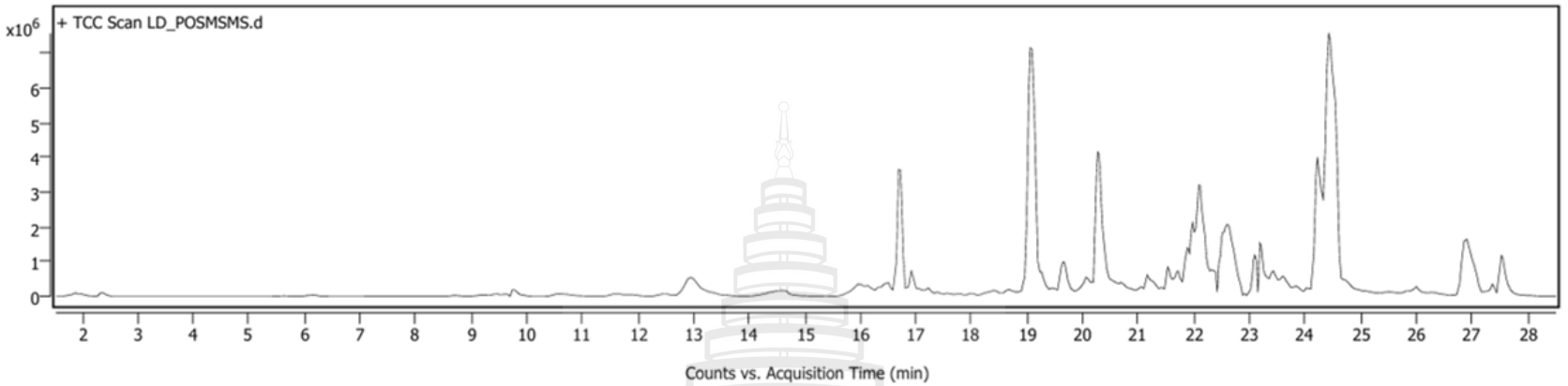

Figure A33 Total compound chromatogram of UHPLC-QTOF of *G. xanthochymus* leave extract with dichloromethane (POS)

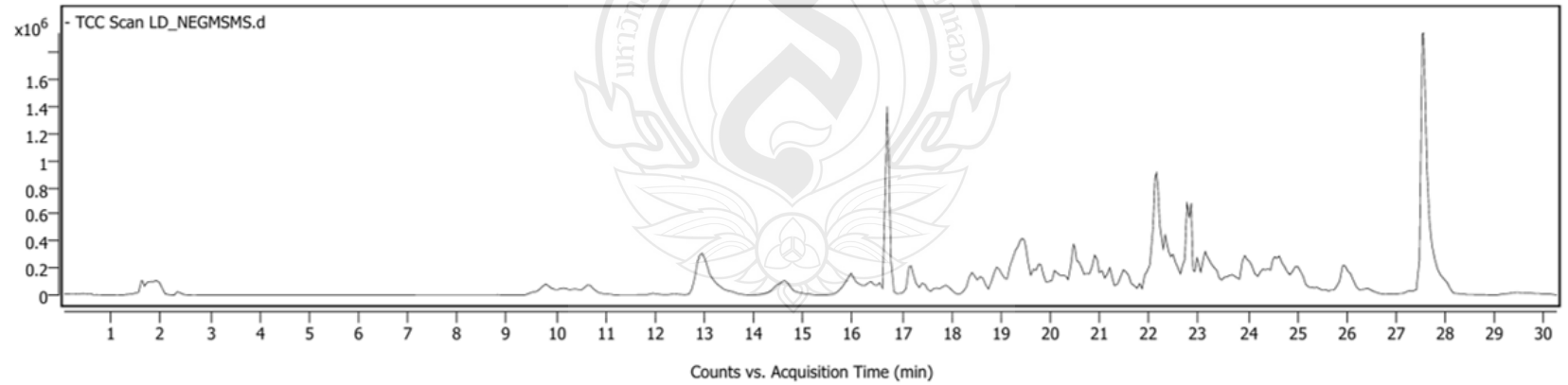

Figure A34 Total compound chromatogram of UHPLC-QTOF of *G. xanthochymus* leave extract with dichloromethane (NEG)

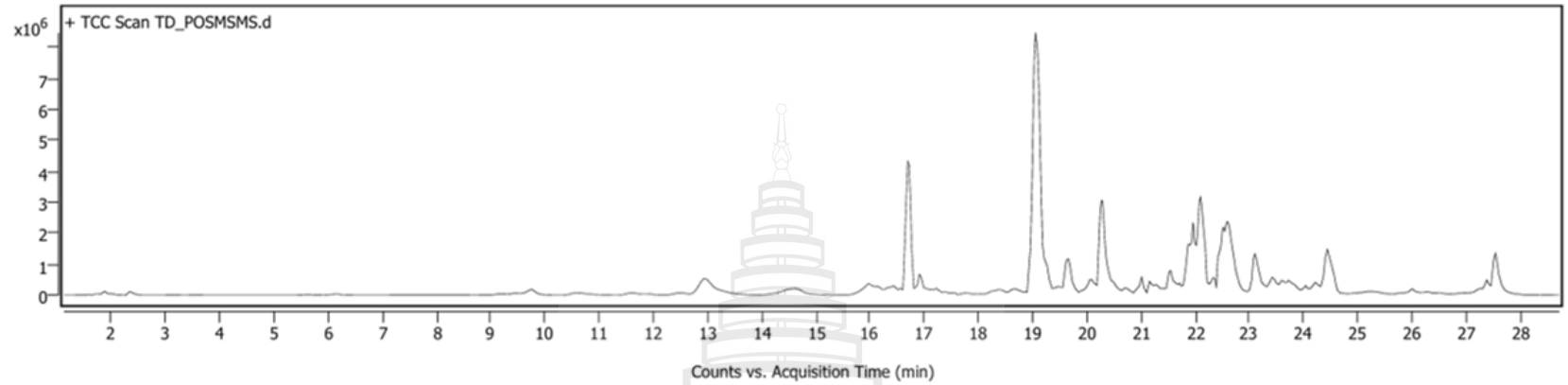

Figure A35 Total compound chromatogram of UHPLC-QTOF of *G. xanthochymus* twig extract with dichloromethane (POS)

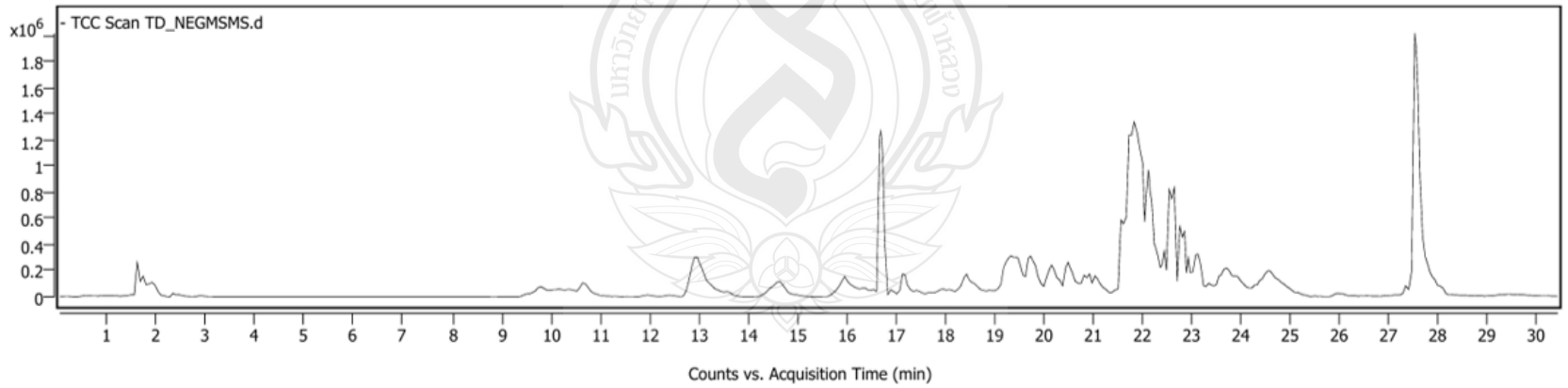

Figure A36 Total compound chromatogram of UHPLC-QTOF of *G. xanthochymus* twig extract with dichloromethane (NEG)

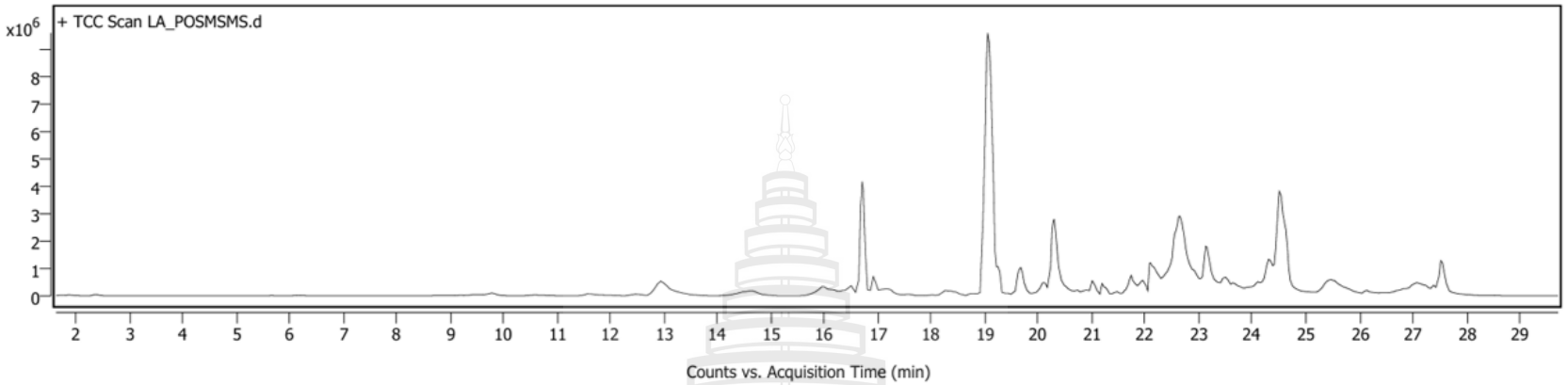

Figure A37 Total compound chromatogram of UHPLC-QTOF of *G. xanthochymus* leave extract with acetone (POS)

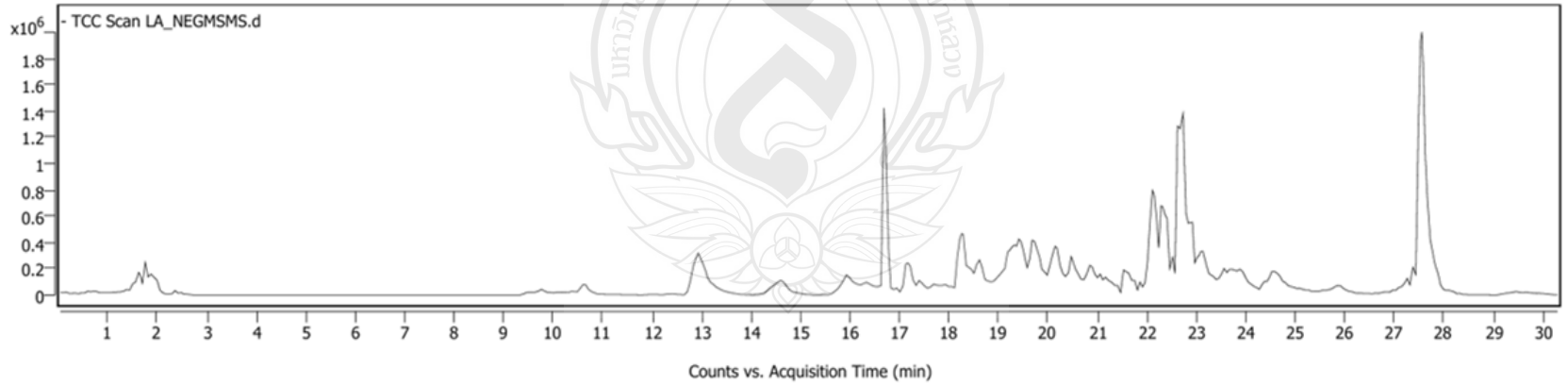

Figure A38 Total compound chromatogram of UHPLC-QTOF of *G. xanthochymus* leave extract with acetone (NEG)

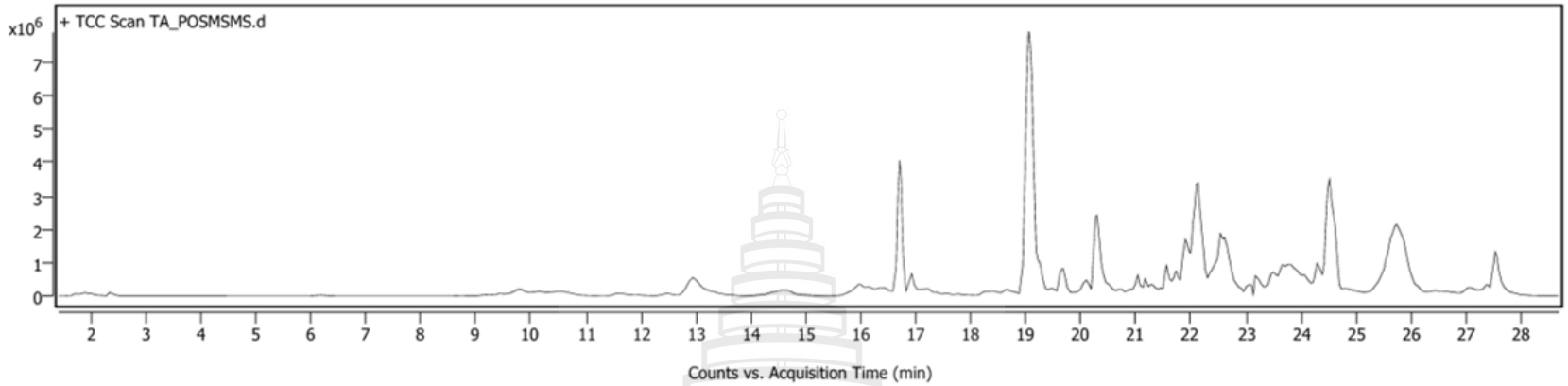

Figure A39 Total compound chromatogram of UHPLC-QTOF of *G. xanthochymus* twig extract with acetone (POS)

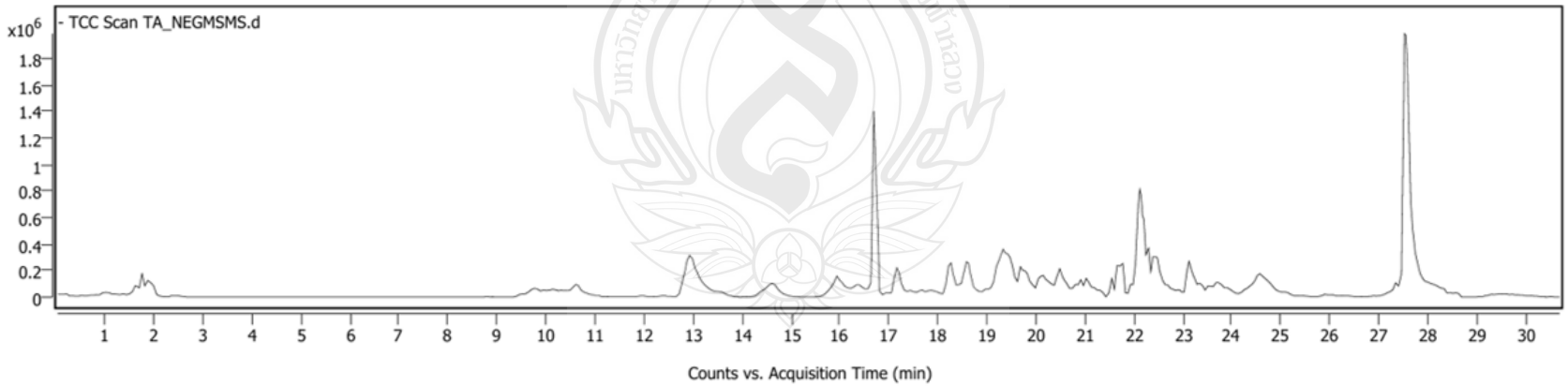

Figure A40 Total compound chromatogram of UHPLC-QTOF of *G. xanthochymus* twig extract with acetone (NEG)

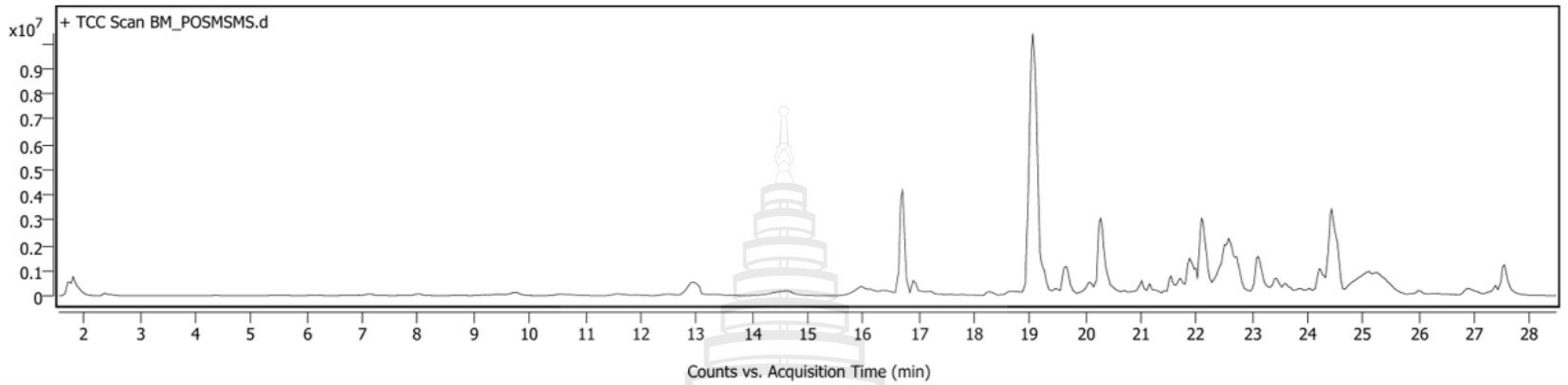

Figure A41 Total compound chromatogram of UHPLC-QTOF of *G. xanthochymus* bark extract with methanol (POS)

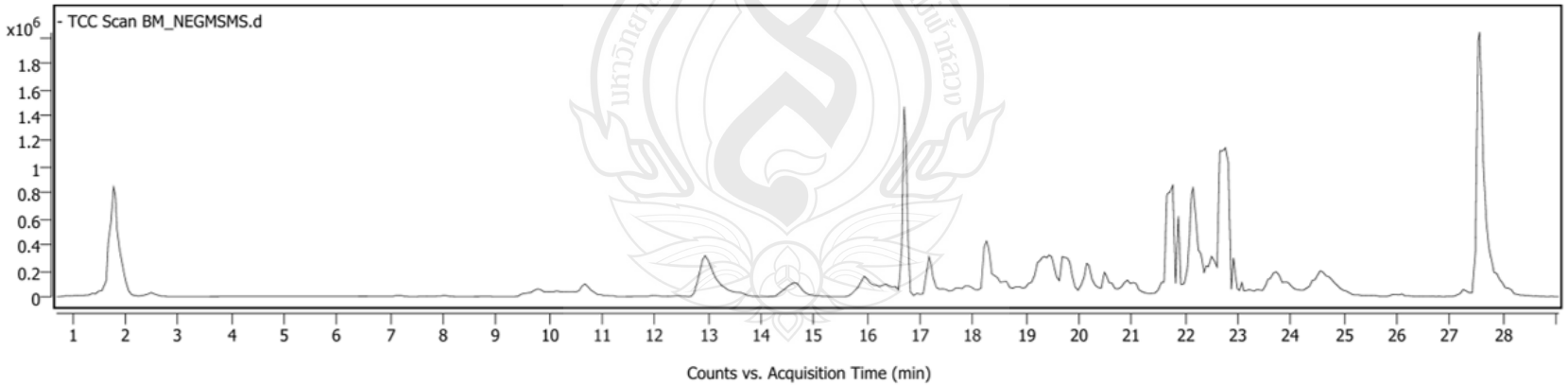

Figure A42 Total compound chromatogram of UHPLC-QTOF of *G. xanthochymus* bark extract with methanol (NEG)

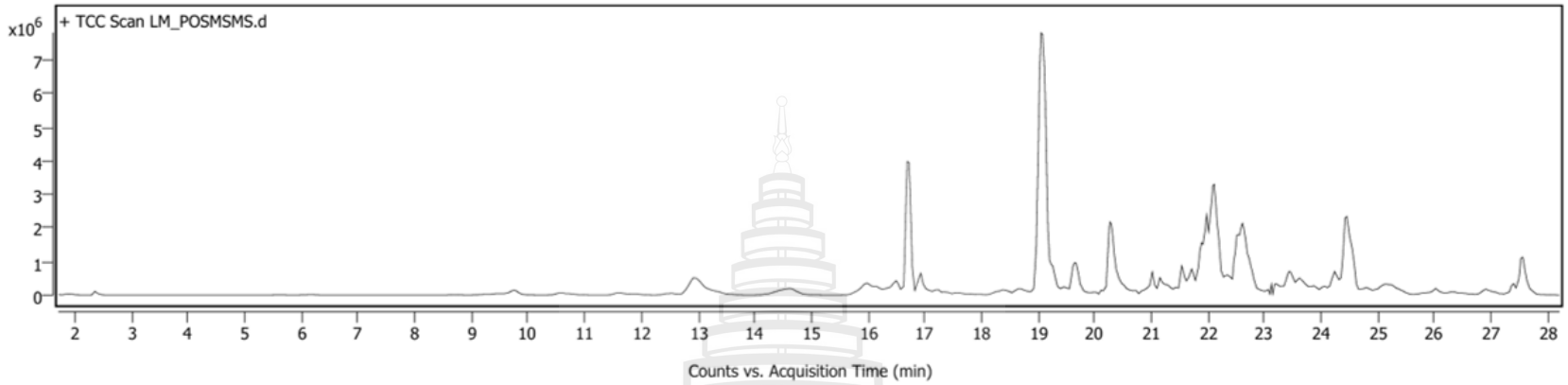

Figure A43 Total compound chromatogram of UHPLC-QTOF of *G. xanthochymus* leave extract with methanol (POS)

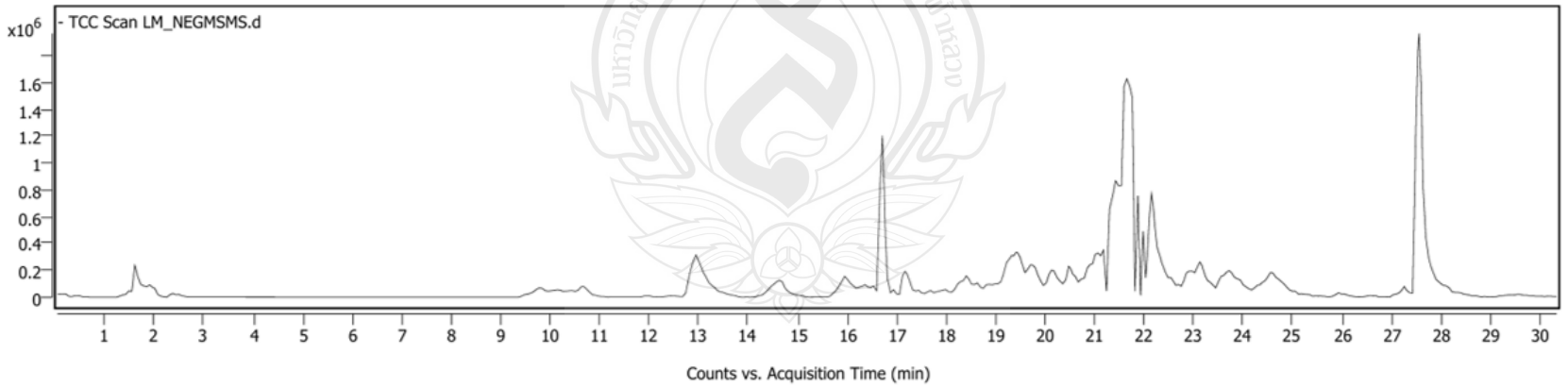

Figure A44 Total compound chromatogram of UHPLC-QTOF of *G. xanthochymus* leave extract with methanol (NEG)

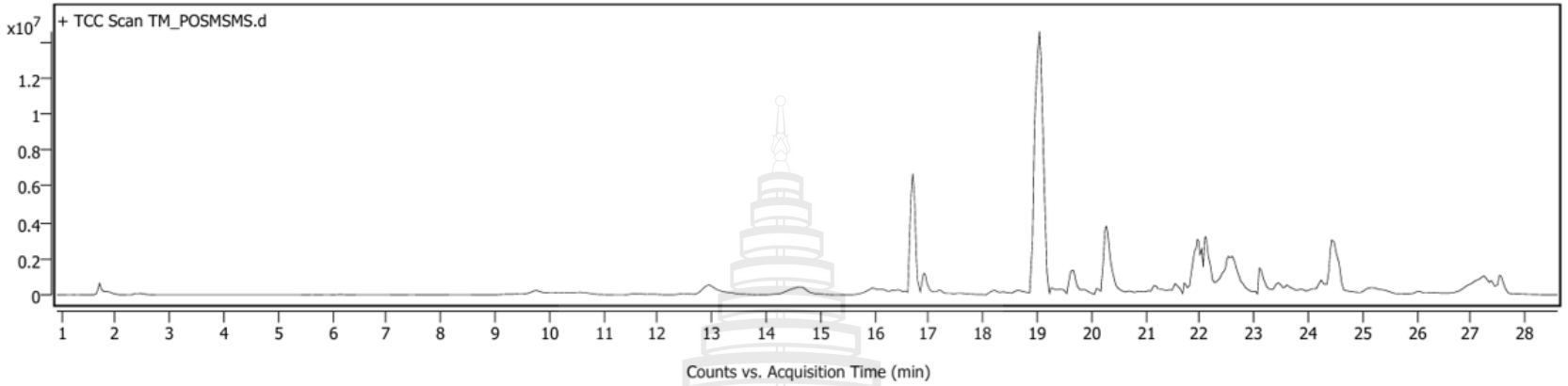

Figure A45 Total compound chromatogram of UHPLC-QTOF of *G. xanthochymus* twig extract with methanol (POS)

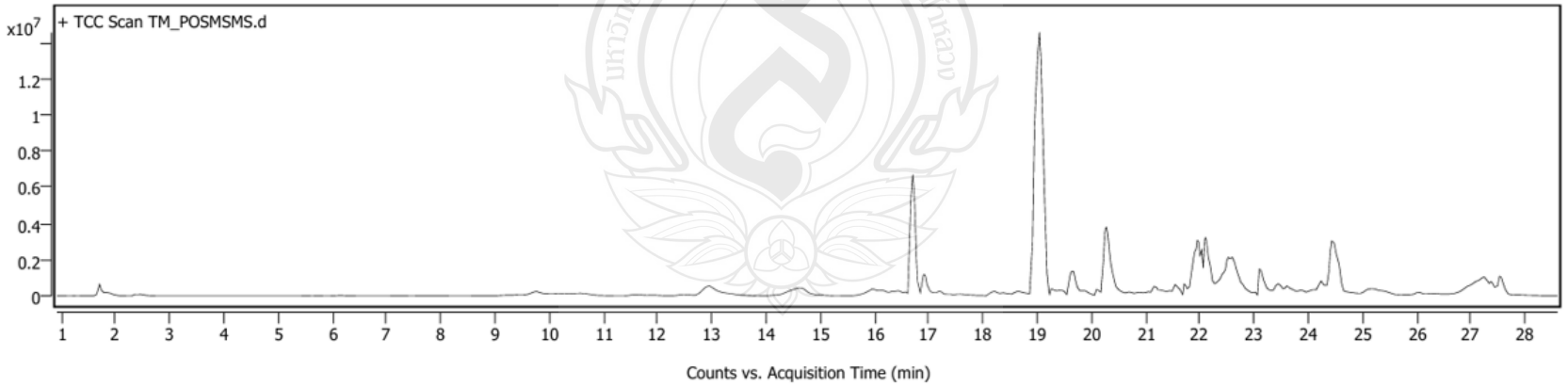

Figure A46 Total compound chromatogram of UHPLC-QTOF of *G. xanthochymus* twig extract with methanol (NEG)

CURRICULUM VITAE

NAME Sirachuch Maungprasert

EDUCATIONAL BACKGROUND

2022 Bachelor of Science
Applied Chemistry
Mae Fah Luang University

SCHOLARSHIP

2023 Postgraduate Scholarship for Tuition Fees

PUBLICATION

Maungprasert, S., Vanden Berghe, W., Kim, C. S., Laphookhieo, S., Somsuan, K., Aluksanasuwan, S., ... Deachathai, S. (2025). Anticancer Activity of *Garcinia xanthochymus* Crude Extracts Against Human Cancer Cells: *In Vitro* Evaluation in MDA-MB-231, Huh-7, A549, and SW480 Cell Lines. *Trends in Sciences*, *22*(10), 10842-10842.